

**Fetteiche Ernährung erhöht das
Melanomzellwachstum in der Knochenmarks-Nische
durch Induktion von Osteopontin und Interleukin 6**

**High fat diet increases melanoma cell growth in the
bone marrow niche by inducing osteopontin and
interleukin 6**

**Der Medizinischen Fakultät
der Friedrich-Alexander-Universität Erlangen-Nürnberg
zur
Erlangung des Doktorgrades Dr. Med.**

**vorgelegt von
Guangliang Chen
Aus Hunan, China**

**Als Dissertation genehmigt von der
Medizinischen Fakultät der Friedrich-Alexander-Universität
Erlangen-Nürnberg**

Vorsitzender des Promotionsorgans: Prof. Dr. Dr. h. c. J. Schüttler

Gutachter: Prof. Dr. G. Schett

Gutachter: Prof. Dr. B. Manger

Tag der mündlichen Prüfung: 25. Juli 2017

Table of Contents

Abstract	1
Zusammenfassung	3
1. Introduction	5
1.1 Obesity as risk factor for cancers	5
1.1.1 Obesity is one major epidemic factor of the 21st century worldwide	5
1.1.2 Obesity as a risk factor for malignant melanoma development and progression	5
1.2 Dysfunctional adipose tissue and adipocytes in obesity and their implications in melanoma growth and metastasis	7
1.2.1 Dysfunctional adipose tissue and adipocytes in obesity	7
1.2.2 Dysfunctional adipocytes are involved in malignant melanoma initiation and metastasis	8
1.2.3 Adipocytes as a major component of the tumor stroma/environment	9
1.2.4 Cancer-associated adipocytes (CAAs).....	10
1.2.5 CAAs contribute to alter cancer cells metabolism	11
1.3 The development and progression of bone metastasis	12
1.3.1 Osteolytic bone metastasis and skeletal-related events.....	12
1.3.2 Current therapies and challenges for metastatic melanoma and osteolytic metastasis	13
1.3.3 Bone metastasis: the “seed and soil” theory.....	14
1.3.4 The bone marrow niche for disseminated melanoma cells	15
1.4 The molecular mechanism for bone metastasis	17
1.4.1 The molecular mechanism for bone metastasis development and progression	17
1.4.2 Role of osteoclasts and macrophages in the tumor-bone niche.....	20
1.4.3 The contribution of inflammatory cytokines in the bone tumor niche: interleukin 6 (IL-6) and osteopontin (OPN).....	23
1.4.4 Role of bone marrow adipocytes in the tumor-bone niche	24
1.5 Aim of the thesis	26
1.5.1 Aim of the thesis.....	26
1.5.2 Declaration	27
2. Materials and Methods	28
2.1 Materials	28
2.1.1 Buffer and staining solutions.....	28
2.1.2 Cell culture media and supplements	31
2.1.3 Oligonucleotides.....	32
2.1.4 Antibodies	36
2.1.5 Molecular weight marker and loading dye.....	37
2.1.6 Reagents for cell culture	37
2.1.7 Dietaries and treatments for mice experiments	38
2.1.8 Kits and enzymes.....	38

2.1.9 Chemicals.....	40
2.1.10 Consumables	41
2.1.11 Laboratory Instruments	42
2.1.12 Software.....	42
2.2 Methods.....	44
2.2.1 Animal experiments.....	44
2.2.2 Bone metastasis mouse models	44
2.2.3 Cell culture.....	45
2.2.4 Flow cytometric analyses.....	47
2.2.5 Methods for RNA levels quantification	48
2.2.6 Methods to study protein levels.....	49
2.2.7 Histology.....	50
2.2.8 Statistical analyses.....	51
3. Results.....	52
3.1 High fat diet (HFD) increases melanoma growth and bone-resorbing osteoclasts in the bone tumor niche	52
3.1.1 Increased melanoma growth in the bone niche of mice exposed to HFD	52
3.1.2 Increased growth rate of disseminating melanoma cells in the bone metastatic niche of mice with HFD	53
3.1.3 HFD induces increased the tumor associated bone-resorbing osteoclasts	54
3.1.4 HFD lead to upregulation of osteopontin and interleukin 6 levels <i>in vivo</i>	57
3.1.5 Increase of OPN-producing macrophages and osteoclasts in the bone marrow tumor niche favor melanoma cell growth.....	60
3.1.6 Increase of IL-6-producing adipocytes in the bone marrow tumor niche by HFD upregulates cancer cell growth	62
3.1.7 Increased CD31+ cells in the bone tumor niche of HFD mice injected with B16F10 cells	63
3.2 The nuclear factor-κB (NF-κB) signalling pathway contributes to alter the biological behaviour of melanoma cells challenged with high fat diet (HFD) serum <i>in vitro</i>	65
3.2.1 Circulating factors present in HFD-fed mice enhance melanoma cells proliferation and migration	65
3.2.2 Enhanced cell migration in melanoma cells pre-treated with HFD serum	66
3.2.3 Upregulation of chemokine (C-X-C motif) ligands secretion by B16F10 cells stimulated with HFD serum.....	68
3.2.4 Activation of NF- κ B pathway in melanoma cells induced by HFD serum	69
3.2.5 Both IL-6 and OPN are essential for CXCLs production by B16F10 melanoma cells <i>in vitro</i>	72
3.3 Activation of osteoclasts differentiation by melanoma cells pre-stimulated with HFD serum is dependent of cell-cell contact.....	73
3.3.1 The secretome of melanoma cells induced by HFD serum is not sufficient to promote osteoclastogenesis <i>in vitro</i>	73

3.3.2 Melanoma cells pre-treated with HFD serum increase osteoclastogenesis in an OPN dependent manner <i>in vitro</i>	74
3.3.3 HFD associated circulating factors also promote osteoclast differentiation <i>in vitro</i>	76
3.4 Melanoma cells potentiate a biological crosstalk with bone marrow adipocytes and osteoclasts in the bone tumor niche.....	77
3.4.1 B16F10 cells become more “aggressive” in the presence of adipocytes.....	77
3.4.2 Upregulation of chemokine (C-X-C motif) ligands and inflammatory gene expression in bone marrow adipocytes by a crosstalk of cancer cells.....	78
3.5 Interruption of IL-6/JAK2-OPN axis rescue melanoma cell growth in mice exposed to HFD	80
3.5.1 Both IL-6 and OPN are essential for tumor growth induced by HFD <i>in vivo</i>	80
3.5.2 Inhibition of JAK2 is essential for reducing the bone tumor cell growth and blocking IL-6 signalling <i>in vivo</i>	82
4. Discussion	85
4.1 Increased melanoma cell growth in the bone tumor niche was triggered by HFD-induced factors.....	85
4.2 Inflammatory cytokines mediated the increased melanoma cell growth in the HFD bone niche.....	87
4.3 Role of adipocytes in the bone melanoma niche for melanoma growth by HFD	88
4.4 Contribution of OPN produced by macrophages and osteoclasts to the bone–melanoma niche.....	90
4.5 HFD exposure drives melanoma cells to orchestrate a stromal cells-rich niche in the bone marrow	91
4.5.1 Impact of circulating factors on melanoma cells via the NF-κB pathway.....	91
4.5.2 Crosstalk of adipocytes and macrophages in the stromal cells-rich bone melanoma niche: role of IL-6-OPN-CXCLs axis	93
4.5.3 CD31+ endothelial cells in the stromal cells-rich bone melanoma niche.....	95
4.6 Conclusions.....	96
5. References	97
6. Appendix.....	120
6.1 Abbreviations	120
6.2 Acknowledgements.....	124

Abstract

The impact of metabolic stress induced by obesity on the bone marrow niche during melanoma growth and metastasis is largely unknown. Here we employed diet induced obese mouse models, where mice received high-fat (HFD) or normal diet (ND) for 6 weeks before challenge with B16F10 melanoma cells. Tumor size, bone loss and osteoclast numbers were assessed histologically in the tibial bones. For defining the molecular pathway, osteopontin (OPN) knock-out mice, interleukin (IL) 6 neutralizing antibody or Janus kinase (JAK) 2 inhibition was carried out in the same model. Mechanistic studies such as adipocyte-melanoma co-cultures for defining adipocyte induced changes of tumor cell proliferation and expression profiles were also performed. Moreover, bone marrow derived monocyte-melanoma co-cultures were set up to define circulating factors present in HFD mice induced activation of osteoclasts. In addition, the effects of systemic factors from HFD mice on B16F10 melanoma cells were also evaluated *in vitro*. As results, HFD enhanced melanoma burden in bone by increasing tumor area and osteoclast numbers. This process was associated with higher numbers of bone marrow adipocytes expressing IL-6 in direct vicinity to tumor cells. Inhibition of IL-6 or of its downstream signalling JAK2 blocked HFD-induced tumor progression. In addition, circulating factors present in HFD mice enhanced melanoma cell proliferation and migration, activated nuclear factor- κ B (NF- κ B) signalling, and upregulated its downstream targets, such as chemokine (C-X-C motif) ligands (CXCLs) and adhesion and angiogenesis molecules in melanoma cells *in vitro*. The phenotypic changes of melanoma cells triggered macrophage and osteoclast accumulations accompanied by increased osteopontin expression and CD31⁺ cells in the bone melanoma niche. In addition, melanoma cells pre-treated with HFD serum increased osteoclastogenesis in an OPN dependent manner *in vitro*. Furthermore, OPN triggered osteoclastogenesis and also exerted a positive feedback loop to tumor cells, which was abrogated in its absence *in vivo* and *in vitro*. Moreover, melanoma cells became more “aggressive” in the presence of bone marrow adipocytes, whereas the latter underwent a dedifferentiation

process into preadipocytes with upregulation of CXCLs and pro-inflammatory genes. Therefore, the bone marrow adipocytes, macrophages/osteoclasts and CD31+ cells constitute a stroma rich environment for melanoma cells in the bone marrow by HFD. Metabolic stress by HFD promotes melanoma cell growth in the bone marrow niche by an increase in IL-6-JAK2-osteopontin mediated activation of tumor cells and osteoclast differentiation.

Zusammenfassung

Der Einfluss von metabolischem Stress auf die Knochenmarks-Nische während des Melanomwachstums und der Metastasierung ist weitestgehend unbekannt. In der vorliegenden Studie verwendeten wir daher ein Diät-induziertes Adipositas-Modell, bei dem Mäuse für sechs Wochen entweder mit normaler Diät (ND) oder Hochfett-Diät (HFD) gefüttert wurden. Im Anschluss wurde den Tieren B16F10 Melanomzellen induziert und die Tumorgröße, der Knochenverlust und die Osteoklasten-Zahl histologisch in den Tibiaknochen analysiert. Um den molekularen Signalweg genauer zu bestimmen wurde dieses Modell zusätzlich auch noch in Osteopontin-defizienten Mäusen sowie unter der Verwendung von Interleukin-6 neutralisierenden Antikörpern und Janus Kinase (JAK) 2 Inhibitoren durchgeführt. Zudem wurden in mechanistischen Studien, wie etwa der Co-Kultur von Adipozyten und Melanomzellen, Veränderungen im Tumor-Wachstum und dem Expressionsprofil untersucht. Darüber hinaus wurden Co-Kulturen von aus dem Knochenmark stammenden Monozyten und Melanomzellen angesetzt um zirkulierende Faktoren zu identifizieren, die unter der HFD zur Aktivierung von Osteoklasten führten. Der Effekt systemischer Faktoren der HFD auf B16F10 Melanomzellen wurde *in vitro* untersucht. Die HFD erhöhte die Tumorlast im Knochen durch eine vergrößerte Tumorfläche und eine erhöhte Osteoklasten-Zahl. Dieser Prozess war zudem mit mehr IL-6 exprimierenden Adipozyten in direkter Nähe zu den Tumorzellen verbunden. Inhibierung von IL-6 oder der IL-6 induzierten Signalprozesse durch JAK2-Blockade hemmte die HFD-induzierte Tumorprogression. *In vitro* Versuche zeigten, dass zirkulierende Faktoren in Mäusen unter HFD die Proliferation von Melanomzellen verstärkten und deren Migration aktivierten. Weiterhin wurden eine Aktivierung des NF- κ B-Signalweges und die Hochregulation von NF- κ B-Zielgenen beobachtet. Darunter befanden sich chemokine (C-X-C motif) ligands (CXCLs) und Gene, welche die Adhäsion und Angiogenese betreffen. Die phänotypischen Veränderungen der Melanomzellen führten zur Akkumulation von Makrophagen und Osteoklasten und waren mit vermehrter Osteopontin-Expression und

mehr CD31-positiven Zellen in der Knochen-Melanoma-Nische verbunden. Weiterhin erhöhten Melanomzellen, die mit dem Serum von Mäusen unter HFD inkubiert wurden, die Osteoklastogenese auf eine OPN-abhängige Art und Weise *in vitro*. Darüber hinaus löste OPN Osteoklastogenese aus und induzierte einen positiven Rückkopplungskreislauf auf Tumorzellen, welcher in Abwesenheit von OPN sowohl *in vitro* als auch *in vivo* ausblieb. Weiterhin wurden Melanomzellen „aggressiver“ in der Gegenwart von Knochemarks-Adipozyten, wobei Letztere eine Differenzierung zu Prä-Adipozyten unterliefen und CXCLs sowie inflammatorische Gene heraufregulierten. Wir schließen daraus dass Adipozyten, Makrophagen/Osteoklasten und CD31-positive Zellen eine Umgebung darstellen, die das Melanomwachstum in der Knochenmarks-Nische unter dem Einfluss einer HFD fördern. Der metabolische Stress, der durch die HFD ausgelöst wird, fördert dabei das Melanomwachstum durch eine erhöhte Zahl an Knochemarks-Adipozyten und IL-6-JAK2-OPN abhängige Aktivierung von Tumorzellen und Osteoklasten.

1 Introduction

1.1 Obesity as risk factor for cancers

1.1.1 Obesity is one major epidemic factor of the 21st century worldwide

Obesity is one major epidemic factor of the 21st century (Kaidar-Person et al., 2011). A basic cause for overweight and obesity is the energy imbalance between calories consumed (by eating) and calories expended (by exercise and everyday living) (Organization, 2015). Currently, overweight and obesity assessment and classification are dependent on a scale known as the body mass index (BMI), which is determined as weight (in kilograms) divided by height (in meters) squared. In 2014, around 39% of the world adult population (aged 18+) was overweight ($BMI \geq 25 \text{ kg/m}^2$) divided for 39% of men and 40% of women; and 13% was obese ($BMI \geq 30 \text{ kg/m}^2$) (11% of men and 15% of women) resulting from analysis of the Global Health Observatory (GHO) data. In addition, overweight and obesity is occurring in children with younger ages (Hurt et al., 2010; Mitchell et al., 2011; Organization, 2015; Wu, 2006). For example, the World Health Organization (WHO) estimates that 42 million children under the age of 5 of the world were overweight or obese in 2013 (Organization, 2015). Moreover, the prevalence of overweight and obesity in developing countries continues to soar (Organization, 2015; Wu, 2006). The alarming increase in obese and overweight population posed a major public health issue worldwide, because overweight and obesity increase the risk of several serious chronic diseases, including certain forms of cancer (WHO and Consultation, 2003).

1.1.2 Obesity as a risk factor for malignant melanoma development and progression

Cancer is another epidemic factor of the 21st century (Kaidar-Person et al., 2011). It has been estimated that around 20% of all cancers are due to excess weight (Berrington de Gonzalez et al., 2010; Calle et al., 2003; De Pergola and Silvestris, 2013; Wolin et al.,

2010). Fortunately, obesity, like tobacco, is a preventable cause of cancer (Organization, 2015). Obesity is linked to cancer susceptibility, including malignant melanoma (MM)(Antoniadis et al., 2011; Berrington de Gonzalez et al., 2010; Calle et al., 2003; De Pergola and Silvestris, 2013; Kaidar-Person et al., 2011; Louer et al., 2012; Mitchell et al., 2011; Sergentanis et al., 2013; Wolin et al., 2010). However, the biological mechanisms are not fully understood (De Pergola and Silvestris, 2013). To explain this, several hypotheses were proposed, such as hyperinsulinemia or insulin resistance, adipose tissue dysfunction with excess amounts of estrogen, adipokines, and inflammatory molecules production, oxidative stress, hypoxia and involvement of nuclear factor kappa beta (NF- κ B) signalling in adipose tissue, shared genetic susceptibility, and altered immune function (Antoniadis et al., 2011; Berrington de Gonzalez et al., 2010; Calle et al., 2003; De Pergola and Silvestris, 2013; Kaidar-Person et al., 2011; Louer et al., 2012; Mitchell et al., 2011; Sergentanis et al., 2013; Wolin et al., 2010). Among these hypotheses, the dysfunctional adipose tissue is highlighted as the central player in the increased susceptibility of cancers (Blucher, 2013; de Ferranti and Mozaffarian, 2008; Diedrich et al., 2015; Iyer et al., 2010; Kloting and Bluher, 2014; Nieman et al., 2013; Nikki A. Ford, 2013; van Kruijsdijk et al., 2009), including melanoma(Brandon et al., 2009; De Pergola and Silvestris, 2013; Dennis et al., 2008; Institute, 2012; Mori et al., 2006; Nieman et al., 2013; Nikki A. Ford, 2013; Odenbro et al., 2007; Sergentanis et al., 2013; Shors et al., 2001; Veierod et al., 1997).

Melanoma is a skin neoplasm disorder, arising from transformed and uncontrolled proliferation of melanocytes. Melanoma is one of the most aggressive cancers. Even though melanoma accounts for only 4% of all skin cancers, melanoma contributes to around 75% of deaths from skin cancer (Maryland, 2003). Moreover, the incidence of melanoma is rising faster than any other malignancy worldwide (Bataille, 2009 -a; Foundation., 2015).

The well-known risks of melanoma include sun exposure, dysplastic nevi, age, race, personal or family history of melanoma, and immune suppression so on (Bataille, 2009

-b; Chen et al., 2013; Foundation., 2015). In recent, obesity as a risk for melanoma was increasingly attracted much attention in the field of melanoma research. Indeed, epidemiological, clinical and experimental studies have shown that over nutrition leading to adipose tissue expansion increases the risk of melanoma (De Pergola and Silvestris, 2013; Dennis et al., 2008; Institute, 2012; Mori et al., 2006; Nieman et al., 2013; Nikki A. Ford, 2013; Odenbro et al., 2007; Sergentanis et al., 2013; Shors et al., 2001; Veierod et al., 1997), melanoma cell growth (Amjadi et al., 2011; Brandon et al., 2009; Kwan et al., 2014), distant metastasis (Jung et al., 2015; Kushiro et al., 2012; Mori et al., 2006), and resistance to chemotherapy and targeted therapy (Chi et al., 2014), and worsens its prognosis (Dennis et al., 2008; Pandey et al., 2012). In addition, obesity is associated with a state of chronic systemic inflammation (Institute, 2012; Kwan et al., 2014; van Kruijsdijk et al., 2009), which may presents a critical role of inflammation in skin carcinogenesis and progression (Maru et al., 2014; Melnikova and Bar-Eli, 2009). Therefore, a better understanding of how obesity contributes melanoma initiation and progression could help us to beat this devastating disease.

1.2 Dysfunctional adipose tissue and adipocytes in obesity and their implications in melanoma growth and metastasis

1.2.1 Dysfunctional adipose tissue and adipocytes in obesity

Metabolic stress induced by obesity is characterized by the hypertrophic expansion of adipose tissue, and in consequence dysfunction of this tissue. In obese setting, activation of some transcription factors (TFs) were observed in adipocytes or stromal cells, which mainly include NF- κ B, signal transducer and activator of transcription 3 (STAT-3), hypoxia-inducible factor-1 alpha (HIF-1 α) (He et al., 2011; Jiang et al., 2013). These TFs induce inflammatory gene targets, such as prostaglandins, cyclooxygenase-2 (COX-2), cytokines (tumor necrosis factor- alpha (TNF- α), interleukin (IL)-1, IL-6), chemokines (CXC-chemokine ligands (CXCLs)) and chemokine receptors, and in consequences trigger a chronic “low-grade” inflammatory response to obesity (Greenberg and Obin, 2006; Kabir et al., 2014). The inflammatory microenvironment

in adipose tissue can predispose individuals to develop metabolic syndromes, including type 2 diabetes mellitus (T2DM) and cardiovascular disease (Gregor and Hotamisligil, 2011; Jung and Choi, 2014; Lumeng and Saltiel, 2011). And the chronic inflammatory state was regarded as critical mediators for both obesity and cancers (Bald et al., 2014; Jung et al., 2015; Malvi et al., 2015; Maru et al., 2014; van Kruijsdijk et al., 2009). Also, the unique influence of adipose tissue providing systemic endocrine factors, such as adipokines and pro-angiogenic factors, favor both melanoma initiation and progression (Nieman et al., 2011; Park et al., 2014; Rivera-Gonzalez et al., 2014).

1.2.2 Dysfunctional adipocytes are involved in malignant melanoma initiation and metastasis

Though, adipocytes were long thought to act as reservoirs for storage of excess energy as lipid, they could also involve in natural cancer history (Tan et al., 2011). In skin, adipocytes exist in a specialized dermal depot and display dynamic changes in number and size during tissue homeostasis (Kruglikov et al., 2016; Rivera-Gonzalez et al., 2014). Recent studies revealed, that the dermal adipocytes is closely associated with the hair cycle, wound healing following injury, and aging in skin (Rivera-Gonzalez et al., 2014). Due to the anatomical structure of adipocytes in skin, crosstalk between melanocytes and adipocytes are likely necessary to melanoma initiation and progression (Figure 1.1).

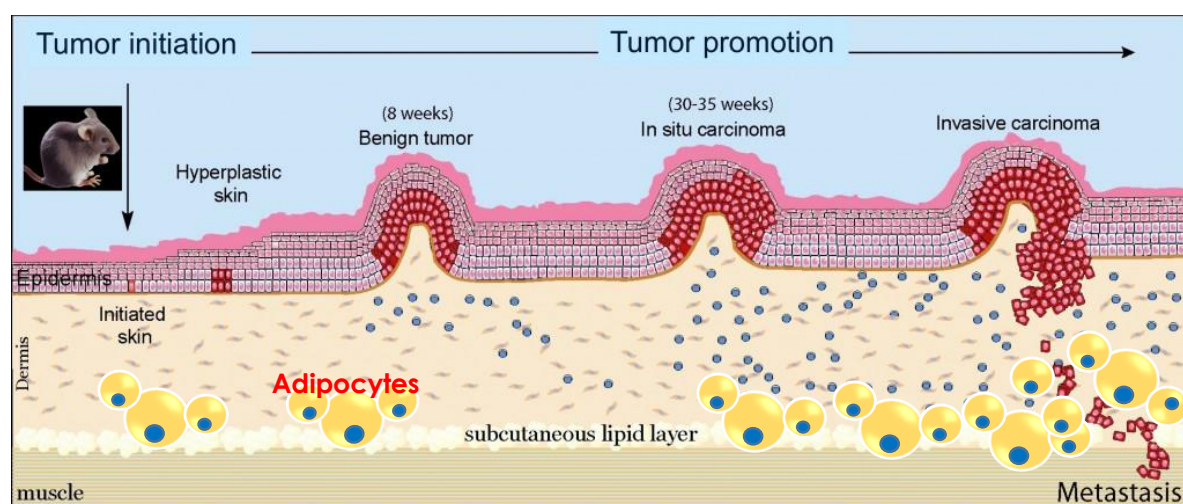


Figure 1.1 A mouse model for skin cancers including melanoma initiation and progression. Carcinogen induces specific mutations in cell of the epidermis or in melanocytes (red) to become

transformed skin cells, which can give rise to benign tumors. They can eventually develop into invasive carcinoma or melanoma, and metastasize to other organs such as lymph nodes, brain, lung and bone. Dermal adipocytes are likely necessary to melanoma initiation and progression. Inflammatory cells are shown as blue dots. (Adapted from Lee Sherman in 2011 on <http://oregonstate.edu/terra/2011/10/how-tumors-begin/>, Illustration: Indra laboratory)

Indeed, melanoma cells invade dermal compartment that are rich with adipose tissue, where adipocytes function as endocrine cells to critically shape their microenvironments and contribute to cancer development and progression (Kwan et al., 2014). In addition, peritumor adipose tissue may be a source of angiogenic factors for melanoma progression (Alasvand et al., 2015; Wagner et al., 2013). Like other cancers in adipocyte-rich soft tissue, such as the breast, adipocytes also interact dynamically with melanoma cells and induce tumor cell growth, invasion and metastasis(Bochet et al., 2011; Chi et al., 2014; Coelho et al., 2015; Jung et al., 2015; Kushiro et al., 2012; Kwan et al., 2014).

1.2.3 Adipocytes as a major component of the tumor stroma/environment

Melanoma like other solid tumors are generally composed of two major components: heterogeneous malignant cells and non-malignant stromal part (Inada et al., 2015; Kucerova and Skolekova, 2013). It is now clear that stromal cells in tumor microenvironment play an important role in cancer development and progression (Inada et al., 2015; Mao et al., 2013). In adipocyte-rich tissue, such as breast, omentum and dermal depot, the adipocytes surrounding tumors are one major component of the tumor stroma, and act as one of the tumor-promoting cell types(Bochet et al., 2013; Dirat et al., 2011; Mao et al., 2013; Nieman et al., 2011; Pollard, 2004; Tan et al., 2011), besides fibroblasts and macrophages(Pollard, 2004).

Mechanistically, the tumor-associated adipocytes contribute to tumor growth by acting as an energy source for the embedded cancer cells(Mao et al., 2013; Nieman et al., 2011; Park et al., 2014; Sturtz et al., 2014; Wagner et al., 2013). For supporting this point, metastatic cancer cells, including melanoma, can recruit adipocyte progenitors into the stromal vascular fractions(Zhang et al., 2009b), and further enhance adipogenesis by

their soluble factors, e.g. IL-8, and bone morphogenetic protein (BMP) 4(Hirano et al., 2008; Wong et al., 2014; Zhang et al., 2009b). The enhanced adipocytes are probably able to recruit fibroblasts and macrophages (Kwan et al., 2014; Rivera-Gonzalez et al., 2014). In obese states, dysfunctional adipose tissue and adipocytes promote tumor growth and metastasis by functioning as an endocrine organ, through secretion of signalling molecules, such as leptin(Brandon et al., 2009), IL-6(Dirat et al., 2011), and IL-8(Nieman et al., 2011), for tumor cells(Park et al., 2014). Thus, adipocytes play an important role in promoting cancer development and progression.

1.2.4 Cancer-associated adipocytes (CAAs)

Indeed, melanoma cells are closely aligned with adipose tissue (Kwan et al., 2014; Wagner et al., 2013). The reciprocal interactions between adipocytes and tumor cells may be essential for melanoma development and progression(Park et al., 2014; Wagner et al., 2013), and that might be amplified in obese individuals(Dirat et al., 2011; Park et al., 2014; Tan et al., 2011; Wagner et al., 2013). Invasive cancer cells induce phenotypic and functional modifications of tumor surrounding adipocytes, such as loss of adipogenic markers, upregulated expression of inflammatory cytokine and protease genes, and enhanced release of free fatty acids(Dirat et al., 2011; Nieman et al., 2011; Park et al., 2014; Tan et al., 2011; Wagner et al., 2013). Due to the dramatic changes in phenotype and specific biological features, tumor surrounding adipocytes are also named cancer-associated adipocytes (CAAs) (Figure 1.2)(Dirat et al., 2011; Nieman et al., 2011; Park et al., 2014; Tan et al., 2011; Wagner et al., 2013). Importantly, all changes occurring in adipocytes support aggressive tumor growth and invasiveness(Dirat et al., 2011; Nieman et al., 2011; Park et al., 2014; Tan et al., 2011; Wagner et al., 2013). In addition, adipocytes also undergo apoptosis or necrosis in tumors setting, which recruits and activates macrophages, contributing to tumor-associated inflammation (Wagner et al., 2013).

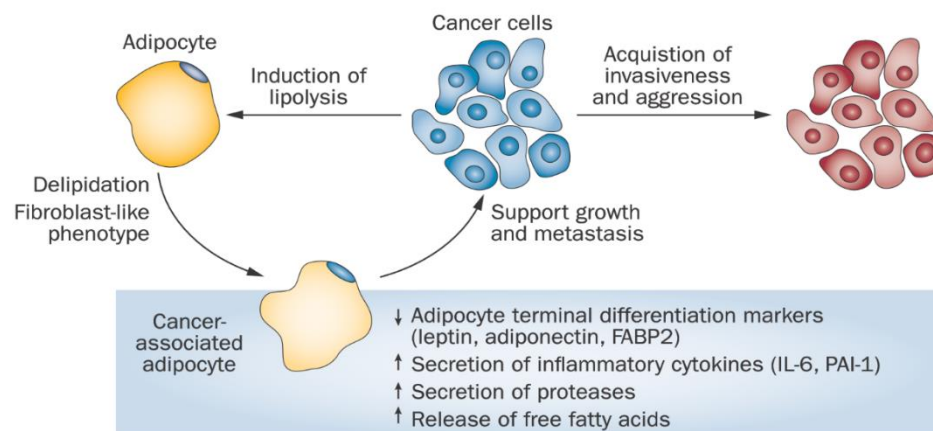


Figure 1.2 Cancer associated adipocytes. Crosstalk between cancer-associated adipocytes and cancer cells within the tumour microenvironment is crucial for creation of a niche that is permissive for cancer cell growth and metastasis. Cancer cells stimulate lipolysis in adipocytes, which leads to delipidation and acquisition of a fibroblast-like phenotype in adipocytes. These alterations in cancer-associated adipocytes are associated with functional changes in the cells, such as loss of adipogenic markers, increased secretion of inflammatory cytokines and proteases, and increased release of free fatty acids, all of which support aggressive tumor growth and invasiveness. (Park J, *et al.* Nat Rev Endocrinol. 2014 Aug; 10(8): 455–465. doi: 10.1038/nrendo.2014.94)

1.2.5 CAAs contribute to alter cancer cells metabolism

Tumor cells can actively direct the metabolism of tumor stromal cells, by transferring high-energy metabolites such as lactate, ketones, glutamine and fatty acids to cancer cells (Park et al., 2014). The adipocyte-rich tissue surrounding tumor cells provides an easily accessible reservoir of lipids (Park et al., 2014). The phenotypic transition of CAAs is likely to reflect the high energy requirements of cancer cells (Park et al., 2014). Indeed, melanoma cells differentially express genes regulating lipid metabolism during melanoma progression (Kwan et al., 2014; Sumantran et al., 2015). Like fatty acid-binding protein 4 (FABP4) in ovarian cancers and prostate cancers, FABP7 is involved in lipid metabolism and is associated with proliferation and invasion of melanoma cells (Slipicevic et al., 2008). Recent studies showed that acquisition of a lipogenic phenotype in melanoma promotes tumorigenesis and progression (Kwan et al., 2014; Sumantran et al., 2015). Indeed, CAAs provide fatty acids to melanoma cells and stimulate melanoma growth via thymoma viral proto-oncogene 1 (Akt) signalling pathway (Kwan et al.,

2014). In addition, fatty acid synthase (FASN) expression is a reliable prognostic marker for human melanomas (Innocenzi et al., 2003; Malvi et al., 2015).

Glucose transport proteins (Glut), including Glut1-4 (Huang and Czech, 2007), participate the process of glycolysis in melanoma cells (Bedogni and Powell, 2009; Ito and Suda, 2014; Kwan et al., 2014; Wang et al., 2016). Enhanced glycolysis, which is highly related to hypoxia and the transcription factor HIF-1 α (Bedogni and Powell, 2009; Hall et al., 2013; Hersey et al., 2009; Ito and Suda, 2014; Robey et al., 2005), is another distinctive feature of melanoma. In obese states, adipocyte-rich tissues such as the skin are hypoxic, which provide a permissive microenvironment for melanocyte transformation and melanoma development (Robey et al., 2005). Thus, cellular interactions between the stroma and melanocyte cells may provide key signals for melanocytes to exit from a quiescent state, and progression (Bedogni and Powell, 2009).

1.3 The development and progression of bone metastasis

1.3.1 Osteolytic bone metastasis and skeletal-related events

Melanoma cell metastasis is the primary cause of deaths of melanoma patient (Tas, 2012), which can occur in multiple sites, including the lung, liver, brain, bone, and lymph nodes (Braeuer et al., 2014). Indeed, bone is a preferred metastatic site of most advanced malignancies including malignant melanoma (Ell and Kang, 2012; Jain et al., 2007; Peinado et al., 2012; Shiozawa et al., 2015). Bone metastases are referred to non-bone tissue derived tumor cells entering and growing in the bones. Bone metastases derived from melanoma are very common in autopsy series (23-49%) but also frequently observed in clinical series (5%-17%) (Costache et al., 2014). Furthermore, elderly patients (60–79 years old) are more prone to occur bone metastasis, with incidence 3 to 4 times higher than middle-aged patients (40-59 years old) (Aebi, 2003). In fact, the skeletal complications in metastatic melanoma are associated with a poor prognosis of patients. After diagnosis of bone metastasis, the patient's life expectancy is rather short with a median survival up to 2-6 months (Costache et al., 2014; Tas, 2012).

Since more than 90% of melanoma patients with bone metastasis are osteolytic metastasis (Brountzos et al., 2001; des Grottes et al., 2001; Hiraga et al., 1995; Lau et al., 2006; Takita et al., 2007), these patients are at high risks of developing skeletal-related events (SREs), which are currently defined as pathologic bone fractures or a need for surgery, palliative radiation therapy for bone pain, spinal cord compression, or hypercalcaemia of malignancy (Brountzos et al., 2001; Cetin et al., 2014; Poon et al., 2013). Importantly, SREs can greatly reduce the quality of life, and are associated with increased mortality and cost (Cetin et al., 2014).

1.3.2 Current therapies and challenges for metastatic melanoma and osteolytic metastasis

The treatment for melanoma usually depends on the size and stage of cancer. An early-stage melanoma just needs a simple surgery to remove the melanoma and possibly requires no further treatment. However, if melanoma has spread beyond the skin, extensive treatments, including surgery, radiation therapy, chemotherapy, and biological therapy, are necessary. Currently, the biological therapy, which includes targeted therapy and immunotherapy, provides significant clinical benefits for patients with metastatic or unresectable melanoma (Hugo et al., 2016; Tomei et al., 2014). The targeted therapies are able to target the cancer cells, which have a certain genetic mutation (Boespflug and Thomas, 2016), such as B-Raf proto-oncogene, serine/threonine kinase (BRAF) and mitogen-activated protein kinase kinase (MEK) inhibitors. In addition, the novel immunotherapy, such as anti-cytotoxic T-lymphocyte-associated protein 4 (CTLA4) or anti-programmed cell death protein 1 (PD1) therapies, seems to be extremely promising in patients with advanced melanoma due to counteract immune checkpoints (Tomei et al., 2014; Wolchok et al., 2013). Although improved overall survival in patients with metastatic melanoma due to better therapies is observed (Hodi et al., 2010; Wolchok et al., 2013), the patients with bone metastasis still has a poor clinical outcome (Bostel et al., 2015; Buijs et al., 2010). To improve the prognosis of melanoma patients with osteolytic metastasis, interventions could be required to

target both the disseminating osteotropic cancers (the seed) and the metastatic soil (or niche) (Buijs et al., 2010).

Currently, targeting the osteolytic components is the main therapeutic strategy for bone metastasis. Inhibition of osteoclast activity (by bisphosphonates) or receptor activator of nuclear factor kappa-B ligand (RANKL) (by denosumab) can effectively reduce the incidence of SREs over time, especially in pathological fractures and the need for surgery (Poon et al., 2013), and improve the quality of life of patients with osteolytic metastases (Ortiz and Lin, 2012). However, less efficacy was observed in improving the osteoblastic bone disease found in prostate cancer (Ortiz and Lin, 2012). In addition, whether their use can effectively prevent recurrences in early-stage disease is not as well established (Ortiz and Lin, 2012).

1.3.3 Bone metastasis: the “seed and soil” theory

The “seeds and soil” hypothesis, firstly proposed by Steven Paget in 1889, was later recognized as a theoretical basis in the field of tumor metastasis (Cox et al., 2015; Hoshino et al., 2015; Liu and Cao, 2016; Paget, 1989; Psaila and Lyden, 2009; Ramakrishna and Rostomily, 2013; Ren et al., 2015). For bone metastasis, a small number of cancer cells in the heterogeneous primary tumor acquires a set of genes mutation or amplification (Kang et al., 2003), and become the osteotropism cancer cells, which can be called as the “seeds”. However how key genes govern the transformation of cancer cell into the seeds remains need to be fully elucidated. Several critical gene sets regulated by transforming growth factor (TGF)- β and/or hypoxia (Dunn et al., 2009; Ell and Kang, 2013; Kang et al., 2003), such as parathyroid hormone-like related protein (PTHrP) (Ell and Kang, 2012; Li et al., 2011) and its regulator v-maf avian musculoaponeurotic fibrosarcoma oncogene homolog (MAF) (Pavlovic et al., 2015), a gene signature composed of IL-11/CXCR4/OPN/connective tissue growth factor (CTGF) (Kang et al., 2003), Lysyl oxidase (LOX) (Cox et al., 2015; Erler et al., 2009), Follistatin-like protein 1 (FSL1) (Kudo-Saito et al., 2013; Kudo-Saito et al., 2009), Vascular Cell Adhesion Molecule 1 (VCAM1) (Lu et al., 2011), Jagged1 (Sethi et al.,

2011), SRC proto-oncogene, non-receptor tyrosine kinase (Src) (Bakewell et al., 2003; Liu et al., 2015; Zhang et al., 2009a) and microRNAs (Ell and Kang, 2014), have been identified as breakthrough for this area.

1.3.4 The bone marrow niche for disseminated melanoma cells

Consistent with Paget's notion, crosstalk between the "seeds" and the "soil" determines the formation of a secondary tumor in bone (Fidler, 2003). Although the seeds have lots of genetic changes, the bones, named as the "soil", also need to be extensively modified during bone metastasis. To achieve this, the osteotropism cancer cells secrete soluble factors and/or exosomes and modify the distant bone marrow microenvironment (designated as the soil or niche) (Fidler, 2003).

In physiology, the hypoxic bone marrow niche is crucial for sustaining a quiescent haematopoietic stem cells (HSCs) pool and supporting glycolytic metabolism (Reagan and Rosen, 2016). When challenged with stress, including metabolic stress and tumor, the quiescent HSCs pool can be activated, mobilize and export out of the bone marrow (Luo et al., 2015; Reagan and Rosen, 2016).

In the bone marrow metastatic niche, the metastasized cancer cells can hijack the HSCs niche and progress by acquiring helps from a variety of cellular components (Herroon et al., 2013; Templeton et al., 2015; Weilbaecher et al., 2011), including endothelial cells, osteoblasts, fat cells, nerve cells, immune cells, such as monocyte-derived macrophages, osteoclasts, T cells, Dendritic cells (DCs), neutrophils and platelets (Figure 1.3).

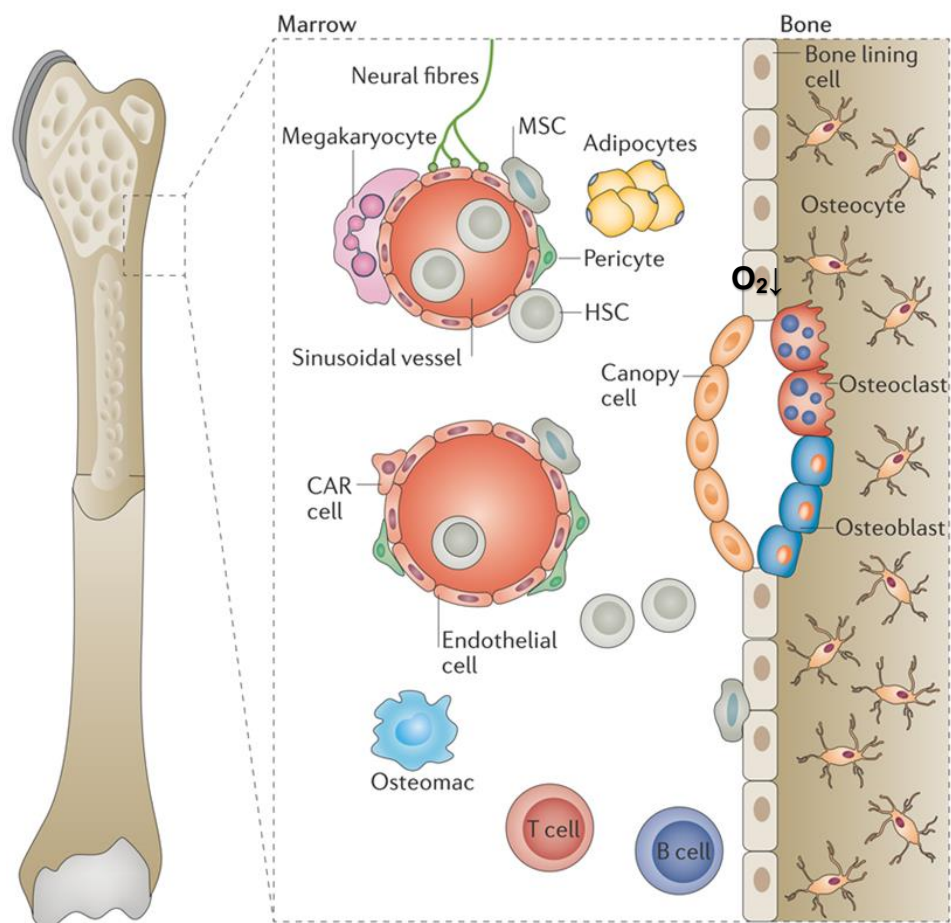


Figure 1.3 The two mini-organs of the bone marrow niche. The bone marrow niche is composed of multiple cells of mesenchymal and haematopoietic lineages. A hypoxic environment, endosteal bone cells and the proximity of sinusoids and microvessels provide a unique environment for haematopoietic stem cells (HSCs) and mesenchymal stromal cells (MSCs). The union of the skeletal remodelling system and the vascular network within the bone marrow provides a unique niche that regulates whole-body homeostasis. CAR cell, CXCL12-abundant reticular cell. (Adapted from Reagan, M. R., & Rosen, C. J.. *Nat Rev Rheumatol.* 2016 Mar;12(3):154-68. doi: 10.1038/nrrheum.2015.160.)

For examples, platelets guard circulating tumor cells from immune attack and support the tumor cells spread to the bone marrow (Gay and Felding-Habermann, 2011). In the early stage of bone colonization, osteoblasts provide an ideal niche for supporting the proliferation and progression of the disseminated cancer cells by heterotypic adherens junctions (hAJs) (Wang et al., 2015). Indeed, these osteoblasts are osteoprogenitors with maturation arrest, which highly expressing OPN, IL-6 and RANKL, directly activating the bone resorbing osteoclasts (Hanoun et al., 2014; Sethi et al., 2011; Wang et al., 2015). In osteolytic metastasis, activated osteoclasts dissolve the bone, and result in release of

bone stored growth factors, including TGF- β , fibroblast growth factors (FGFs), insulin like growth factors (IGFs) and BMPs as well as calcium and phosphorous(Chen et al., 2010). Since all of these factors favor disseminated cancer cell progression, the activated osteoclasts are regarded as a vicious cycle generator and the key targets for the treatment of patients with osteolytic metastases. Furthermore, angiogenesis promote tumor growth in bone indicating the involvement of endothelial cells in bone metastasis (Morgan and Lipton, 2010; Stacer et al., 2015). Therefore, targeting niche-cancer interactions is a promising therapeutic avenue (Reagan and Rosen, 2016).

1.4 The molecular mechanism for bone metastasis

1.4.1 The molecular mechanism for bone metastasis development and progression

The development of bone metastasis is a complex multistep process. For any metastasis, the first essential step is how cancer cells escape the primary tumor and enter into circulation (Chambers et al., 2002; Patel et al., 2011). In the early stages of bone metastasis, osteotropism cancer cells must lose their cell polarity and adhesion molecules, and gain migratory and invasive properties. This whole process is usually called epithelial-mesenchymal transition (EMT) (Kudo-Saito et al., 2009; Zheng and Kang, 2015). The transcription factors related to EMT for bone metastasis have also been identified, such as Snail Family Zinc Finger 1 (Snail)(Kudo-Saito et al., 2009), Twist Basic Helix-Loop-Helix Transcription Factor 1 (Twist1)(Chang et al., 2015; Croset et al., 2014), Zinc finger E-box binding homeobox 1 (Zeb1)(Liu et al., 2012; Mock et al., 2015), and Fos-related antigen 1 (Fra1)(Desmet et al., 2013). Next, these osteotropism cancer cells have to escape through the basement membrane and intravasation into the blood or lymphatic vessel. Genes related to this process include increased expression of matrix metalloproteinase (MMPs) and urokinase-type plasminogen activators (uPAs), while lower expression of tissue inhibitors of metalloproteinase (TIMPs) (Ell and Kang, 2012; Lu et al., 2009).

To gain insights into the mechanisms of bone marrow metastasis *in vivo*, certain transgenic or syngeneic mouse models are used to delineate early stages of metastasis; however, little of them develop bone metastasis lesions despite long period of observations (Fantozzi and Christofori, 2006). To the next choice, models with implantation of tumor cells into the primary site are used to recapitulate the homing step in the study of bone metastasis (Francia et al., 2011; Sakamoto et al., 2015; Yang et al., 1999), such as injection of 4T1 murine breast cancer cells into the 4th mammary gland (Monteiro et al., 2013).

The later stages of bone marrow metastasis include tumor cells circulating in the bloodstream, rolling and arrest at a distant bone marrow capillary, extravasation across the endothelial lining, and colonization of the bone marrow niche (Reagan and Rosen, 2016). Up to now, scientists found that the cancer cells target the hypoxic bone marrow HSC niche and compete with HSCs for this niche (Shiozawa et al., 2011). Then, they reprogramme the bone marrow and finally establish their footholds in a bone tumor niche (Hanoun et al., 2014; Price and Sipkins, 2014; Reagan and Rosen, 2016), in favor for tumor cell growth, dormancy, recurrence and/or resistance (Wang et al., 2015; Zheng and Kang, 2015) (Figure 1.4). The commonly used mouse models such as intracardiac (i.c.) injection and direct orthotopic injections (intrafemoral or intratibial (i.t.) injection) (Reagan and Rosen, 2016; Shiozawa et al., 2011; Weilbaecher et al., 2011), ideally reflect the later stage of bone marrow metastasis (Reagan and Rosen, 2016).

CXCL10/CXCR3 axis and chemokine (C-C motif) ligand 2 (CCL2)/chemokine (C-C motif) receptor (CCR2) axis, play a pivotal role in cancer cells targeting and growing in the bone marrow niche (Lee et al., 2012; Mizutani et al., 2009; Wang et al., 2006). Also, interaction between integrins ($\alpha 5\beta 1/3$, $\alpha 2\beta 1$ and $\alpha 4\beta 1$) and adhesion molecules, such as intercellular cell adhesion molecule-1 (ICAM1), VCAM1, E-cadherin, fibronectin and vitronectin, and the small integrin-binding ligand N-linked glycoproteins (SIBLINGs) family, such as OPN and bone sialoprotein (BSP), contribute to malignant cell proliferation, detachment, invasion, metastasis and recurrence of several osteotropic cancers in the bone marrow (Gay and Felding-Habermann, 2011; Kruger et al., 2014; Lu et al., 2011; Wu et al., 2007). In addition, the inflammatory cytokines, such as IL-1, IL-6, IL-8, IL-17, TNF- α , RANKL, M-CSF, prostaglandin E2 (PGE2), and macrophage inflammatory protein (MIP)-1 α , are involved in activating monocyte derived osteoclastogenesis and also promote tumor cell growth in the bone niche (Ara and Declerck, 2010; Kwan Tat et al., 2004). In the meanwhile, MMPs and cathepsin K are related to osteoclasts resorption of the bone matrix and release bone-stored growth factors, such as TGF β , IGF1, BMPs, FGFs, platelet-derived growth factors (PDGFs) and collagens, known to be critical for cancer cells growth in the bone marrow niche (Ren et al., 2015). Furthermore, a CXCL1/2-S100A8/9 loop causes cancer cells chemoresistance (Acharyya et al., 2012; Hiraga et al., 2012). Moreover, angiogenesis associated molecules, such as vascular endothelial growth factor (VEGF), heparanase, TGF- β , IGF1, PDGF, IL-8 and IL-6, are increased in the process of bone metastasis (Pluijm et al., 2000; Roberts et al., 2013). Noticeably, most of these molecules have overlapping functions at multiple stages of bone metastasis (Reagan and Rosen, 2016).

1.4.2 Role of osteoclasts and macrophages in the tumor-bone niche

At present, bone metastasis can be generally divided into two types, i.e. osteolytic and osteoblastic metastasis (Ell and Kang, 2012; Ortiz and Lin, 2012). The osteolytic metastasis, such as in breast cancer (Ell and Kang, 2012; Roodman, 2004), lung cancer (Ell and Kang, 2012), and melanoma (Costache et al., 2014; Hiraga et al., 1995;

O'Connell et al., 1989), are characterized by destruction of normal bone, while the osteoblastic metastasis, such as in prostate cancer (Ell and Kang, 2012; Roodman, 2004), with the deposition of new bone based upon the predominant radiologic appearance (Ell and Kang, 2012). This distinction is not absolute. In fact, mainly the osteolytic metastasis develop mortality can be observed in melanoma patients with bone metastasis (Broutzos et al., 2001; Ell and Kang, 2012; Steiner and MacDonald, 1972). Bone resorption is one of the key features of osteolytic metastasis. The osteoclasts, a specialized bone-resorbing cell type, were recognized as major players in bone marrow tumor niche during osteolytic metastasis (Lau et al., 2006; Perez et al., 2001). By releasing bone-deposited matrix, osteoclasts activated by tumor cells direct the self-perpetuating vicious cycle for disseminating tumor cells growth, dormancy, or recurrence in the bones (Akunuru et al., 2011; Cox et al., 2015; Ell and Kang, 2012; Furugaki et al., 2011; Roato, 2014; Roodman, 2004; Wang et al., 2006; Weilbaecher et al., 2011). In addition, myeloid derived monocyte cells (MDSCs), a mixed population of granulocytic Ly6C+Ly6G+ cells and monocytic Ly6C+Ly6G-, can differentiate into osteoclasts in the bone tumor niche (Lau et al., 2006; Sawant et al., 2013; Stiff et al., 2016; Zhuang et al., 2012). Other cells, such as eosinophils, basophils, neutrophils and mast cells, share also common progenitors with osteoclasts (Vasiliadou and Holen, 2013). In bone tumor microenvironment, melanoma cells can produce soluble factors or cell surface molecules that directly or indirectly stimulate osteoclastic bone resorption (Hiraga et al., 1995; Lau et al., 2006; Perez et al., 2001). These factors include IL-1, IL-6, IL-8, granulocyte macrophage colony-stimulating factor (GM-CSF), PGE2, CXCL1/2/10, CCL2, TGF- α/β , RANKL, ICAM1, VCAM1, PTHrP and colony stimulating factor 1 (CSF-1) (Hiraga et al., 1995; Hirbe et al., 2007; Inada et al., 2015; Jones et al., 2006; Lau et al., 2006; Lee et al., 2012; Takita et al., 2007). Also, tumor associated stromal cells and/or extracellular matrices stimulate osteoclastogenesis, such as fibroblasts, osteoblasts, heparan sulfate proteoglycan (HSPG) and fibronectin (FN) (Hiraga et al., 1995; Inada et al., 2015; Lau et al., 2006; Perez et al., 2001; Takita et al.,

2007). Activation of transcription factors such as c-Fos, NF- κ B, and nuclear factor-activated T cells c1 (NFATc1) is sufficient to promote osteoclast differentiation (Kim and Kim, 2014; Takayanagi, 2007), leading expression of tartrate-resistant acid phosphatase (TRAP), cathepsin K, and MMP-9 in osteoclasts (Takayanagi et al., 2002). Indeed, all of them are known to play key functions in resorbing the bone matrix (Sawant et al., 2013).

In melanoma, osteoclasts can be derived from tumor associated macrophages (TAMs), which *per se* play a significant role in the bone tumor niche, in the presence of macrophage colony stimulating factor 1 (M-CSF) and RANKL (Lau et al., 2006). Macrophages can be generally categorized into two types, i.e. classically activated macrophages (M1) promoted by ‘classical activators’, such as interferon γ and lipopolysaccharide (LPS) and alternatively activated macrophages (M2) induced by IL-4, IL-10 and or IL-13 (Roszer, 2015; Vasiliadou and Holen, 2013). In tumor microenvironment, the phenotype and the function of differentiated mature TAMs resembles the anti-inflammatory macrophages named as M2, rather than the M1 (Shiozawa et al., 2015; Vasiliadou and Holen, 2013). The main characteristics of TAMs are their poor capacity for antigen presentation and nitric oxide (NO) production, while they have a strong ability to express anti-inflammatory cytokines, such as IL-10, TGF- β 1, chitinase-like 3 (Ym-1), cysteine-rich secreted A12-alpha-like protein 1 (FIZZ1) and Arginase-1 (Raes et al., 2002; Shiozawa et al., 2015; Vasiliadou and Holen, 2013). Moreover, they are able to suppress the function of cytotoxic CD8⁺ T-cell (Shiozawa et al., 2015; Vasiliadou and Holen, 2013). In addition, TAMs are considered as one of the most important regulators of angiogenesis in tumors (Vasiliadou and Holen, 2013), due to their ability to produce VEGF, TGF- β and PDGF. By these, TAMs are able to promote tumor growth and facilitate the survival and metastatic spread of cancer cells (Shiozawa et al., 2015; Vasiliadou and Holen, 2013). Furthermore, tumor-derived molecules, such as IL-6, CXCL10, PDGF, VEGF, M-CSF and TGF β are chemotactic for macrophages, stimulate their differentiation and maintain their survival (Shiozawa

et al., 2015; Vasiliadou and Holen, 2013). However, more researches are necessary to fully reveal the roles of TAMs in bone metastasis (Vasiliadou and Holen, 2013).

1.4.3 The contribution of inflammatory cytokines in the bone tumor niche: IL-6 and OPN

As mentioned above, inflammatory cytokines produced by either tumor cells or stromal cells, are crucial for recruitment and activation of osteoclasts and/or macrophages in the bone tumor niche (Kim et al., 2011b).

IL-6 is one of the most important cytokines in bone metastasis, based on its multiple effects on bone metabolism, tumor cell proliferation and survival, angiogenesis, and inflammation (Ara and Declerck, 2010; Hoejberg et al., 2012; Yang et al., 2010). These effects are mediated by the signaling pathways Janus kinase/signal transducer and transcription activator (JAK/STAT-3), and amplified in the presence of soluble IL-6 receptor (sIL-6R) (Hiraga et al., 1995; Hoejberg et al., 2012; Yang et al., 2010). Indeed, human melanoma tissues express high amount of the IL-6 receptors. Melanoma patients with bone metastasis showed remarkable elevation in IL-6 level, which is also associated with a poor clinical outcome, supporting the role of IL-6 in melanoma bone metastasis (Ara and Declerck, 2010; Mouawad et al., 1996).

Similarity, OPN is another important cytokine in bone metastasis. OPN originally isolated from bone by Heingard *et al.* in 1985, also known as BSP-1, or secreted phosphoprotein 1 (SPP1) or early T-lymphocyte activation-1 (Eta-1) (Franzen and Heinegard, 1985; Kahles et al., 2014; Lund et al., 2009). OPN is both a matricellular protein and a soluble cytokine, which can bind to the cell surface via integrins or CD44. Consequently, OPN activates several pathways, including phosphoinositide 3-kinase (PI3K), extracellular signal-regulated kinase (ERK), and c-Jun NH₂-terminal kinase (JNK), and NF- κ B (Franzen and Heinegard, 1985; Kahles et al., 2014; Lund et al., 2009). OPN is involved in normal physiological processes and enhanced the cell to facilitating cell adhesion, migration, extracellular matrix invasion and cell proliferation, as well as escaping complement-mediated cell lysis (Franzen and Heinegard, 1985; Kahles et al.,

2014; Lund et al., 2009). OPN is implicated in the pathogenesis of a variety of disease states, including several chronic inflammatory diseases, obesity and bone metastasis (Franzen and Heinegard, 1985; Kahles et al., 2014; Lund et al., 2009). Indeed, host OPN deficiency exhibits decreased markers of inflammation, melanoma growth, angiogenesis and bone metastasis (Carlinfante et al., 2003; Hayashi et al., 2007; Kumar et al., 2013; Nemoto et al., 2001; Nomiya et al., 2007; Ohyama et al., 2004). It was also known that OPN expressed in the cytoplasm of osteoclasts could be an important determinant for the osteolytic metastasis process (Carlinfante et al., 2003; Ibrahim et al., 2000; Nemoto et al., 2001; Ohyama et al., 2004).

Interestingly, both IL-6 and OPN levels are increased in individuals with obesity or cancers, and are linked to macrophages and osteoclasts activities. Signaling by IL-6 can also promote M2 macrophages in obesity (Mauer et al., 2014) and act as pro-inflammatory in other circumstance such as chronic inflammatory disorders like Crohn's disease and rheumatoid arthritis (Scheller et al., 2011). OPN can skew macrophages toward M2 or TAMs, by a feedback loop action during cancer progression (Kale et al., 2014; Lin et al., 2015; Rao et al., 2013). However, despite a close connection between IL-6 and OPN (Wen et al., 2015), their link in obesity and cancer bone metastasis might be worth to explore.

1.4.4 Role of bone marrow adipocytes in the tumor-bone niche

Adipocytes, are not only present in subcutaneous fat tissue, but are also found in large quantities in the bone marrow. Indeed, bone marrow adipocyte content increases with obesity (Luo et al., 2015), as well as with age (Justesen et al., 2001; Krings et al., 2012). In the bone marrow, mesenchymal stem cells differentiate into the bone forming osteoblasts or into adipocytes (Luo et al., 2015). Balance between bone marrow osteoblasts and adipocytes assure the maintenance of the bone mass and the integrity of the bone marrow space (Luo et al., 2015). Bone marrow adipocytes have both white and brown adipose tissue characteristics (Krings et al., 2012), and have the capability to

enhance osteoclasts differentiation and activity (Goto et al., 2011; Hozumi et al., 2009; Muruganandan and Sinal, 2014).

In one hand, inflammatory cytokines can affect adipocytes function. For example, in obese adipose tissue, macrophages are the primary cells expressing OPN, which can induce inflammatory signaling in both adipocytes and macrophages (Zeyda et al., 2011). OPN can also be a chemotactic cytokine for PDGFR α ⁺ progenitors, which proliferate and differentiate into adipocytes at sites of dead adipocyte clearance (Lee et al., 2013). On another hand, adipocytes can secrete pro-inflammatory cytokines and adipokines, such as MCP-1, TNF- α , IL-6, IL-8, MMP-11, TGF- β , plasminogen activator inhibitor-1 (PAI-1) and collagen VI (Andarawewa et al., 2005; Dirat et al., 2011; Nieman et al., 2011; Nieman et al., 2013; Park and Scherer, 2012), in the tumor microenvironment. The effects of bone marrow adipocytes on bone metastasis is a new frontier in bone metastasis (Reagan and Rosen, 2016), which just start to be investigated.

During obesity, the HSC niche is largely disturbed by the increased presence of adipocytes in the bone marrow (Luo et al., 2015). As bone marrow adipocytes are perturbing HSC maintenance and myeloid cell differentiation (Luo et al., 2015; Naveiras et al., 2009), they may exert an important role in building tumor cell niches, or promoting tumors within the bone marrow (Reagan and Rosen, 2016). In support of this concept, one previous study mentioned that bone marrow adipocytes modulate the FABP4-IL-1 β pathway in prostate cancer cells, when homing into bone (Herroon et al., 2013). Recently, an interesting research showed that the marrow adipose tissue might provide a niche for extensive breast cancer cell colonization of the bone marrow, via expression of Leptin and IL-1 β (Templeton et al., 2015). Moreover, adipocytes seem to promote cancer stem cell self-renewal via cathepsin B (CTSB) (Tang et al., 2016; Wolfson et al., 2015). However, it is still unknown whether obesity-induced bone marrow changes affect the homing and survival of melanoma cells into the bone niches.

1.5 Aim of the thesis

1.5.1 Aim of the thesis

Dietary fat increases melanoma growth, metastasis, and mortality (Kushiro et al., 2012; Kushiro and Nunez, 2011; Kwan et al., 2014; Malvi et al., 2015; Sergentanis et al., 2013; Shors et al., 2001). Bone metastasis is a devastating complication for melanoma patients, which is not curable. To decipher the crosstalk among metabolic stress by obesity, bone marrow niche and melanoma cells might be of potential interest. Because it might provide insight into the disease, and possibly new targets to develop innovative therapeutic strategies for improving prognosis of obese patients with melanoma and/or bone metastasis. It might also improve our understanding of the relationship between obesity or metabolic disorders and cancer risk and/or poor patient outcome (Tan et al., 2011).

The aim of this thesis was to determine the role of obesity induced fat bone marrow on the homing and survival of melanoma cells into the bone. To do this, we first established high fat diet (HFD) induced obese mouse model in C57BL/6N male mice, and then performed two classical bone metastasis mouse models (intratibial and intracardiac injection of B16F10 melanoma cells) in the overweight mice. We delineated the bone tumor niche changes and the serum cytokine profiles in these mice after challenge of metabolic stress by HFD and melanoma cells. In addition, we analyzed the effects of obesity-related systemic factors on melanoma cells and osteoclasts differentiation *in vitro*. Moreover, we performed bone marrow adipocyte/melanoma cell co-cultures to assess the changes in melanoma cells and adipocytes. Furthermore, we tested whether inhibition of inflammatory cytokines could counterbalance the induced melanoma burden *in vivo*. We made use of osteopontin-deficient (OPN^{-/-}) mice, and blockade of IL-6/JAK2 signaling pathway with neutralizing monoclonal antibody to IL-6 and small inhibitor AG490, respectively, where we applied and assessed in the intratibial mouse model.

1.5.2 Declaration

The present thesis is in part based on results, which are already published in a peer-review journal. *Chen, G.L., Luo, Y., Eriksson, D., Meng, X., Qian, C., Bauerle, T., Chen, X.X., Schett, G., and Bozec, A.. High fat diet increases melanoma cell growth in the bone marrow by inducing osteopontin and interleukin 6. Oncotarget. (2016). doi: 10.18632/oncotarget.8474.*

I declare that the thesis work is done by me independently under the supervision of my supervisors at the Department of Internal Medicine 3, Rheumatology and Immunology, University of Erlangen-Nuremberg.

2. Materials and Methods

2.1 Materials

2.1.1 Buffer and staining solutions

Tail Lysis Buffer	50ml	Tris-HCl (1M), pH 8.5
	5ml	EDTA (0.5M), pH 7.5-8.0
	10ml	SDS (10%)
	20ml	NaCl (5M)
	dH ₂ O (autoclave)	<i>ad</i> 500ml,
	Add, 10µl Proteinase K (20mg/ml)	per 100µl

Erythrocyte lysis buffer	4.012g	NH ₄ Cl
	0.5g	KHCO ₃
	50mM	EDTA
	dH ₂ O	<i>ad</i> 500ml

PBS(10×)	80g	NaCl
	2g	KCl
	14.4g	Na ₂ HPO ₄
	2.4g	KH ₂ PO ₄
	dH ₂ O <i>ad</i> 1000ml	adjust pH to 7.4

TBS(10×)	24.2g	Tris
	80g	NaCl
	dH ₂ O <i>ad</i> 1000ml	adjust pH to 7.6

PBS-T	1×	PBS
	0.05%	Tween-20

TBS-T	1× 0.05%	TBS Tween-20
Running buffer (10×)	30.3g 144.0g 10.0g dH ₂ O	Tris-base glycine SDS <i>ad</i> 1000ml
Transfer buffer (1×)	3.03g 14.4g 200ml dH ₂ O	Tris base glycine Methanol <i>ad</i> 800ml
SDS-PAGE gel (10%)	2ml 1.67ml 1.25ml 25μl 25μl 2.5μl	dH ₂ O 30% acrylamide/Bis 1.5M Tris (pH 8.8) 20% SDS 10% ammonium persulfate TEMED
FACS buffer	1× 1%	PBS BSA
IHC block buffer	5% 0.1%	Serum (from Dako kits) BSA in PBS
IHC staining solution	2%	FBS

	0.05%	Tween-20 in PBS
Citrate buffer	1.92g	Citrate Acid
	0.05%	Tween-20
	dH ₂ O	<i>ad</i> 1000ml
Fixation buffer	12.5ml	Citrate buffer
	4ml	37% Formaldehyde
	32.5ml	Acetone
ELISA coating Buffer	15mM	Na ₂ CO ₃
	35mM	NaHCO ₃
HRP-Substrate	20mM	Na ₂ HPO ₄
	7mM	Citric acid
	0.1%	O-Phenylendiamin
	0.1%	H ₂ O ₂ (30%)
Oil Red-O stock solution	0.5g	Oil Red-O powder
	100ml	Isopropanol
Oil Red-O working solution	3 parts	Oil Red-O stock solution
	2 parts	dH ₂ O
	mix well, and filter with 0.45 µm syringe filter	
TRAP staining solution	9ml	dH ₂ O
	100µl	Naphtol
	400µl	Acetate

200 μ l	Tartrate
100 μ l	Sodium Nitrate
100 μ l	Fast Garnet

2.1.2 Cell culture media and supplements

DMEM medium	500ml	DMEM
	10%	FBS
	1%	Penicillin/Streptomycin
α -MEM medium	500ml	α -MEM+GlutaMAX
	10%	FBS
	1%	Penicillin/Streptomycin
Osteoclast medium	500ml	α -MEM+GlutaMAX
	10%	FBS
	1%	Penicillin/Streptomycin
	20ng/ml	M-CSF
	5ng/ml	RANKL
Bone marrow-derived macrophages (BMM) medium	500ml	DMEM
	10%	FBS
	1%	Penicillin/Streptomycin
	10%	L929-conditioned medium
Adipogenic cocktail	5 μ g/ml	Insulin
	0.5mM	3-isobutyl-1-methylxanthine
	1 μ M	Dexamethasone

2 μ M

Rosiglitazone

2.1.3 Oligonucleotides

Primers were ordered from Invitrogen.

RT-PCR

<i>β-actin</i>	fw 5' TGT CCA CCT TCC AGC AGA TGT 3'
	rev 5' AGC TCA GTA ACA GTC CGC CTA GA 3'
<i>HPRT</i>	fw 5' GCT TGC TGG TGA AAA GGA CCT C 3'
	rev 5' CAA ATC AAA GTC TGG GGA CGC 3'
<i>Adiponectin</i>	fw 5' GCG ATA CAT ATA AGC GGC TTC T 3'
	rev 5' GCA GGC ATC CCA GGA CAT C 3'
<i>Akt1</i>	fw 5' GGA CTA CTT GCA CTC CGA GAA G 3'
	rev 5' CAT AGT GGC ACC GTC CTT GAT C 3'
<i>Ang-2</i>	fw 5' CTC TGT CTC AGG ATG ACT CCA G 3'
	rev 5' AGG TGT TGA CAT CTT TGC AGA AAG 3'
<i>aP-2</i>	fw 5' TGA AAT CAC CGC AGA CGA CAG G 3'
<i>(FABP-4)</i>	rev 5' GCT TGT CAC CAT CTC GTT TTC TC 3'
<i>Cathepsin K</i>	fw 5' AGG GCC AAC TCA AGA AGA AAA CT 3'
	rev 5' TGC CAT AGC CCA CCA CCA ACA CT 3'
<i>Cyclin D1</i>	fw 5' GCA GAA GGA GAT TGT GCC ATC C 3'
	rev 5' AGG AAG CGG TCC AGG TAG TTC A 3'
<i>CD11c</i>	fw 5' TGCCAGGATGACCTTAGTGTCG 3'
	rev 5' CAGAGTGACTGTGGTTCCGTAG 3'
<i>CD44</i>	fw 5' CGG AAC CAC AGC CTC CTT TCA A 3'
	rev 5' TGC CAT CCG TTC TGA AAC CAC G 3'
<i>CD74</i>	fw 5' GCT GGA TGA AGC AGT GGC TCT T 3'
	rev 5' GAT GTG GCT GAC TTC TTC CTG G 3'
<i>CD206</i>	fw 5' GTTCACCTGGAGTGATGGTTCTC 3'

	rev 5' AGGACATGCCAGGGTCACCTTT 3'
<i>CEBPα</i>	fw 5' AAG AGC CGC GAC AAG GC 3'
	rev 5' GTC AGC TCC AGC ACC TTG TG 3'
<i>CEBPβ</i>	fw 5' CAA CCT GGA GAC GCA GCA CAA G 3'
	rev 5' GCT TGA ACA AGT TCC GCA GGG T 3'
<i>c-Fos</i>	fw 5' CGG GTT TCA ACG CCG ACT AC 3'
	rev 5' CAG GTC TGG GCT GGT GGA GA 3'
<i>c-Myc</i>	fw 5' TCG CTG CTG TCC TCC GAG TCC 3'
	rev 5' GGT TTG CCT CTT CTC CAC AGA C 3'
<i>CTGF</i>	fw 5' CTG TCA AGT TTG AGC TTT CTG G 3'
	rev 5' GGA CTC AAA GAT GTC ATT GTC C 3'
<i>CXCL1</i>	fw 5' TCC AGA GCT TGA AGG TGT TGC C 3'
	rev 5' AAC CAA GGG AGC TTC AGG GTC A 3'
<i>CXCL2</i>	fw 5' CAT CCA GAG CTT GAG TGT GAC G 3'
	rev 5' GGC TTC AGG GTC AAG GCA AAC T 3'
<i>CXCL5</i>	fw 5' CCG CTG GCA TTT CTG TTG CTG T 3'
	rev 5' CAG GGA TCA CCT CCA AAT TAG CG 3'
<i>CXCL14</i>	fw 5' TAC CCA CAC TGC GAG GAG AAG A 3'
	rev 5' CGC TTC TCG TTC CAG GCA TTG T 3'
<i>CXCR2</i>	fw 5' CTC TAT TCT GCC AGA TGC TGT CC 3'
	rev 5' ACA AGG CTC AGC AGA GTC ACC A 3'
<i>CXCR4</i>	fw 5' GTG TAA GGC TGT CCA TAT CAT C 3'
	rev 5' GAC AGC TTA GAG ATG ATG ATG C 3'
<i>CXCR7</i>	fw 5' GAC CGC TAT CTC TCC ATC ACC T 3'
	rev 5' GTT GGA AGC AGA TGT GAC CGT C 3'
<i>Fizz-1</i>	fw 5' GAACGCGCAATGCTCCTTTGAG 3'
	rev 5' AGCCACAAGCACATCCAGTGAC 3'
<i>Foxal</i>	fw 5' GCC TTA CTC CTA CAT CTC GCT C 3'

	rev 5' CTG CTG GTT CTG GCG GTA ATA G 3'
<i>ICAM1</i>	fw 5' AAA CCA GAC CCT GGA ACT GCA C 3'
	rev 5' GCC TGG CAT TTC AGA GTC TGC T 3'
<i>IGF1</i>	fw 5' GTG GAT GCT CTT CAG TTC GTG TG 3'
	rev 5' TCC AGT CTC CTC AGA TCA CAG C 3'
<i>IL-1β</i>	fw 5' TGG ACC TTC CAG GAT GAG GAC A 3'
	rev 5' GTT CAT CTC GGA GCC TGT AGT G 3'
<i>IL-6</i>	fw 5' TCC TTC CTA CCC CAA TTT CC 3'
	rev 5' GCC ACT CCT TCT GTG ACT CC 3'
<i>INOS</i>	fw 5' GAGACAGGGAAGTCTGAAGCAC 3'
	rev 5' CCAGCAGTAGTTGCTCCTCTTC 3'
<i>Jagged-1</i>	fw 5' AAC GAC CGT AAT CGC ATC GT 3'
	rev 5' TAT CAG GTT GAA TAG TGT CAT TAC TGG AA 3'
<i>Krt-18</i>	fw 5' AAT CAG GGA CGC TGA GAC CAC A 3'
	rev 5' GCT CCA TCT GTG CCT TGT ATC G 3'
<i>Leptin</i>	fw 5' ATC TGA AGC AAG CCA TCA GC 3'
	rev 5' CCA GTC ACC AGA GGT CAA GC 3'
<i>M-cadherin</i>	fw 5' AGG ACG AGC ATA GCT GAA GGA G 3'
	rev 5' GTC CAC TTG CAG CCA GTC TTC T 3'
<i>MCSF</i>	fw 5' GCC TCC TGT TCT ACA AGT GGA AG 3'
	rev 5' ACT GGC AGT TCC ACC TGT CTG T 3'
<i>MMP-9</i>	fw 5' GCT GAC TAC GAT AAG GAC GGC A 3'
	rev 5' TAG TGG TGC AGG CAG AGT AGG A 3'
<i>Mpa3K</i>	fw 5' GGC TTT CTG ACG GAG TAT GTG G 3'
	rev 5' GTT GGA GAG CAT CTC AGC CAG A 3'
<i>N-cadherin</i>	fw 5' TCG CTG CTT TCA TAC TGA ACT TT 3'
	rev 5' AGC GCA GTC TTA CCG AAG G 3'
<i>NFATc1</i>	fw 5' GGT GCC TTT TGC GAG CAG TAT C 3'

	rev 5' CGT ATG GAC CAG AAT GTG ACG G 3'
<i>Notch1</i>	fw 5' GCT GCC TCT TTG ATG GCT TCG A 3'
	rev 5' CAC ATT CGG CAC TGT TAC AGC C 3'
<i>Nrp-1</i>	fw 5' TAC CTC ACA TCT CCC GGT TAC C 3'
	rev 5' GAA GAT TTC ATA GCG GAT GG 3'
<i>Osteopontin</i>	fw 5' TCC TTA GAC TCA CCG CTC TT 3'
	rev 5' TCT CCT TGC GCC ACA GAA TG 3'
<i>PDGFa</i>	fw 5' CTG GCT CGA AGT CAG ATC CAC A 3'
	rev 5' GAC TTG TCT CCA AGG CAT CCT C 3'
<i>PI3K</i>	fw 5' CAA ACC ACC CAA GCC CAC TAC T 3'
	rev 5' CCA TCA GCA GTG TCT CGG AGT T 3'
<i>PIGF</i>	fw 5' AGT TTC ACA GGA GCG TGG CTT G 3'
	rev 5' GAT CCA GAG TGG CGA GAT AAC C 3'
<i>PPARγ2</i>	fw 5' CTG ATG CAC TGC CTA TGA GC 3'
	rev 5' GGG TCA GCT CTT GTG AAT GG 3'
<i>Pref-1</i>	fw 5' GAC ACT CGA AGC TCA CCT GG 3'
	rev 5' GGA AGG CTG GGA CGG GAA AT 3'
<i>Pten</i>	fw 5' TGA GTT CCC TCA GCC ATT GCC T 3'
	rev 5' GAG GTT TCC TCT GGT CCT GGT A 3'
<i>S100a8</i>	fw 5' CAA GGA AAT CAC CAT GCC CTC TA 3'
	rev 5' ACC ATC GCA AGG AAC TCC TCG A 3'
<i>Sema3a</i>	fw 5' GAC ATC TAT GGC AAA GCC TGT GC 3'
	rev 5' GTG AGT CAG TGG GTC TCC ATT C 3'
<i>TGF-β1</i>	fw 5' TGA TAC GCC TGA GTG GCT GTC T 3'
	rev 5' CAC AAG AGC AGT GAG CGC TGA A 3'
<i>TGF-β3</i>	fw 5' AAG CAG CGC TAC ATA GGT GGC A 3'
	rev 5' GGC TGA AAG GTG TGA CAT GGA C 3'
<i>VCAM1</i>	fw 5' GCT ATG AGG ATG GAA GAC TCT GG 3'

	rev 5' ACT TGT GCA GCC ACC TGA GAT C 3'
<i>VEGF-α</i>	fw 5' CTG CTG TAA CGA TGA AGC CCT G 3'
	rev 5' GCT GTA GGA AGC TCA TCT CTC C 3'
<i>VEGF-c</i>	fw 5' CCT GAA TCC TGG GAA ATG TGC C 3'
	rev 5' CGA TTC GCA CAC GGT CTT CTG T 3'
<i>VEGF-R2</i>	fw 5' CAT CAC CGA GAA CAA GAA CA 3'
	rev 5' CAT TGA TCT TTG CCT CAC AG 3'
<i>YM-1</i>	fw 5' TACTCACTTCCACAGGAGCAGG 3'
	rev 5' CTCCAGTGTAGCCATCCTTAGG 3'

2.1.4 Antibodies

Immunohistochemistry

Name	Company	Catology	Dilutions
Mouse anti-human HMB45	Pierce™, ThermoFisher, Inc.	Cat#MA1-34759	1:50
Rat anti-mouse IL-6	BioXCell, Inc.	Cat#BE0046	1:100
Goat anti-mouse OPN	R&D system, Inc.	Cat#AF808	1:100
Goat anti-Rat IgG H&L	Abcam	Cat# ab150157	1:1,000
Donkey anti-Mouse IgG H&L	Abcam	Cat#ab150103	1:1,000
DAPI solution	Vector Laboratories Inc.	Cat#H-1200	-

Western Blot

NF- κ B(p65)	Cell Technology, Inc.	signaling Cat#8242	1:500
phospho-NF- κ Bp65 (Ser468)	Cell Technology, Inc.	signaling Cat#3039	1:500
β -actin mouse mAb	Sigma-Aldrich, Inc.	Cat#A5316	1:5,000

FACS

Antigen	Antibody	Source, dilution
CD11b	FITC rat anti-mouse CD11b	BD Pharmingen, 1:200
CD11c	Alex Flour 488 anti-mouse CD11c	BD Pharmingen, 1:200
B220	Percp anti-mouse B220	BD Pharmingen, 1:100
SiglecF	PE rat anti-mouse SiglecF	BD Pharmingen, 1:200
CD31	PE-Cy7 anti-mouse CD31	eBiosciences, 1:100
Ly6C	APC rat anti-mouse Ly6C	BD Pharmingen, 1:100
Ly6G	PerCP-Cy5.5 rat anti-mouse Ly6G	Biologend, 1:200
Propidium Iodide		Sigma-aldrich

2.1.5 Molecular weight marker and loading dye

GeneLadder 100bp plus 1.5kb	Genaxxon	Cat#M3094
Loading Buffer DNA II	Applichem	Cat#A2571.0025

2.1.6 Reagents for cell culture

Cell culture

DMEM	Invitrogen™	Cat#10566
α-MEM	Invitrogen™	Cat#32561
Dulbecco's PBS (1×)	Gibco™	Cat#14190-144
Fetal Bovine Serum	Biochrom, Inc.	Cat#s0113
Fetal Bovine Serum (for Osteoclast)	Biochrom, Inc.	Cat#s0415
Penicillin/Streptomycin	Gibco™	Cat#15140
MCSF	PeptoTech, Inc.	Cat#315-02
RANKL	PeptoTech, Inc.	Cat#315-11
Insulin	Sigma	Cat#I2643
3-isobutyl-1-methylxanthine	Sigma	Cat#I7018
Dexamethasone	Sigma	Cat#D4902
Rosiglitazone	Sigma	Cat# R2408

Cell stimulation

Interleukin-6 Protein Sino Biological Inc. Cat#50136-MNAE-100

2.1.7 Dietaries and treatments for mice experimentsMice diet

Name	Company	Catolog number
Normal diet (ND)	Sniff	Cat#D59494
High fat diet (HFD)	Research Diets	Cat#D12330

Food content

Main Ingredient	ND	HFD
Protein	19.00%	23.0%
Fats and oil	3.30%	35.8% [Coconut oil (33.5%) + soybean oil (0.225%)]
Carbohydrates	4.9%	3.5%
kcal	3059.3/kg	5558.5/kg
Mineral Mix	3.07%	5.09%
Vitamine	0.93%	1%

In vivo injection

IL-6 monoclonal antibody	BioXCell, Inc.	Cat#BE0046
AG490	AdooQBioScience	Cat#A10047

2.1.8 Kits and enzymesRNA isolation

Water, nuclease-free	Fermentas	Cat#R0582
peqGold Trifast	PeQlab, Inc.	Cat#30-2020
peqGold RNAPure™ reagent	PeQlab, Inc.	Cat#30-1030
RNAlater® Solution	Ambion	Cat#AM7021
TRIzol® Reagent	Invitrogen	Cat#15596018

cDNA synthesis and RT-PCR

DNase I	Fermentas	Cat#EN0521
GeneAmp® 10×PCR Buffer II & MgCl ₂	Applied Biosystems	Cat#N8080130
GeneAmp® dNTPs	Applied Biosystems	Cat# N8080007
MuLV Reverse Transcriptase	Applied Biosystems	Cat#N8080018
Oligo d(T) ₁₆ (50 μM)	Applied Biosystems	Cat#N8080128
RNase Inhibitor	Applied Biosystems	Cat#N8080119
High-Capacity RNA-to-cDNA™ Kit	Applied Biosystems	Cat#4368813
SYBR Green I-dTTP	Eurogentec	Cat#RT-SN2X-03+WOUN

Immunohistology

StreptABComplex/HRP	Dako	Cat#K0377
Liquid DAB+Substrate	Dako	Cat#K3468

FlowCytomix™ Multiple Analyte Detection Kits

Mouse Th1/Th2 10plex	ebioscience	Cat#BMS820FF
----------------------	-------------	--------------

ELISA

IL-6	R&D system, Inc.	Cat#DY406
Osteopontin	R&D system, Inc.	Cat#DY441
Leptin	R&D system, Inc.	Cat#DY498
CXCL-1	R&D system, Inc.	Cat#DY453

Western Blot

2x Laemmli Sample Buffer	Bio-Rad Laboratories, Inc.	Cat#1610737
Bradford Protein Assay	Bio-Rad Laboratories, Inc.	Cat#5000205

ECL™ Prime	GE Healthcare	Cat#RPN2232
------------	---------------	-------------

Genotyping

AmpliTaq® DNA Polymerase	Applied Biosystems	Cat#N8080161
Taq DNA Polymerase	Peqlab	Cat#01-1030
dNTP Mix PCR	Roth	Cat#L541.2
Proteinase K	Invitrogen	Cat#25530031

2.1.9 Chemicals

Acrylamide stock (30%)	Bio-Rad Laboratories
Agarose	AppliChem
Ammonium peroxydisulphate	Roth
Bovine Serum Albumin	Sigma
DEPC	Roth
DMSO	Merck
EDTA	Roth
Eosin	Sigma
Ethanol pure	Roth
Ethanol denatured	Roth
Glycine	Roth
Glycerol	Roth
Hematoxylin Solution, Mayer's	Sigma
Hemalum Mayer	Merck
Hydrogen peroxide 30%	Merck
Isopropanol	Roth
KCl	Roth
KHCO ₃	Roth
KH ₂ PO ₄	Roth
Magnesium chloride hexahydrate	Roth

Magnesium sulphate heptahydrate	Roth
Methanol	Roth
β -Mercaptoethanol	Roth
Na ₂ HPO ₄	Roth
NaCl	Roth
NH ₄ Cl	Roth
Oil red O	Sigma
Roti-Histofix 4%	Roth
Rotiphorese 50× TAE Buffer	Roth
Sodium bicarbonate	Roth
Sodium hydroxide solution	Roth
Sodium dodecyl sulfate	Roth
TEMED	Life Technologies, Gibco®
Tween-20	Roth
Tris Base	Roth
Triton X-100	Sigma-Aldrich
Xylene	Roth
Vectashield Mounting Medium	Vector

2.1.10 Consumables

Cell strainer	BD Falcon	Cat#352350
Cell lifter	Corning	Cat#3008
Injection needles(27G ³ / ₄)	BD	Cat#03086999
Injection needles(29G)	Micro-Fine™, BD	Cat#320926
MicroAmp Optical 96-well Plate	Applied Biosystems	Cat#N8010560
MicroAmp Optical Adhesive Film	Applied Biosystems	Cat#4311971
Hyperfilm ECL	GE Healthcare	Cat#28906837
96 well ELISA Microplates	Greiner Bio-one	Cat#655001

Optical adhesive cover sheeting	Excel Scientific	Cat#100-seal-PLT
Cell Culture Insert	Merck Millipore	Cat#PICM01250
Filter Tip 10-1000 μ l, Flasks, Dishes, plates		Greiner Bio-one

2.1.11 Laboratory Instruments

Name	Company
Biological Safety Cabinet Nu-440-600E	Nuair
Centrifuge Heraeus Fresco 17	Thermo Electron Corporation
Centrifuge Rotina 420R	Hettich Zentrifugen
Color digital camera DP72	Olympus
Color digital camera DS-5Mc	Nikon
FACS Calibur	BD
Gallios TM flow cytometer	Beckman Counter
Homogenizer Precellys 24	PeqLab
Thermocycler	PeqLab
Incubator	Heraeus Instruments
Microscope Nikon Eclipse 80i	Nikon
Microtome SLIDE 2003	mpo pfm
Neubauer counting chamber	Laborcenter
pH meter HI 9321	HANNA Instruments
Photometer BioPhotometer	Eppendorf
Real-time PCR Cycler	Applied Biosystems
CFX96 Touch TM Real-Time PCR	Bio-Rad
Thermocycler GeneAmp [®] PCR system	Applied Biosystems
Thermocycler Mastercycler	Eppendorf
Thermomixer comfort	Eppendorf

2.1.12 Software

Beckman flow cytometry	Beckman Coulter, Inc.
------------------------	-----------------------

ImageJ	NIH, Bethesda, Maryland, USA
Microsoft Office	Microsoft®, Unterschleißheim
GraphPad Prism	GraphPad Software, Inc, USA
NIS-Elements BR2.2	Nikon Instruments Inc.

2.2 Methods

2.2.1 Animal experiments

Mice and treatment

Male C57BL/6N mice (6 week-old) were purchased from Jackson Labs and maintained at 25°C with 12-h light and dark cycles. Mice were fed with normal (ND; sniff, Cat#D59494) or high fat diet (HFD; Research Diets, Cat#D12330) ad libitum for 6 weeks. OPN deficient mice were purchased from Jackson Labs (B6.128S6(Cg)-Spp1^{tm1Blh}/J). All mice were housed in a temperature and humidity controlled facility with free access to water. All experiments were performed according to the rules and regulations of the animal facilities in the Franz Penzoldt Center (FPZ) at the University Erlangen-Nürnberg and University Hospital Erlangen in Germany and approved by the local ethics authorities.

Anti-IL-6 antibody and JAK2 inhibitor injection

For blocking IL-6, 0.5 mg of IL-6 monoclonal antibody (BioXCell, Inc. Cat#BE0046) was injected intraperitoneally (i.p.) every other day after the intratibial injection of B16F10 cells. For Janus kinase 2 (JAK2) inhibition, 17µg/kg of the JAK2 inhibitor AG490 (AdooQBioScience, Inc. Cat#A10047) was daily administrated i.p. after the injection of B16F10 cells into the tibia.

2.2.2 Bone metastasis mouse models

Intratibial and intracardiac injection of B16F10 cells were performed as previously described by Bakewell *et al.* (Bakewell et al., 2003). Briefly, mice were anaesthetized with isoflurane (Abbott; IsoFlo®, Cat#05260-05). For intratibial (i.t.) injection, 1×10^4 B16F10 melanoma cells suspended in 50µl PBS or only PBS (vehicle) were injected into the tibiae of anaesthetized mice within 30 minutes after the cells were trypsinized. The 27G $\frac{3}{4}$ needle (BD, Cat#03086999) was inserted into the mouse tibia for delivering the cells into the metaphysis. For intracardiac (i.c.) injection, 29G needles (BD Micro-Fine™, Cat#320926) were used to inject 1×10^5 B16F10 cells suspended in 100 µl PBS

into the left cardiac ventricle within 30 minutes after trypsinization of the cells. All mice were sacrificed at the indicated time point after B16F10 cells inoculation.

2.2.3 Cell culture

B16F10 cells culture and serum stimulations

Murine melanoma cell lines (B16F10) were obtained from the American Type Culture Collection (ATCC), and were maintained in alpha minimum essential medium (α -MEM, Invitrogen™, Cat#32561) containing 10% fetal bovine serum (FBS, Biochrom, Inc. Cat#s0113) with 1% penicillin and streptomycin (Gibco™, Cat# 15140) at 37°C (5% CO₂ , 95% air). B16F10-cells were starved in serum-free α -MEM medium containing 1% antibiotics and antimycotics for 24-48h. Then, 5×10^5 cells/well or 5×10^4 cells/well were plated on 6-well plates or 12-well plates, respectively, and stimulated with medium containing 2% serum from ND or HFD exposed mice.

In vitro osteoclast differentiation assay

For primary osteoclast assays, total bone marrow cells were isolated from C57BL/6 mice (6~8 weeks) by flushing femur and tibia. After filtered in 70 μ m cell strainer, cells were incubated at 37°C in 100mm dish in α -MEM medium supplemented with 5 ng/ml macrophage colony-stimulating factor (M-CSF) (PeproTech, Inc. Cat#315-02) overnight (5% CO₂ , 95% air). Non-adherent cells were collected, washed and further cultured in osteoclast medium in 24-well plate at the concentration of 1×10^6 cells/ml. In some experiments, 2% serum from ND or HFD mice was added. Medium was changed every 2-3 days. Osteoclast differentiation was evaluated around day 5-7 by tartrate-resistant acid phosphatase (TRAP) activity staining using the leukocyte acid phosphatase kit (Sigma-Aldrich, Inc. Cat#387A) according to the manufacturer's instructions. TRAP+ multi-nucleated ($n \geq 3$) cells were considered as osteoclasts.

In vitro bone marrow-derived macrophages differentiation assay

Bone marrow-derived macrophages (BMM) were prepared following the protocol described previously by Weischenfeldt J. and Porse B. (Weischenfeldt and Porse, 2008). Briefly, fresh primary bone marrow cells were collected following the same protocol to

osteoclast differentiation assays. The bone marrow cells with a concentration of 2×10^6 cells/mL were plated on 12-well plates in DMEM medium containing 10% L929-conditioned medium (BMM medium). BMM were incubated in BMM medium for 7 d, and were used for next experiments after an additional 24h incubation in DMEM medium.

Co-culture of adipocyte and melanoma

A purified population of bone marrow (BM) mesenchymal stem cells (MSCs) (BM-MSCs) were prepared following the method reported previously by Soleimani M, *et al.* (Soleimani and Nadri, 2009). BM-MSCs or the murine adipocyte cell line (14F1.1 cells) were provided by Prof. Dov Zipori of the Weizmann Institute of Science, Rehovot, Israel) were differentiated into BM adipocytes by the addition of the adipogenic cocktail (5 μ g/ml insulin, Sigma Cat#I2643; 0.5mM 3-isobutyl-1-methylxanthine, Sigma Cat#I7018; 1 μ M dexamethasone, Sigma Cat#D4902; and 2 μ M rosiglitazone, SigmaCat#R2408) for 2 days, and followed by maintaining within a DMEM medium supplemented with 5 μ g/ml insulin for additional 7-10 days. B16F10 cells were cultured on 24-well Transwell inserts with a 0.4 μ m pore size (Merck Millipore, Cat#PICM01250) within DMEM medium. After 48h of co-culture, BM adipocytes (lower chamber) and B16F10 cells (upper chamber) were separately harvested for Oil red O staining or gene expression profile analysis.

Co-culture of melanoma cells and osteoclasts

B16F10 cells were first cultured in α -MEM medium supplemented with a low concentration of FBS (0-2%) for 48h. The starved B16F10 cells were either treated with 2% heat-inactivated (56°C, 30 min) serum from ND or HFD mice. After removal of the serum from mice, the B16F10 cells were cultured in FBS-free α -MEM medium for additional 48h. In order to evaluate melanoma-secreted factors, supernatants were harvested after the 2 days starvation, and then were added during the process of osteoclasts differentiation, which was described above (refer to *In vitro* osteoclast differentiation assay).

For the study of melanoma cells surface alteration, the procedure for tumour cell/osteoclast co-culture was adapted from Yagiz and colleagues (Yagiz and Rittling, 2009). Briefly, 5×10^4 B16F10 cells were pre-incubated with 2% serum from ND or HFD mice at 37°C for 12h. The cells were then fixed with 2.5% glutaraldehyde for 1 min and immediately quenched with 1.5% glycine in PBS for 20 minutes. Fixed cells were washed and incubated overnight in complete DMEM medium before the co-culture with monocytes. The co-culture cells were cultured in osteoclast medium. Medium was replaced every 2-3 days. TRAP staining and TRAP⁺ cells quantification were performed as described above (refer to *In vitro* osteoclast differentiation assay).

2.2.4 Flow cytometric analyses

FACS analyses of bone tumor niche

To analyze infiltrated immune cells into the bone tumor niche, tibial bone marrow injected with B16F10 cells (i.t model) at day 7 were isolated from ND or HFD mice. The cells were washed, filtered through 70µm cell strainer, and followed by staining with antibody mixtures at 4°C. The following Antibodies were used: FITC-labeled anti-CD11b, CD11c, PE-labeled anti-SiglecF (both from BD Pharmingen), APC-labeled anti-F4/80, PerCP-Cy5.5-labeled anti-Ly6G, Ly6C, B220 (all from Biolegend). Cells were washed in 1ml FACS buffer twice, and then re-suspended in 200µl FACS buffer and analyzed by GalliosTM flow cytometer (Beckman Coulter, Inc.).

FACS analyses of serum cytokines

Serum levels of IL-1α, IL-2, IL-4, IL-5, IL-6, IL-10, IL-17, TNFα, IFN-γ and GM-CSF were detected by Mouse Th1/Th2 10plex Multiple Analyte Detection Kits (FlowCytomixTM, ebioscience, Cat#BMS820FF) according to the manufacturer's instructions. Briefly, 10µl microbeads mixture (vortex before pipetting) were added to 25µl serum, followed by 10µl biotin conjugate, vortex and incubate for 2h in the dark at room temperature (25°C). After wash with 1ml FACS buffer, add 10µl Streptavidin-PE dilution to each sample, vortex and incubate for 1h in the dark at room temperature.

Then wash again, re-suspend in 300 μ l FACS buffer and analyzed by GalliosTM flow cytometer.

FACS analyses of cell cycle

To analyze the cell cycle changes induced by HFD in melanomas, 2×10^5 B16F10 cells were coating on 6-well plates and starved overnight before incubation of serum from ND or HFD mice. The trypsinized and detached B16F10 cells were fixed with ethanol for 15min on ice. After centrifuged at 1500 rpm for 5 min, the cells were suspended in 500 μ l PI-solution in PBS (50 μ g/ml PI from 50x stock solution (2.5 mg/ml), 0.1 mg/ml RNase A, 0.05% Triton X-100), and incubated for 40 min at 37°C. After wash twice with 1ml FACS buffer, the cells were re-suspended in 200 μ l FACS buffer and analyzed by GalliosTM flow cytometer.

2.2.5 Methods for RNA levels quantification

RNA extraction

Frozen tissue was homogenized in Precelly tubes containing ceramic beads (1.4mm) and Trizol (Invitrogen) or Trifast (Peqlab) (6500rpm, 2 \times 20sec, break 30sec) with a Precellys 24 (Peqlab). RNA was isolated according to the manufacturer's instructions. RNA from cells in osteoclast cultures were isolated in 500 μ l Trizol reagent (Invitrogen) according to the manufacturer's instructions.

DNase I digestion and cDNA synthesis

One microgram RNA was digested with 1 μ l of DNase I in a total of 10 μ l for 30min at 37°C, followed by a 10min inactivation step at 65°C. For reverse transcription into cDNA, 4 μ l of the DNase I digested RNA was used (20°C for 10min, 42°C for 15min, 95°C for 5min):

Magnesium chloride (25mM)	4 μ l
10 \times PCR buffer	2 μ l
dNTPs (10 μ M)	8 μ l
Oligo d(T) primer (50 μ M)	1 μ l

RNase Inhibitor (20U/ μ l)	1 μ l
Reverse Transcriptase (50U/ μ l)	1 μ l
DNase I digested RNA	4 μ l

Quantitative PCRs (qPCRs)

Q-PCRs were performed using SYBR Green I-dTTP (Eurogentec). The following reaction mixture and program was used:

Reaction mixture:	SYBR Green I-dTTP	7.5 μ l
	RNase free water	5.5 μ l
	cDNA	1 μ l
	forward primer	0.5 μ l
	reverse primer	0.5 μ l

Program:	1 \times 50 $^{\circ}$ C for 2min
	1 \times 95 $^{\circ}$ C for 10min
	40 \times 95 $^{\circ}$ C for 2min, 60 $^{\circ}$ C for 1min
	1 \times 95 $^{\circ}$ C for 15min
	1 \times 60 $^{\circ}$ C for 1min
	1 \times 95 $^{\circ}$ C for 5min

Samples were analyzed in duplicate and normalized to the levels of β -actin or *HPRT*. The threshold cycle (C_T) values were exported from the CFX96 system (Bio-Rad). The fold changes in target genes were determined by using the $2^{-\Delta\Delta C_T}$ method (Livak and Schmittgen, 2001).

2.2.6 Methods to study protein levels

Western blot

B16F10 cells were pre-incubated with 2% serum from ND or HFD mice at 37 $^{\circ}$ C for 5 to 30 minutes, and then were handled with a denaturing and electrophoretic method named sodium dodecyl sulfate polyacrylamide gel electrophoresis (SDS-PAGE). The proteins were then transferred to 0.45 μ M nitrocellulose membrane (BD, Cat#1620115),

where they are stained with the following antibodies: nuclear factor kappa B (NF- κ B) p65 (Cell signaling Technology, Inc. Cat#8242; 1:500 dilutions), phospho-NF- κ B p65 (Ser468) (Cell signaling Technology, Inc. Cat#3039; 1:500 dilutions) and anti- β -actin mouse mAb (Sigma-Aldrich, Inc. Cat#A5316; 1:5,000 dilutions).

2.2.7 Histology

Immunohistochemistry

Mouse tibia paraffin sections were deparaffinized at 60°C for 1h, washed 3 \times 5min in xylene, re-hydrated in 100% (2 \times), 96% (2 \times), 80% and 70% ethanol for 2min and washed in dH₂O. Antigens were unmasked by citrate buffer (95°C for 10min), cooled for 20min, and rinsed in dH₂O. Endogenous peroxidase was blocked with hydrogen peroxide (3% in PBS, 10min) and washed in PBS (2 \times 5min). Slides were blocked with 5% serum (the host in which the secondary antibody was produced), and incubated with goat anti-mouse OPN (R&D system, Inc. Cat#AF808; 1:100 dilutions). Slides were washed and incubated with biotinylated secondary IgG and avidin-biotin complex (Vector laboratories) according to the manufacturer's instructions. Sections were stained with DAB substrate. After washing in dH₂O for 5min, slides were counterstained with Hemalum and washed in PBS for 5min, and then mounted in Roti-Histokitt II (Roth). Images were acquired using a Nikon Eclipse 80i microscope, equipped with Sony DXC-390P digital camera and NIS-Elements BR2.2 software.

For fluorescence immunostaining, slides were then treated with 0.2% Triton X-100 and blocked with 5% normal serum control after antigen retrieval with citrate buffer (10mM Citric Acid, 0.05% Tween 20, pH 6.0), and incubated with mouse anti-human HMB45 (Pierce™, ThermoFisher, Inc. Cat#MA1-34759; 1:50 dilutions), Ki-67 (Pierce™, ThermoFisher, Inc. Cat# PA5-19462; 1:50 dilutions), or rat anti-mouse IL-6 (BioXCell, Inc. Cat#BE0046; 1:100 dilutions). Slides were washed and incubated with pre-adsorbed goat anti-Rat IgG (Alexa Fluor® 488) and donkey anti-Mouse IgG (Alexa Fluor® 647) (All from abcam; 1:1,000 dilutions). Slides were counterstained and covered with DAPI solution (Vector Laboratories Inc. Cat#H-1200). Images were acquired as described above.

Bone histomorphometric analyses

Tibiae were fixed overnight in 4% formalin and then decalcified in 14% EDTA until bones became flexible. Long bones were embedded in paraffin and sliced at equivalent coronal sections through the centre of the bone with 1~2 μm thickness. Histological sections were stained with Hematoxylin and Eosin (H&E), and TRAP activity. Area of tumor, bone erosions, number of osteoclasts (N.Oc) per tibia, osteoclast surface per bone surface (Oc.S/BS), number of osteoclasts per bone perimeter (N.Oc/B.Pm) were assessed by Osteomeasure Analyses System (OsteoMetrics, Decatur, Georgia, USA) according to previously reported protocol (Diarra et al., 2007; Luo et al., 2015; Parfitt et al., 1987). Tumor area was assessed in H&E stained sections by OsteoMeasure according to a standard protocol (Li et al., 2010). Briefly, tissue sections were investigated at 4 \times magnifications using Zeiss Axioskop 2 microscope (Zeiss, Inc. Marburg, Germany) directly below the growth plate at the distal end of the tibia or at the bone tumor area.

2.2.8 Statistical analyses

All data are expressed as means \pm SEM. The statistical significance was determined by Student's *t* test, or Mann-Whitney U test, or One-Way ANOVA by using GraphPad Prism software Version 5.0 (Graphpad software, La Jolla, CA). Significance is shown as ns, not significant, or * $P < 0.05$; ** $P < 0.01$; *** $P < 0.001$; **** $P < 0.0001$.

3. Results

3.1 High fat diet (HFD) increases melanoma growth and bone-resorbing osteoclast numbers in the bone tumor niche

3.1.1 Increased melanoma growth in the bone niche of mice exposed to HFD

To determine whether obesity impacts melanoma growth in the bone, C57BL/6N male mice (6-week-old) were first fed with high fat diet (HFD, 60 kcal% fat) or normal diet (ND, 10 kcal% fat). The mice were overweight and body mass index were significantly increased 6 weeks after HFD exposure as was previously reported by our group (Luo et al., 2015). Next, ND and HFD-fed mice were injected with B16F10 melanoma cells into the tibial bone marrow (Figure 3.1A). In the intratibial (i.t.) tumor model, bone tumor volume was significantly higher in HFD tumor-bearing (HFD-T) compared to ND tumor-bearing (ND-T) mice already 6 days after melanoma cell injection (Figure 3.1B).

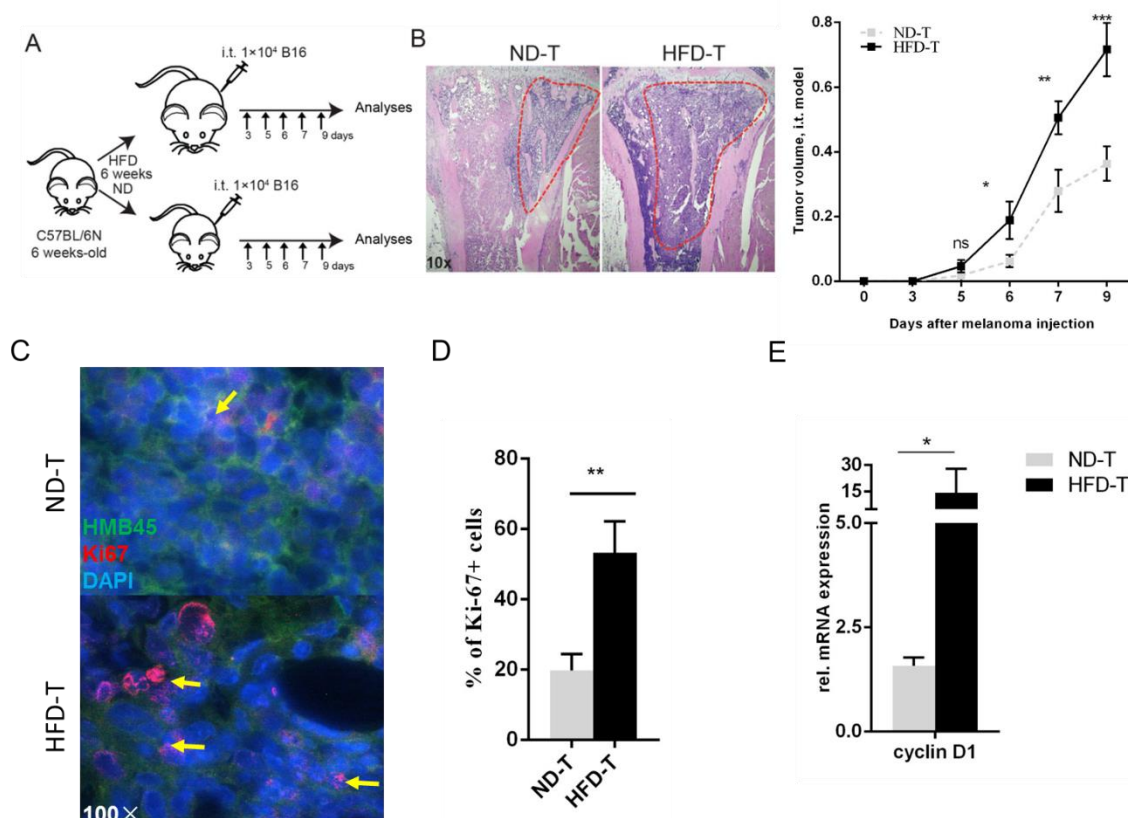


Figure 3.1 Mice induced by high fat diet have an increased bone tumor growth. (A) Experimental scheme: C57BL/6N mice fed for 6 weeks with normal diet (ND) or high fat diet (HFD) were injected intratibially (i.t.) with B16F10 cells (1×10^4) in PBS (50 μ l) or with vehicle (PBS, 50 μ l). Mice were

sacrificed at day 3, 5, 6, 7, and 9 post tumor inoculation. Normal diet (ND)- and high fat diet (HFD)-fed mice with injection of tumor cells were defined as ND-T and HFD-T, respectively. (B) Representative hematoxylin & eosin (H.E.) stained pictures of tibiae from ND and HFD mice at day 7 post i.t. injection of B16F10 cells (magnification $\times 10$). Tumor areas are shown by red dashed line. Quantification of the normalized tumor area at the indicated time point (n=6-8 per group). (C-D) Representative Ki67 staining (C) and Ki67 + cells quantification (D) in bone tumor area from ND and HFD mice at day 7 post i.t. B16F10 cell injection (magnification $\times 100$). Arrows in the color of yellow indicate Ki67 + cells. (E) *Cyclin D1* mRNA levels in bone from ND and HFD mice at 7 days post i.t. B16F10 cells injection (n=6-8 per group). Data are shown as means \pm SEM. Asterisks show statistically significant difference (ns, not significant; * $P < 0.05$; ** $P < 0.01$; *** $P < 0.001$).

When characterizing tumor cell proliferation, an increased number of Ki67 positive cells, consistent with increased *Cyclin D1* mRNA levels were found in tumor cells of HFD compared to ND mice (Figure 3.1C-E) (Chen et al., 2016).

3.1.2 Increased growth rate of disseminating melanoma cells in the bone metastatic niche of high fat diet fed mice

To confirm the observed increase of tumor growth in mice fed HFD, we also performed another well-established bone metastasis mouse model, i.e. the intracardiac (i.c.) injection of B16F10 cells into ND or HFD-exposed mice (Figure 3.2 A). In general, we observed that disseminated melanoma cells delivered through the left-ventricle form an overt bone tumor foci (defined as re-activation stage (Croucher et al., 2016) and indicated with dashed lines in Figure 3.2B) for around 4 days earlier in ND than HFD mice, i.e. at day 6 vs. day 10, respectively (Figure 3.2 B). Surprisingly, tumor growth rate at the re-activation stage in the bone metastatic niche were strikingly higher around 24-fold in HFD than ND mice (Figure 3.2 B), suggesting that HFD promotes melanoma cell growth in the bone metastatic niche when the disseminated melanoma cells are re-activated (Croucher et al., 2016).

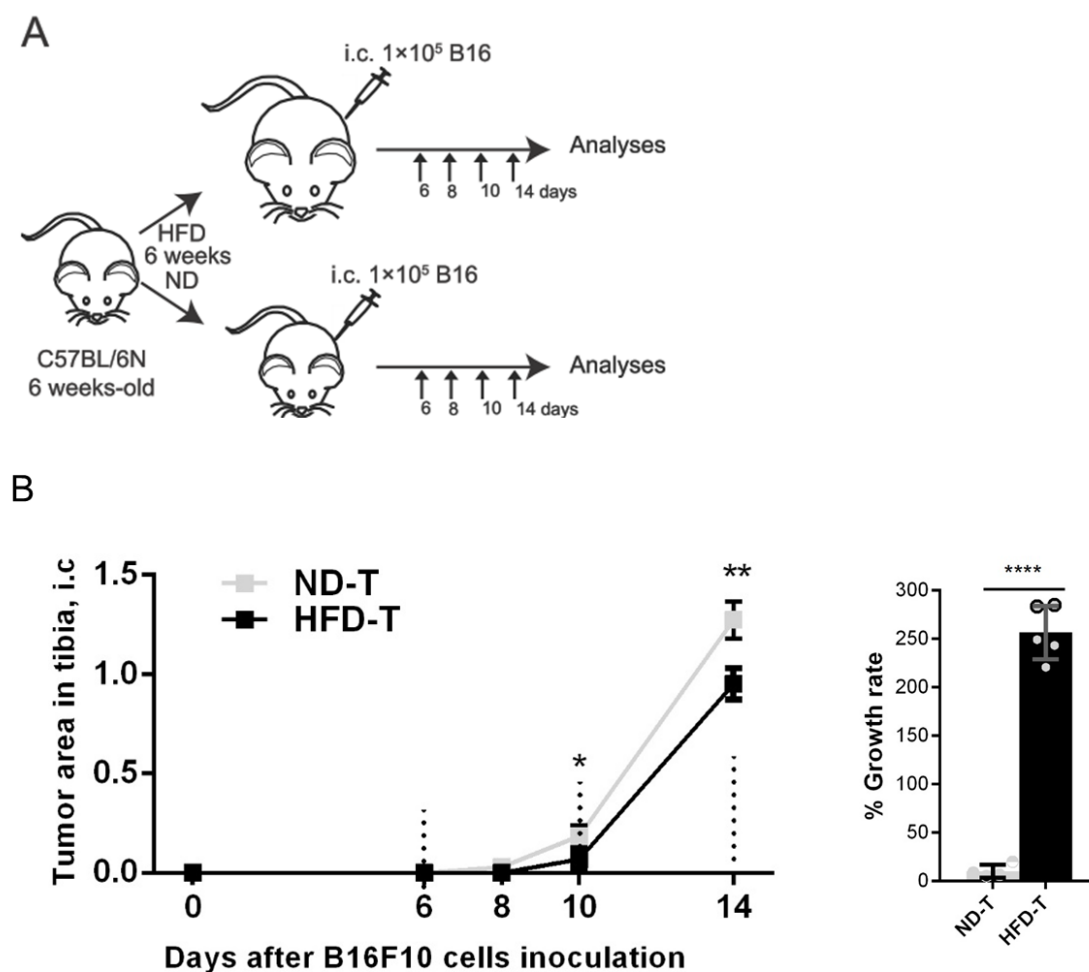
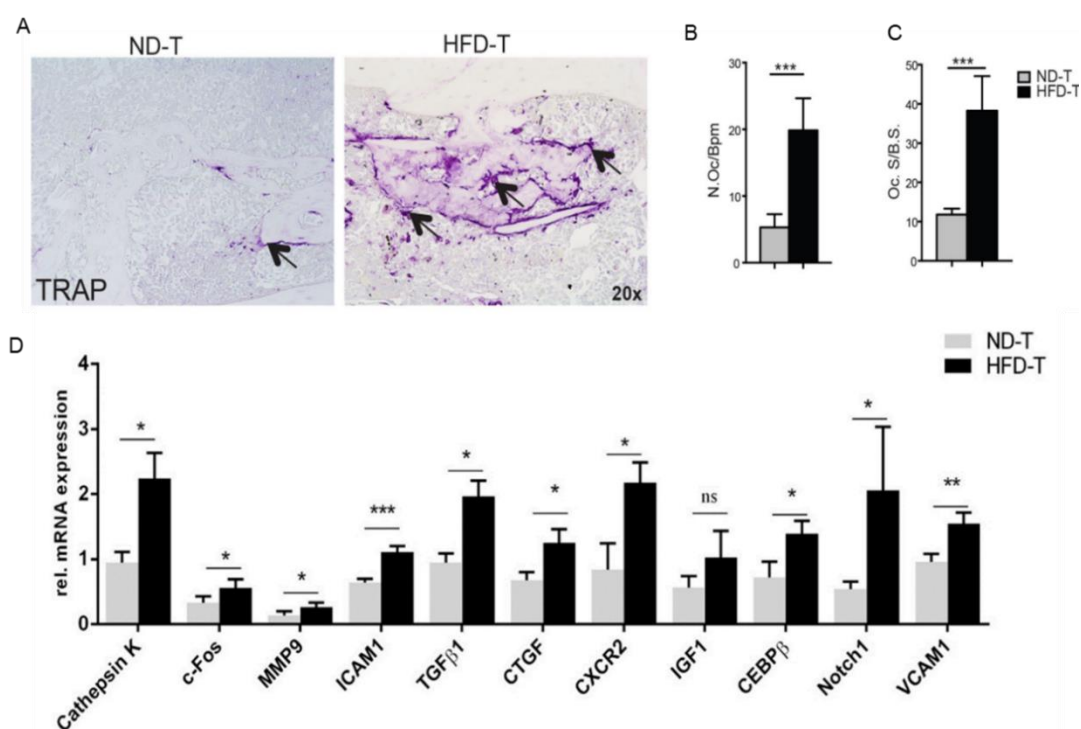


Figure 3.2 Analyses of melanoma cell growth in the intracardiac (i.c.) injection mouse model. (A) Overview of experimental designs: C57BL/6N mice fed for 6 weeks with normal diet (ND) or high fat diet (HFD) were injected intracardially with B16F10 cells (1×10^5) in PBS ($100 \mu\text{l}$). Mice were sacrificed at day 6, 8, 10, and 14 post tumor inoculation. Normal diet (ND)- and high fat diet (HFD)-fed mice with injection of tumor cells were defined as ND-T and HFD-T, respectively. (B) Quantification of the normalized tumor area in the tibial bone marrow at the indicated time point after B16F10 cells inoculation. Growth rate was calculated with the following equation. % Growth rate = $100 \times ((\text{the } 4^{\text{th}} \text{ day's tumor area} - \text{the } 1^{\text{st}} \text{ day's tumor area}) / \text{the } 1^{\text{st}} \text{ day's tumor area})$. (n=6-10 per group) All data are expressed as means \pm SEM. Asterisks mark statistically significant difference (* $P < 0.05$; ** $P < 0.01$; **** $P < 0.0001$).

3.1.3 HFD induces increased numbers of tumor associated bone-resorbing osteoclast

Melanoma bone metastases are commonly osteolytic (Lau et al., 2006). Crosstalk between tumor cells and bone marrow resident cells promotes a self-amplifying cycle of tumor growth and bone destruction (Ell and Kang, 2012; Hirbe et al., 2009; Lau et al., 2006; Yoneda and Hiraga, 2005). To determine whether the bone marrow resident

cell populations are affected, osteoclasts were quantified. Indeed, osteoclast numbers and size were significantly increased in the tumor microenvironment of HFD mice compared to ND-fed mice from i.t. model (Figure 3.3A-C). Consistently, molecular profiling for osteoclasts markers revealed increased expression of *Cathepsin-K*, *matrix metalloproteinase 9 (MMP-9)*, *FBJ Murine Osteosarcoma Viral Oncogene Homolog (FOS) (c-Fos)*, *intercellular adhesion molecule 1 (ICAM1)*, *transforming growth factor β 1 (TGF β 1)*, *connective tissue growth factor (CTGF)*, *chemokine (C-X-C motif) receptor 2 (CXCR2)*, *CCAAT/enhancer-binding protein beta (CEBP β)*, *notch homolog 1, translocation-associated (Notch1)* and *vascular cell adhesion molecule 1 (VCAM1)* in HFD- compared to ND-treated mice 7 days after tumor cell challenge (Fig 3.3D). In addition, an increased mRNA expression levels of *X-box binding protein 1 (Xbp1)*, *Jagged1* and *chemokine (C-X-C motif) ligand 1 and 2 (CXCL-1, -2)*, while decreased mRNA expression of *Glucose transporter type 4 (Glut-4)* was found in HFD tumor-bearing mice (Fig 3.3E). Furthermore, osteoclast numbers and size were also significantly increased in the tumor microenvironment of HFD- compared to ND-fed mice from the i.c. model (Figure 3.3F-H), suggesting that the enhanced tumor associated osteoclasts by HFD are independent of the delivery route of tumor cells .



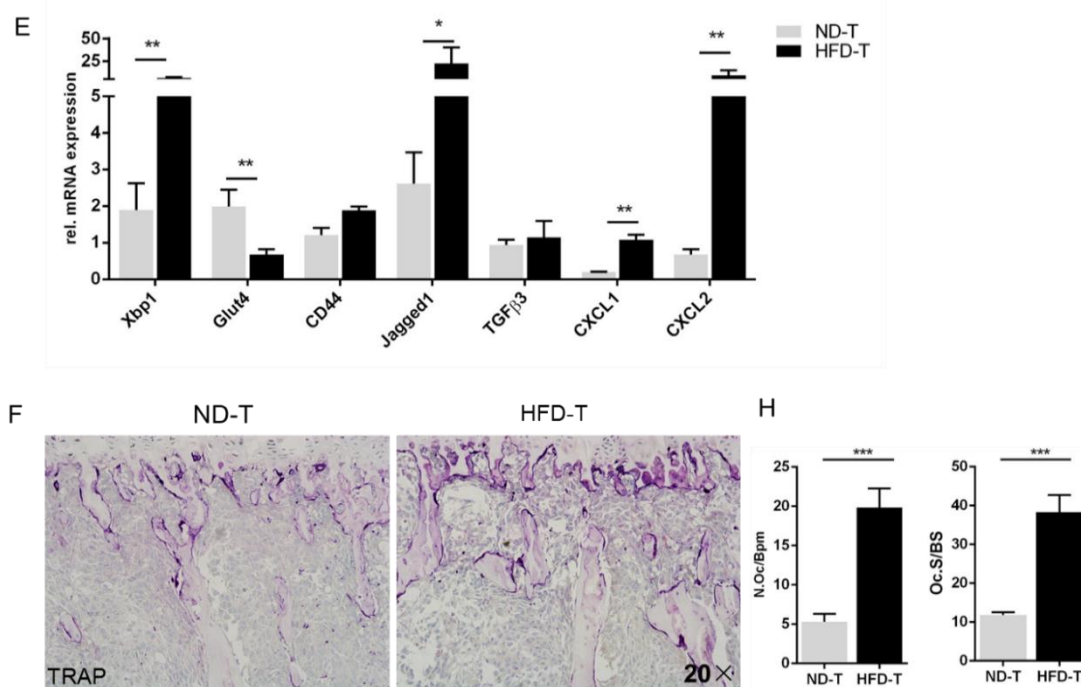


Figure 3.3 Increased osteoclasts marker genes expression in the tibiae of HFD mice injected with B16F10 cells. (A) Representative pictures of tartrate-resistant acid phosphatase (TRAP) activity staining in bone tumor area from ND or HFD mice (magnification $\times 20$). Normal diet (ND)- and high fat diet (HFD)-fed mice with injection of tumor cells were defined as ND-T and HFD-T, respectively. (B-C) Histomorphometric osteoclast quantification in the tumor center of ND or HFD mice. Abbreviations: N.Oc/B.Pm, number of osteoclasts per bone perimeter; Oc.S/BS, osteoclast surface/bone surface. (D-E) Osteoclast gene markers expression (D) and other bone metastasis-related gene profile (E) in bone from ND and HFD mice 7 days post intratibial (i.t.) B16F10 cells injection. (F-H) Representative pictures of TRAP staining (F) in bone tumor area from ND or HFD mice (magnification $\times 20$). Histomorphometric osteoclast quantification (H) in the tumor center of ND or HFD mice 10 days post intracardiac (i.c.) B16F10 cells injection. (n=6-10 per group) All data are expressed as means \pm SEM. Asterisks mark statistically significant difference (* $P < 0.05$; ** $P < 0.01$; *** $P < 0.001$).

To determine whether metabolic stress *per se* might activate bone-resorbing osteoclasts after the *in vivo* injection, bone slides were stained with H&E and for TRAP activity. Despite a decreased bone volume and trabecular bone thickness (Figure 3.4 A-B), no difference in osteoclast numbers and size were observed in HFD-fed compared with ND-fed mice without tumor injection (Figure 3.4C-D). Moreover, most of mRNA levels of osteoclast marker genes showed no difference between ND- and HFD-fed mice (Figure 3.4E). All together, these data indicates that the enhanced bone-resorbing osteoclast numbers and size are closely associated with an increased melanoma cell growth in the murine bone tumor niche after exposure to HFD.

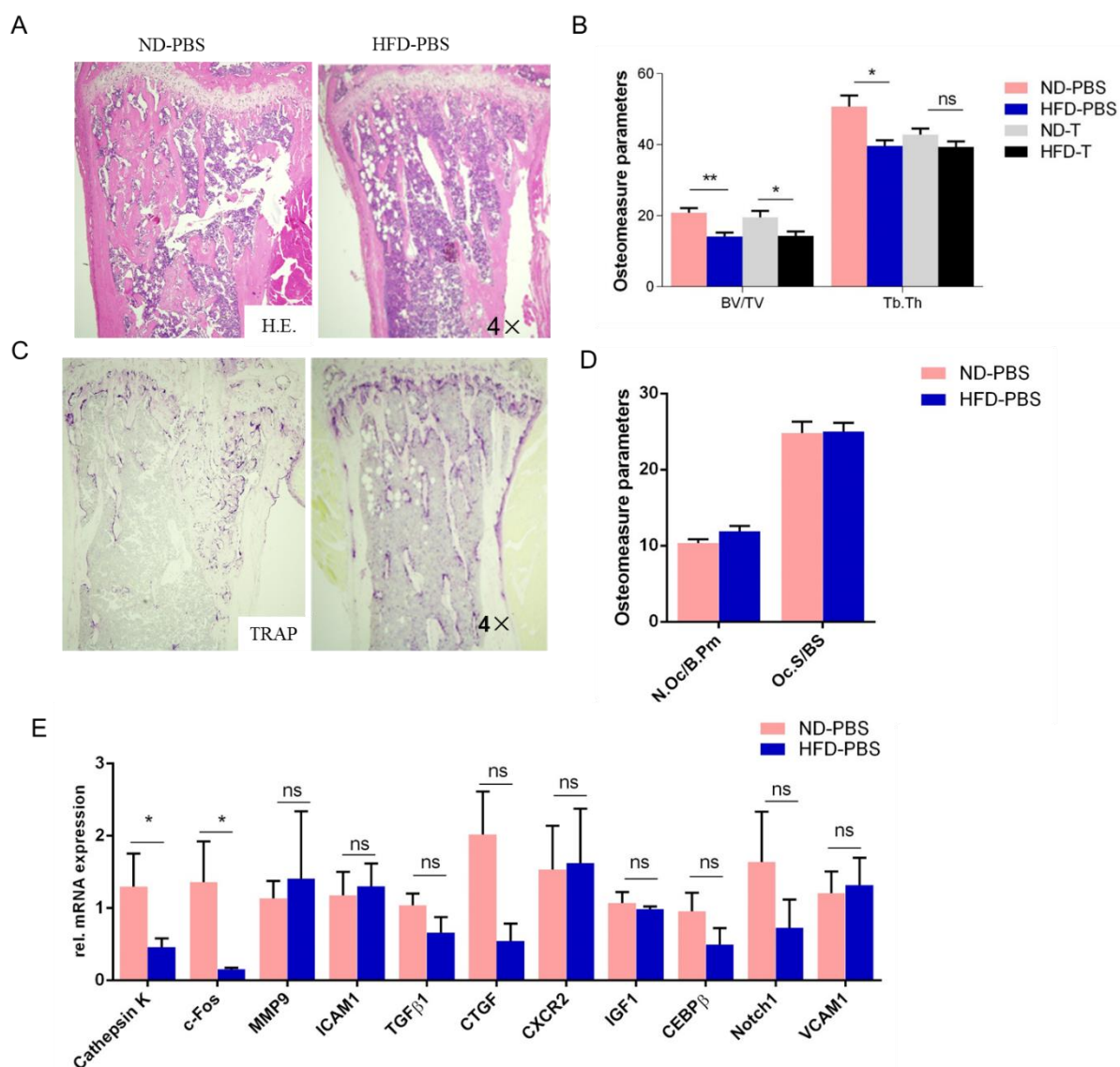


Figure 3.4 HFD do not affect the number of osteoclasts in the tibial bone from PBS-injected mice. (A-B) Representative images of H&E stained tibia section (A) from normal diet (ND) or high fat diet (HFD) mice injected with PBS (ND-PBS and HFD-PBS, respectively). Histomorphometric quantification of bone volume and trabecular bone thickness (B) in bone section from (A). Abbreviations: BV/TV, bone volume per total volume; Tb.Th, trabecular bone thickness. (C-D) Representative images of tartrate-resistant acid phosphatase (TRAP) activity stained tibia section (C) from mice injected with PBS. Histomorphometric quantification of osteoclasts (D) in the bone section from (C). Abbreviations: N.Oc/B.Pm, number of osteoclasts per bone perimeter; Oc.S/BS, osteoclast surface/bone surface. (E) Osteoclast marker genes expression in the bone from ND and HFD mice 7 days post i.t. injection of PBS. (n=6-8 per group) Data are shown as means \pm SEM. Asterisks mark statistically significant difference (ns, not significant; * P <0.05).

3.1.4 HFD leads to upregulation of osteopontin and interleukin 6 levels *in vivo*

Since obesity is known to induce inflammation (Shalapour and Karin, 2015), we hypothesized that increased cytokine levels in sera of HFD tumor-bearing mice could

be responsible for melanoma cell and osteoclasts activation in the bone tumor niche. Therefore, cytokine levels in the sera were analyzed by multiplex arrays and ELISA. Out of the 13 cytokines tested in mice from i.t. model (Figure 3.5 and table 1), osteopontin (OPN) and interleukin (IL)-6 levels were significantly higher in the sera of HFD-fed mice compared to ND-fed mice and further increased after melanoma cell challenge at day 7 (Figure 3.5A, table 1). Although an elevated leptin level in serum was detected in naïve HFD compared to ND mice, leptin serum levels were downregulated after melanoma cell inoculation at day 7 (Figure 3.5B). In addition, CXCL1 levels in serum were significantly increased in HFD mice with or without tumor (Figure 3.5C). Moreover, IL-17 levels were increased in HFD compared to ND mice after melanoma cell transplantation at day 7 based on the results of the multiplex arrays (table 1), while no significant alteration in serum levels of IL-1 α and β , IL-2, 4, 5, 10, IFN γ , GM-CSF and TNF α was observed (Figure 3.5 and table 1). Taken together, the increased IL-6, OPN and CXCL1 suggested that they might have an important role in the crosstalk between melanoma cells and osteoclasts/macrophages in the bone tumor niche after HFD exposure.

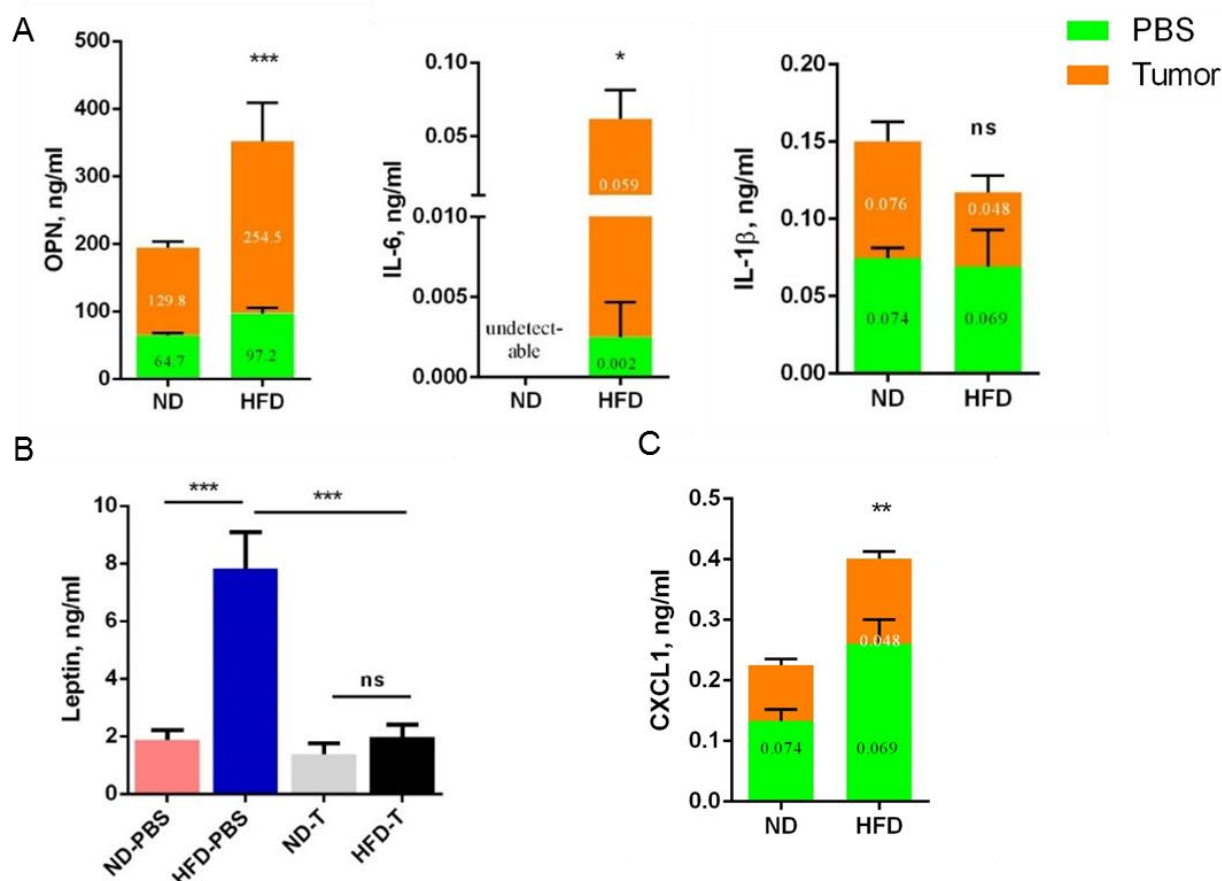


Figure 3.5 Cytokine levels in naïve or tumor-bearing HFD mice compared to ND mice. (A) Cytokine levels of osteopontin (OPN), interleukin (IL)-6, and IL-1 β in serum were detected by ELISA. (B-C) Leptin (B) and CXCL1 (C) levels in serum. (n=6-8 per group). Data are shown as means \pm SEM. Normal diet (ND)- and high fat diet (HFD)-fed mice with injection of tumor cells were defined as ND-T and HFD-T, respectively. ND- and HFD-fed mice injected with PBS were defined as ND-PBS and HFD-PBS, respectively. Asterisks mark statistically significant difference (ns, not significant; * P <0.05; ** P <0.01; *** P <0.001).

Table 1, Cytokine multiplex arrays analysis of serum from naïve and B16F10 injected mice.

Cytokine (pg/ml)	ND-PBS (n=4)	HFD-PBS (n=4)	ND-T (n=6)	HFD-T (n=6)	P value
IL-10	16.64 \pm 0.6502	15.7 \pm 0.4788	16.81 \pm 0.8853	16.4 \pm 1.129	0.3259
IL-6	23.11 \pm 0.4793	23.06 \pm 0.2533	25.01 \pm 0.9555	75.46 \pm 16.79	0.0017
IL-1 α	30.04 \pm 5.599	27.56 \pm 2.248	27.57 \pm 1.522	52.32 \pm 52.79	0.5318
IL-2	19.11 \pm 1.531	19.2 \pm 1.053	18.78 \pm 1.457	18.5 \pm 1.951	0.8959
IL-5	41.52 \pm 2.258	40.91 \pm 4.24	41.77 \pm 1.387	44.04 \pm 8.007	0.7912
GM-CSF	9.048 \pm 0.5649	9.15 \pm 0.25	9.209 \pm 0.1484	9.224 \pm 0.2568	0.8562
IFN γ	43.33 \pm 2.106	44.23 \pm 1.398	47.85 \pm 7.667	46.31 \pm 6.85	0.6525
IL-17	89.17 \pm 1.743	91.17 \pm 2.603	90.19 \pm 0.5007	103.2 \pm 11.08	0.0167
IL-4	26.81 \pm 0.9498	27.97 \pm 0.6894	27.52 \pm 0.5861	27.19 \pm 0.5928	0.1590
TNF α	55.02 \pm 2.837	56.11 \pm 2.028	55.36 \pm 1.349	60.8 \pm 14.86	0.7086

All data represent the mean \pm SEM. One-way analysis of variance. Normal diet (ND)- and high fat diet (HFD)-fed mice with injection of tumor cells were defined as ND-T and HFD-T, respectively. ND- and HFD-fed mice injected with PBS were defined as ND-PBS and HFD-PBS, respectively.

3.1.5 Increase of OPN-producing macrophages and osteoclasts in the bone marrow tumor niche favor melanoma cell growth

To address which cells express OPN in the bone marrow of HFD and ND treated mice having been challenged with melanoma cells, histological sections were prepared and stained with an anti-OPN monoclonal antibody (mAb) and TRAP activity in the bone tumor niche (Figure 3.6A). Indeed, OPN was expressed by macrophages and osteoclasts (TRAP+) in the bone marrow (Figure 3.6A). Additionally, TRAP-negative multinucleated cells around the tumor expressed OPN (Figure 3.6A). Monocytes progenitor cells are known to be shared by macrophages and osteoclasts (Udagawa et al., 1990). It has been also established that CD11b+Ly6C+Ly6Gint inflammatory monocytes, also known as myeloid-derived suppressor cells (MDSCs), have the potential to infiltrate into the tumor area and differentiate into bone-resorbing osteoclasts in the bone tumor niche (Sawant et al., 2013), we next examined the bone marrow monocyte population by flow cytometry. In line with increased TRAP activity in bone tumor area, a higher percentage of CD11b+ cells and CD11b+Ly6C+Ly6Gint cells was found in HFD compared to ND mice bearing melanoma (Fig 3.6B-C). Besides, mRNA profiling of macrophage gene markers revealed a decreased mRNA level of *CD206*, *Ym-1*, *Fizz-1* and *CD11c* in HFD PBS-injected (HFD-PBS) mice than ND PBS-injected (ND-PBS) mice, while markedly increased mRNA expression level of *Ym-1* and *Fizz-1* was observed, which both are main markers of alternatively activated macrophages (Raes et al., 2002), in HFD tumor-bearing (HFD-T) mice compared with ND tumor-bearing (ND-T) mice (Figure 3.6D). Collectively, these data imply that OPN produced by osteoclasts and macrophages may play significant roles in promoting melanoma cell growth in the bone tumor niche of HFD mice.

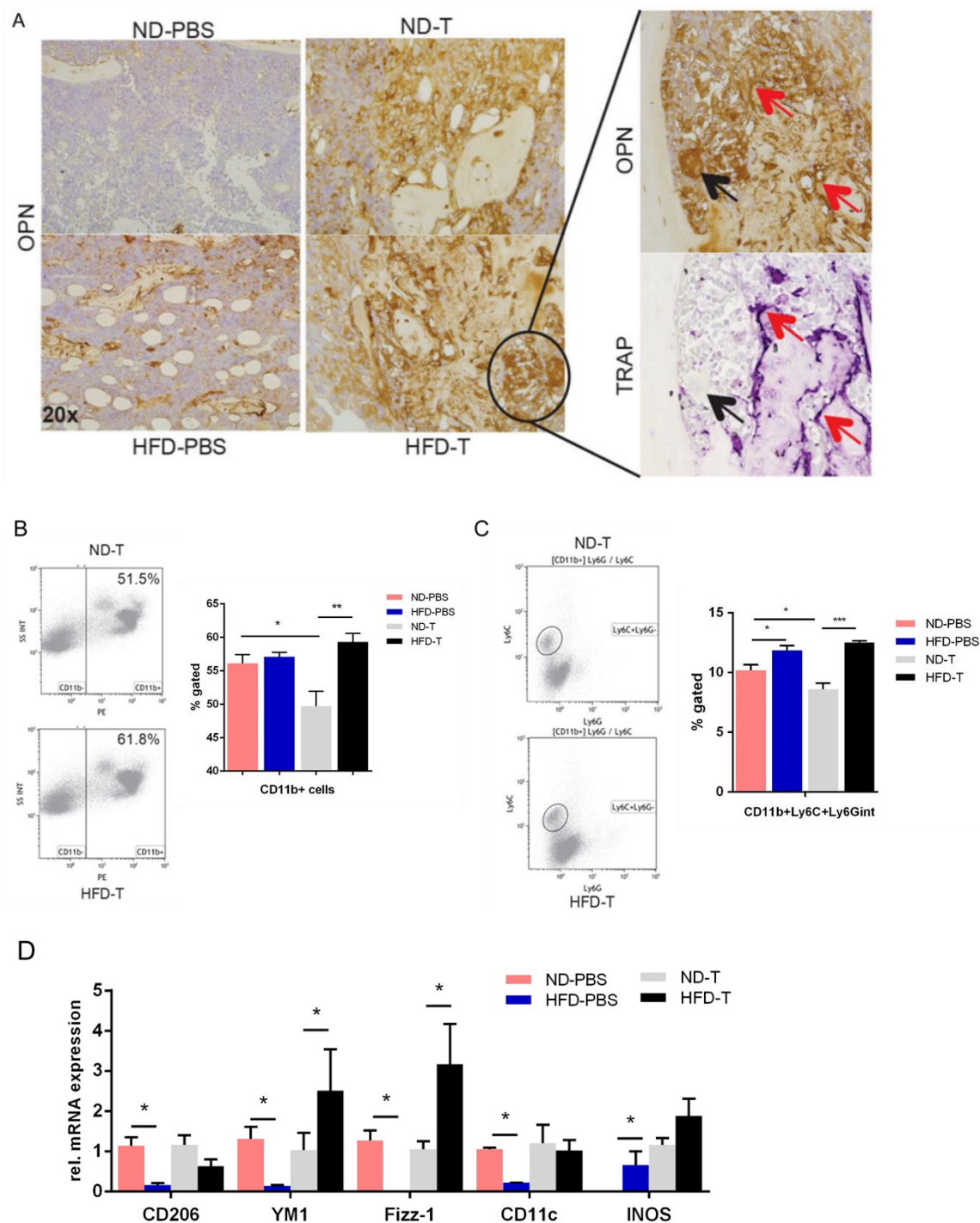


Figure 3.6 Osteopontin (OPN) expressed by macrophages and osteoclasts in bone tumor niche. (A) Staining of OPN and tartrate-resistant acid phosphatase (TRAP) activity in tibial bone with or without B16F10 i.t. injection. Red arrows indicate OPN expression TRAP-positive osteoclast. Black arrows mark OPN expression TRAP-negative multinucleated cells. Magnification 20 \times . (B-C) CD11b $^{+}$ and CD11b $^{+}$ Ly6C $^{+}$ Ly6G int cells from tumor-bearing mice in the bone tumor niche were analysed with FACS. (D) Macrophage genes markers expression level in tibial bone with or without B16F10 i.t. injection. (n=4-8 per each group). Normal diet (ND)- and high fat diet (HFD)-fed mice with injection of tumor cells were defined as ND-T and HFD-T, respectively. ND- and HFD-fed mice injected with PBS were defined as

ND-PBS and HFD-PBS, respectively. Data are shown as means \pm SEM. Asterisks mark statistically significant difference (* P <0.05; ** P <0.01; *** P <0.001).

3.1.6 Increase of IL-6-producing adipocytes in the bone marrow tumor niche by HFD upregulates cancer cell growth

More than as storage cells for fat, adipocytes were recently identified as being a critical source of IL-6 within adipocyte-rich connective tissue in tumor microenvironments such as breast cancer (Dirat et al., 2011). To better understand the remarkable increase of osteoclasts and macrophages in the bone tumor niche of mice challenged with HFD and tumor cells, we hypothesized an interaction between fat cells and tumor cells, which would elicit local inflammatory responses. Therefore, we first examined whether HFD triggers an enhanced anatomical connection between tumor cells and adipocytes in the bone tumor niche. As shown in Figure 3.7A-B, bone marrow adipocytes were more abundant in the bone marrow of HFD-fed tumor-bearing mice than ND-fed tumor-bearing mice in both the i.t. and the i.c. model. Indeed, we found that a higher number of bone marrow adipocytes in vicinity to the site of tumor growth in HFD-fed mice with injection of melanoma cells than ND-fed mice with injection of melanoma cells (Figure 3.7A-B). Since adipocytes are the IL-6 expressing cells in the tumor microenvironment (Dirat et al., 2011; Nieman et al., 2011). We performed an immuno-staining of IL-6 in the bone tumor niche and confirmed that adipocytes indeed actively expressed IL-6 (Figure 3.7C). These data suggested that an accumulation of IL-6-producing adipocytes probably play an important role in boosting melanoma cell growth in the bone tumor niche of mice exposed to HFD (Chen et al., 2016). The IL-6-expressing adipocytes together with OPN-producing macrophages and osteoclasts were hypothesised to provide a 'fertile soil', which is possibly generated by a crosstalk of bone marrow adipocytes and osteoclasts in the bone tumor niche.

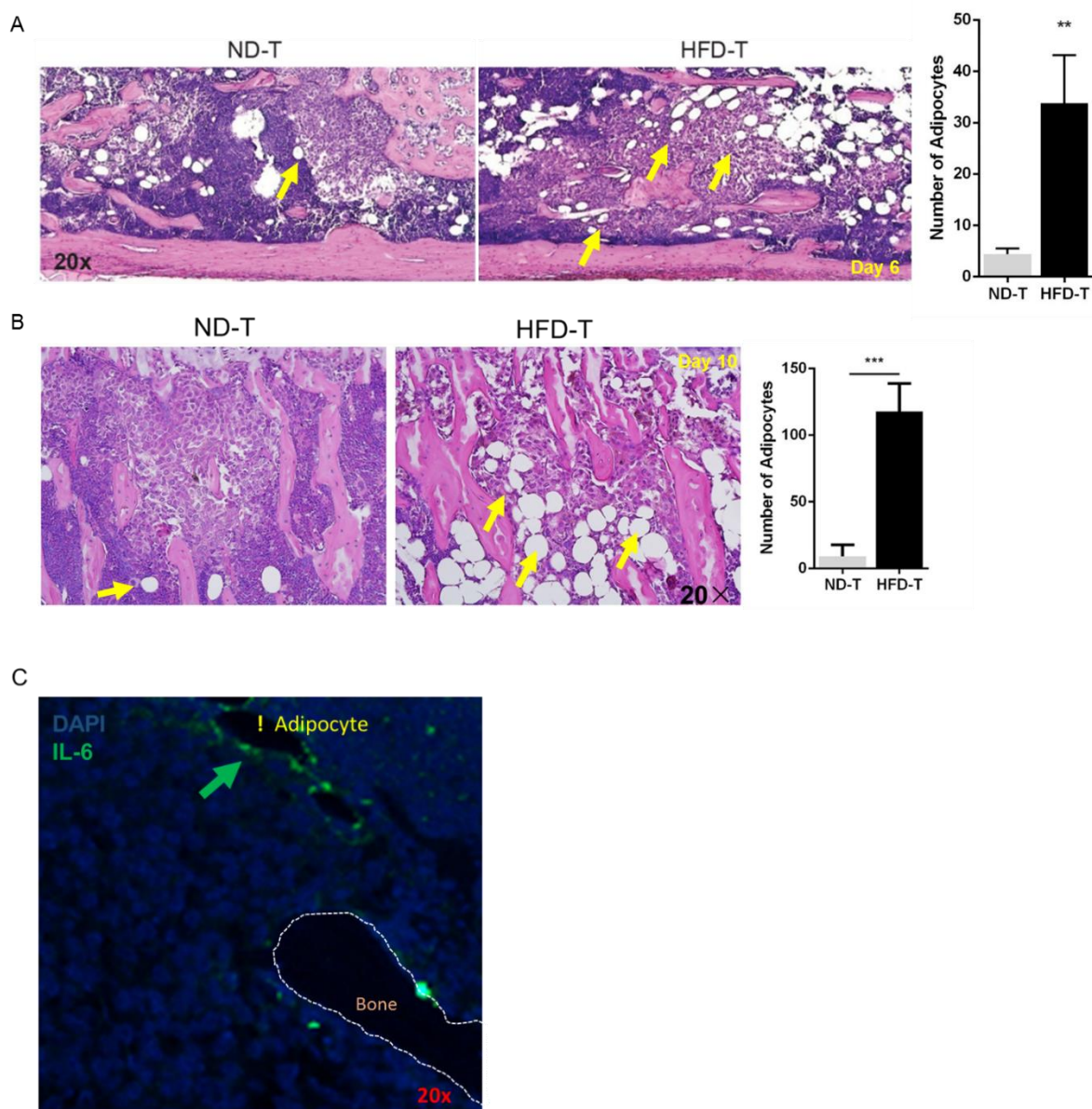


Figure 3.7 IL-6 expressing adipocytes in bone tumor niche in HFD mice. (A-B) Representative H&E stained pictures from bone tumor area at day 6 (intratibial model) (A) and at day 10 (intracardiac model) (B). Quantification of the number of adipocytes in bone marrow tumor area by Photoshop software. (Magnification 20×). (n=5-8 per group). Yellow arrows indicate bone marrow adipocytes. Normal diet (ND)- and high fat diet (HFD)-fed mice with injection of tumor cells were defined as ND-T and HFD-T, respectively. (C) Staining of IL-6 in bone marrow tumor area from HFD-fed mice. Blue arrow indicate IL-6 secreting adipocytes. (Magnification 20×). Data are shown as means ± SEM. Asterisks mark statistically significant difference (* P <0.05; ** P <0.01 determined by Student's t test).

3.1.7 Increased CD31+ cells in the bone tumor niche of HFD mice injected with B16F10 cells

To further profile the cells involved in the bone tumor niche induced by HFD, we assessed CD31+, B cells (B220+), eosinophils (siglec-F+), and dendritic cells (DC)

(CD11c+) cells population in the tibial bone marrow from ND and HFD-treated tumor bearing mice. As shown in Figure 3.8A, the percentage of CD31+ cells was significantly upregulated in HFD melanoma cells injected mice compared to ND melanoma cells injected mice. The decreased percentage of B220+ cells in HFD mice was attributed to the difference in naïve stage (Figure 3.8B). Both siglec-F+ and CD11c+ cells remained unchanged (Figure 3.8C-D). As CD31+ cells in bone marrow are highly angiogenic and vasculogenic cells (Kim et al., 2010a; Kim et al., 2010b). The upregulation of CD31+ cells indicates that tumor-associated angiogenesis might also induce the increased melanoma cell growth in the bone tumor niche of mice fed with HFD.

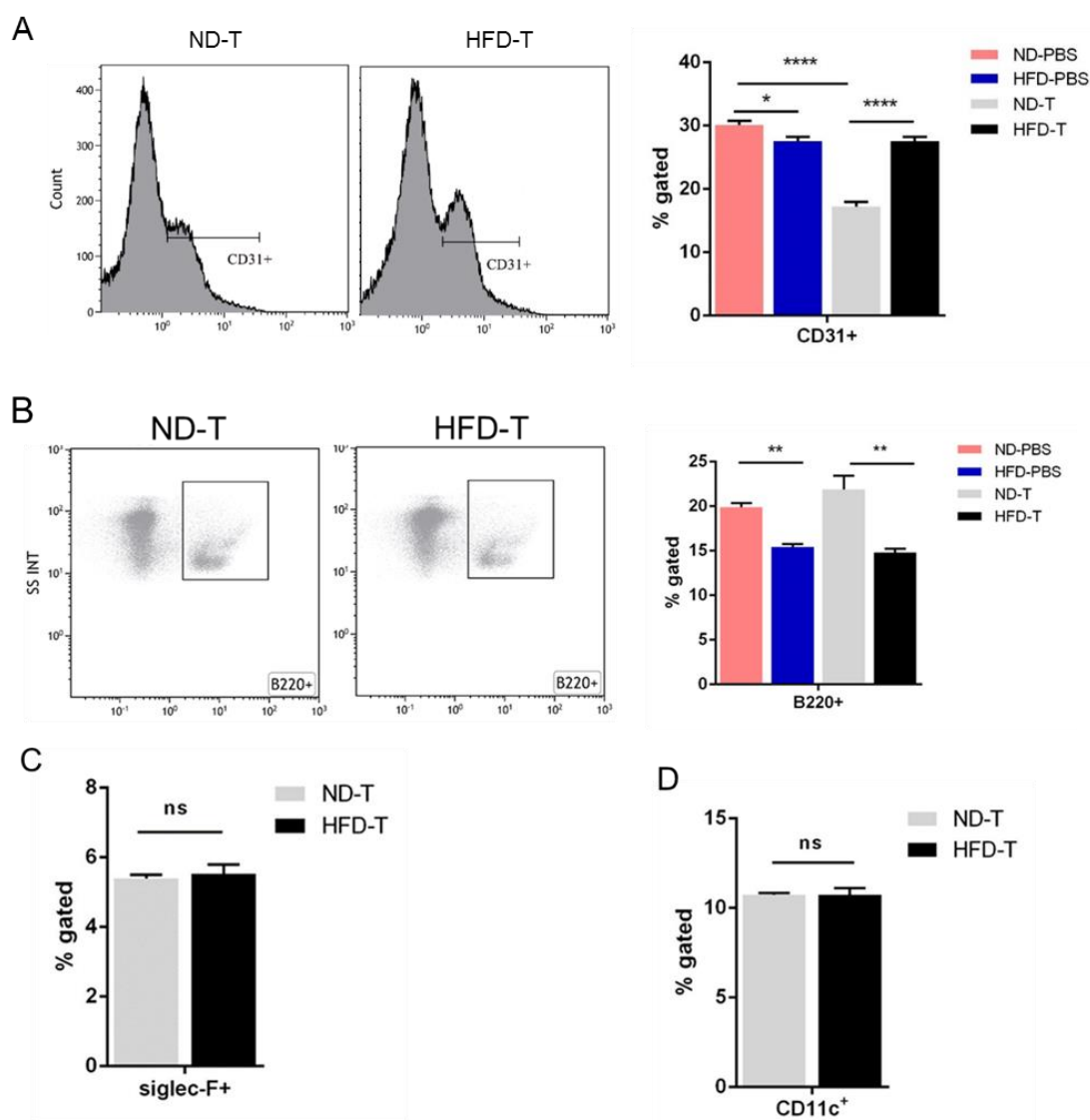


Figure 3.8 HFD increased CD31+ cells in the bone melanoma metastatic niche. (A) Representative contour plots of CD31+ cells in HFD and ND mice intratibially treated with melanoma. Numbers

represent percentage of the gated population. (B) Representative contour plots of B220+ cells in HFD and ND mice intratibially treated with melanoma. Numbers represent percentage of the gated population. (C-D) Percentage of tibial bone marrow eosinophils and dendritic cells (DC) cells (defined as siglec-F+ and CD11c+ cells, respectively) in HFD mice injected or not with melanoma at day 7 post B16F10 intratibial injection (n=3 per group). Normal diet (ND)- and high fat diet (HFD)-fed mice with injection of tumor cells were defined as ND-T and HFD-T, respectively. ND- and HFD-fed mice injected with PBS were defined as ND-PBS and HFD-PBS, respectively. Data are shown as means \pm SEM. Asterisks mark statistically significant difference (ns, not significant; * P <0.05; ** P <0.01; **** P <0.0001).

3.2 The nuclear factor- κ B (NF- κ B) signalling pathway contributes to alter the biological behaviour of melanoma cells challenged with high fat diet (HFD) serum *in vitro*

3.2.1 Circulating factors present in HFD-fed mice enhance melanoma cells proliferation

Apart from the local effect on melanoma cell growth, circulating factors could also potentially influence tumor cells. To figure out whether circulating factors present in HFD-fed mice could influence melanoma cell proliferation *in vitro*, we treated B16F10 cells with 2% heat-inactivated serum derived from ND- or HFD-fed mice. As shown in Figure 3.9A, a significant increase of melanoma cell numbers was detected after HFD compared to ND serum exposure. Flow cytometry analysis of cell cycle phase revealed that the length of the S- and G2M-phases decreased in B16F10 cells after HFD serum treatment (Figure 3.9B-C). Gene expression analyses of proliferation markers showed a significant increase in expression levels of *cyclin D1 (CCND1)*, *v-akt murine thymoma viral oncogene homologue 1 (Akt1)*, *mitogen-activated protein kinase 3 (Map3K)*, and *forkhead box a1 (Foxa1)* in melanoma cells treated with HFD-fed mice derived serum, while a decrease in *B-cell lymphoma 2 (Bcl-2)* expression and no difference for the other parameters were observed (Fig 3.9D). Taken together, these results suggest that HFD enhances melanoma cell growth *in vitro*.

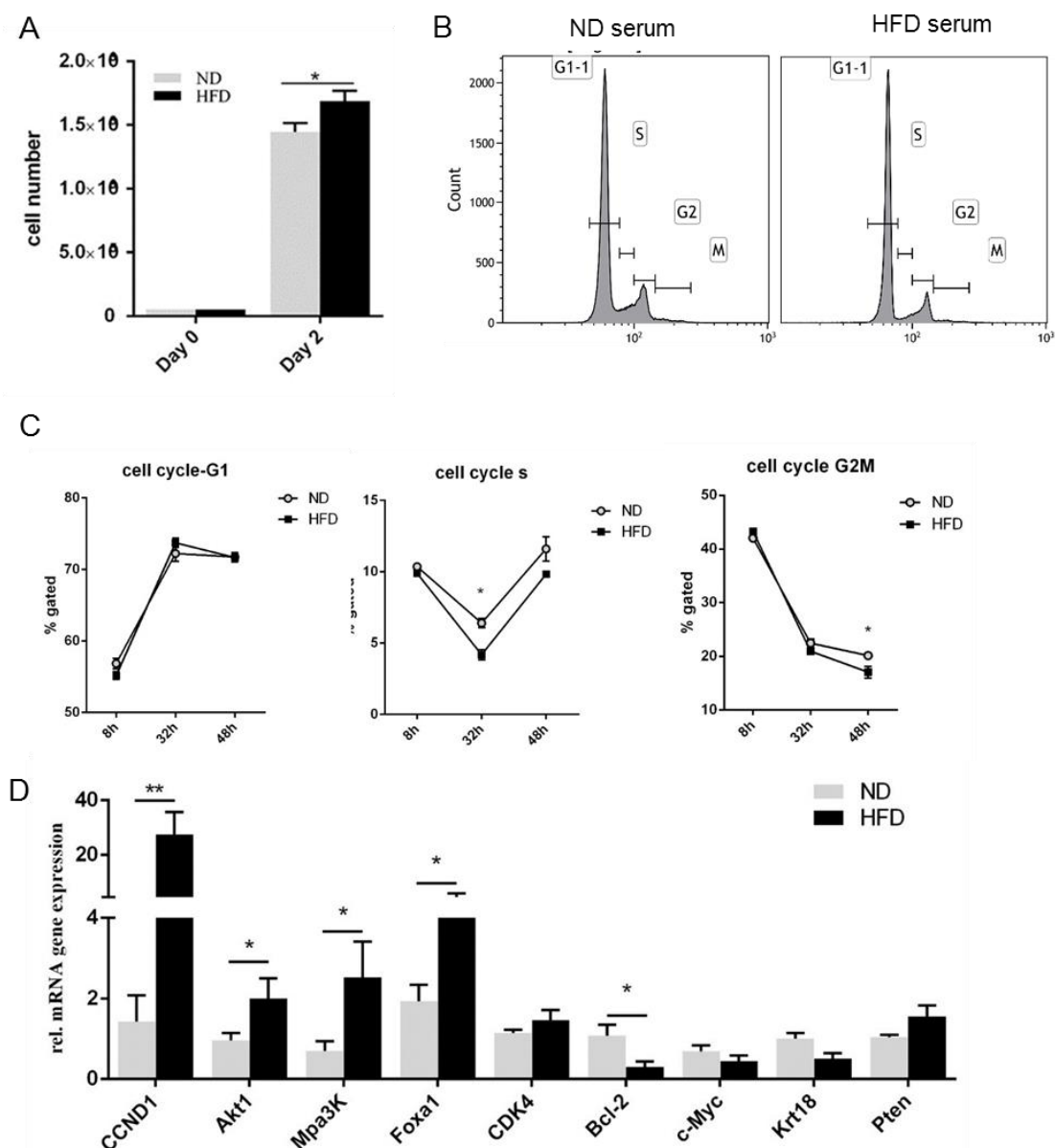


Figure 3.9 HFD enhance proliferation rate of melanoma cells *in vitro*. (A) Cell number was determined after ND or HFD serum exposure within 2 days. (B-C) Cell cycle was detected by flow cytometry and quantified after B16F10 cells treatment with serum from ND or HFD mice for 48h. (D) Proliferation genes expression was analysed by RT-qPCR. Three independent experiments were carried out in triplicates. Normal diet-fed mice, ND; high fat diet-fed mice, HFD. Data are shown as means \pm SEM. Asterisks mark statistically significant difference (ns, not significant; * $P < 0.05$; ** $P < 0.01$).

3.2.2 Enhanced cell migration in melanoma cells pre-treated with HFD serum

To determine whether cell morphology or migration of B16F10 cells would be modulated by HFD, B16F10 cells were treated with HFD serum or ND serum. After 24h of exposure, a phase contrast microscope was used to morphologically analysis of these cells. However, no striking difference was observed between two groups (Figure

3.10A). Interestingly, HFD serum promoted the migration ability of melanoma cells more than ND serum already at the time point of 8h, as indicated by a ~20% increase of coverage percentage in HFD group compared with the ND group (Figure 3.10B). These data indicate that metabolic stress by HFD does not alter the cell shape but promote migration of murine melanoma cells *in vitro*.

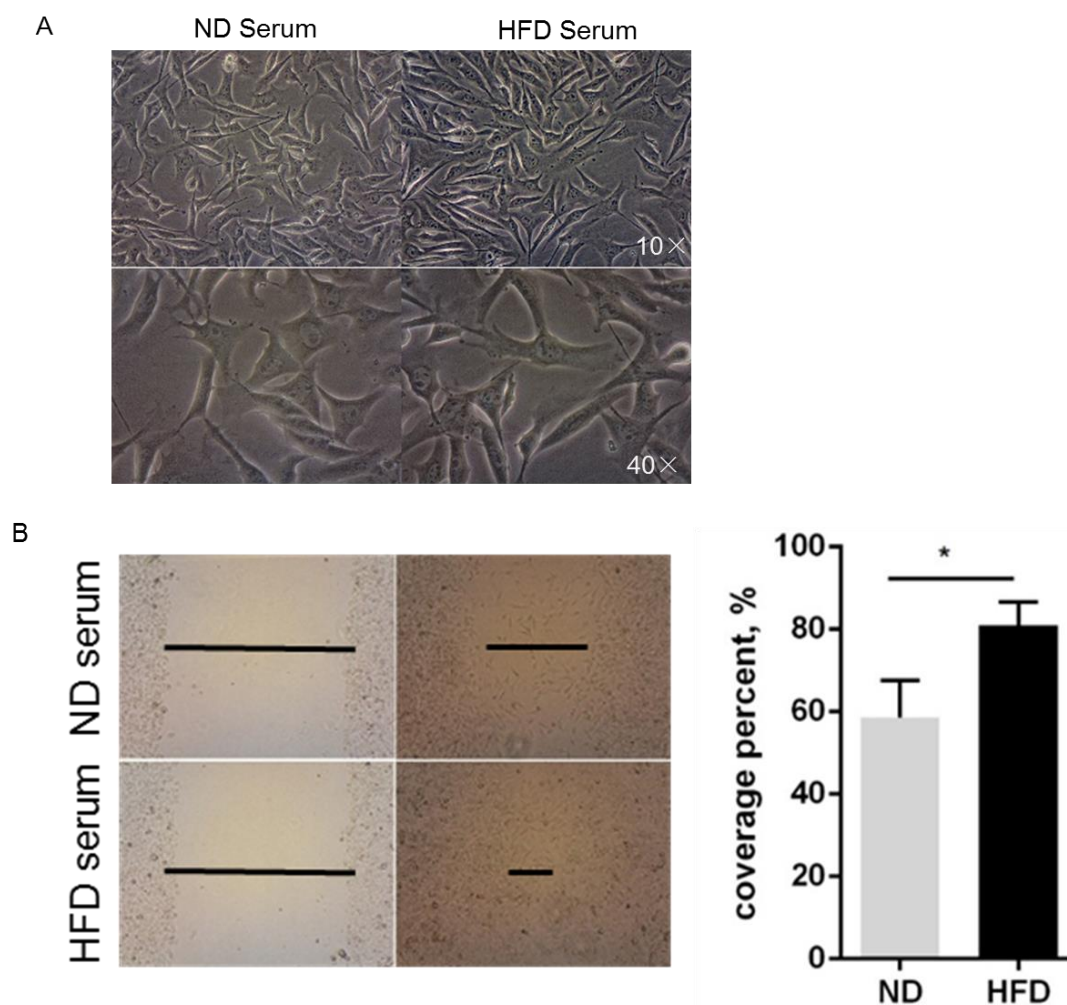


Figure 3.10 Cell shape and migration were assessed *in vitro*. (A) Cell morphology was evaluated by phase contrast microscope after 24h of ND or HFD serum treatment. (B) Wound healing assay was performed in B16F10 cells after 8h of HFD or ND serum stimulation. Coverage percentage was calculated and compared between HFD and ND group. Three independent experiments were carried out in triplicate. Normal diet-fed mice, ND; high fat diet-fed mice, HFD. Data are shown as mean \pm SEM. Asterisks mark statistically significant difference (* $P < 0.05$ determined by Student's t test).

3.2.3 Upregulation of chemokine (C-X-C motif) ligands secretion by B16F10 cells stimulated with HFD serum

To further investigate gene profile altered by HFD, matrix metalloproteinases (MMPs), chemokine (C-X-C motif) ligands (CXCLs), and inflammatory related genes expression levels were first analysed by quantitative PCR. As demonstrated in Figure 3.11A, *MMP-1 α* was significantly upregulated while *MMP-9* was reduced in B16F10 cells treated with HFD than ND serum. Except for *CXCL-12* and *CXCL-14*, almost all CXCLs mRNA expression levels were higher with a range of two to six fold changes in B16F10 cells treated HFD than ND serum (Figure 3.11B). Indeed, CXCL1 levels in culture supernatant of B16F10 cells are induced by HFD serum stimulation (Figure 3.11C). A serial number of pro-inflammatory genes were downregulated in B16F10 cells treated with HFD than ND serum, including *IL-1 β* , *IL-6*, *IL-11*, *TNF- α* , *G-CSF*, *CTGF*, and *MIP-2 α* (Figure 3.11D). To determine the protein levels changes, we collected B16F10 cells-conditioned medium (CM) pre-treated with ND or HFD serum. However, no difference in pro-inflammatory cytokines between HFD and ND group was detected by the Th1/Th2 cytokine multiplex kit (ebioscience) (Figure 3.11E). These data suggest that upregulation of chemo-attractants such as CXCLs in melanoma cells induced by HFD possibly plays a vital role in tumor cell crosstalk with adipocytes and osteoclasts/macrophages in bone tumor metastatic niche *in vivo*.

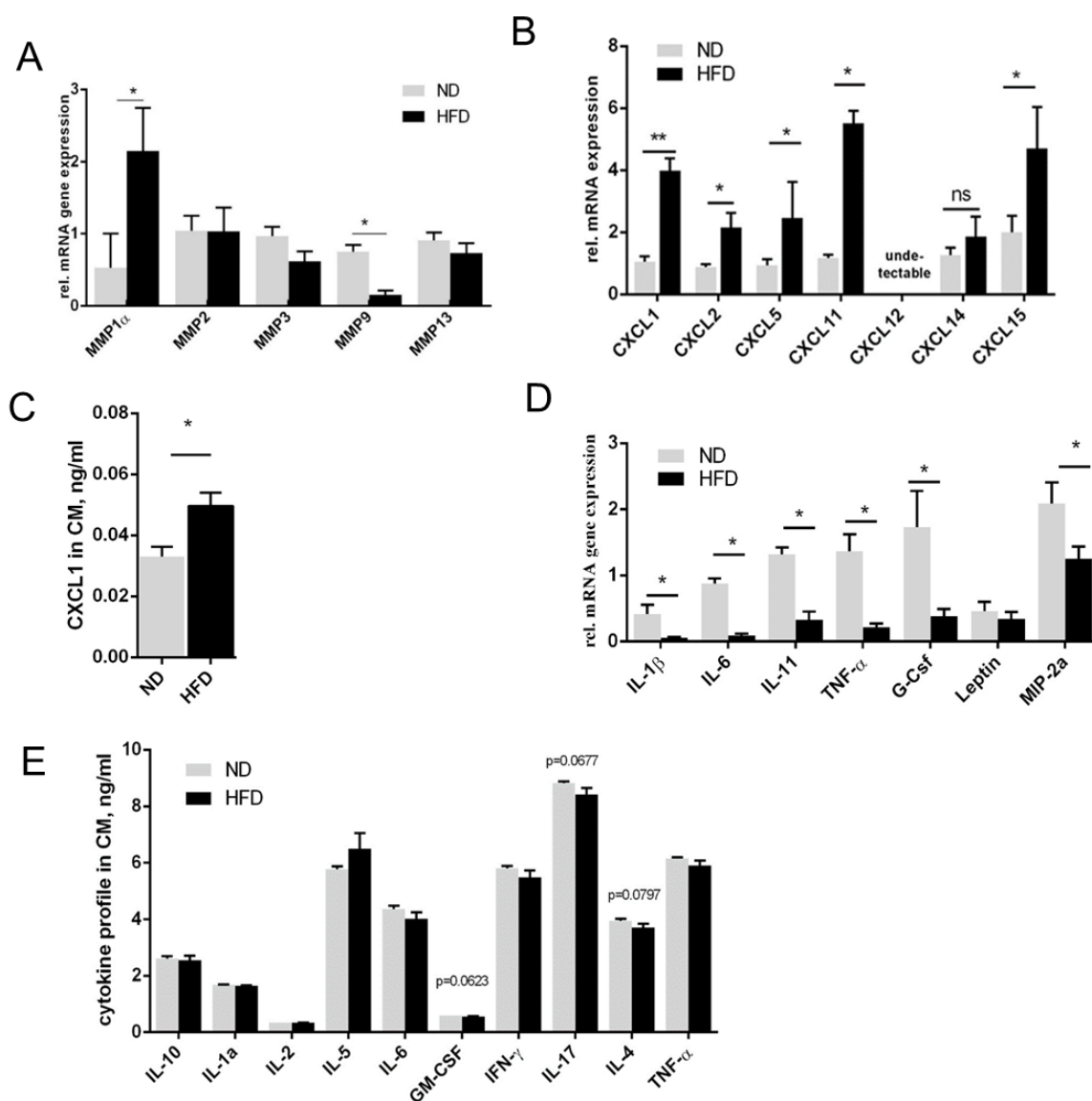


Figure 3.11 Treatment with HFD serum boost chemokine (C-X-C motif) ligands (CXCLs) gene mRNA levels in melanoma cells. (A) Matrix metalloproteinase (MMPs) genes mRNA expression were semi-quantified by the method of polymerase chain reaction (PCR). rel., relative. (B) Chemokine (C-X-C motif) ligands (CXCLs) gene mRNA expression. rel., relative. (C) CXCL1 levels in B16F10 cells derived conditioned medium (CM) pre-treated with 2% ND or HFD serum. (D) Pro-inflammatory and bone metastasis related gene mRNA expression. rel., relative. (E) Cytokine levels in B16F10 cells derived CM were detected by Th1/Th2 cytokine multiplex. Three independent experiments were carried out in triplicate. Normal diet-fed mice, ND; high fat diet-fed mice, HFD. Data are shown as mean \pm SEM. Asterisks mark statistically significant difference (ns, not significant; * P <0.05, ** P <0.01, *** P <0.001 determined by Student's t test).

3.2.4 Activation of NF- κ B pathway in melanoma cells induced by HFD serum

To get an insight into possible pathways activated by HFD, we tested NF- κ B and signal transducer and activator of transcription 3 (STAT3) phosphorylation levels in B16F10

cells after HFD serum stimulation. As shown in Figure 3.12A, the phosphorylated protein levels of p65 were upregulated in B16F10 cells treated with HFD serum when compared to ND serum. However, no difference in phosphorylated STAT3 was observed (data not shown). However, Activator protein 1 (AP-1) transcription factors gene mRNA levels were downregulated in B16F10 cells after incubated with HFD serum, e.g. *Fos-related antigen 2 (Fra2)*, *c-Fos*, and *c-Jun* (Figure 3.12B). No difference in *Fra1*, *hypoxia-inducible factor (HIF)1 β* , *runt-related transcription factor 2 (Runx2)*, and *Catenin (Cadherin-Associated Protein)*, *Beta 1 (CTNNB1)* mRNA level, while increase of *PPAR γ* mRNA level were detected in B16F10 cells treated with HFD serum (Figure 3.12B). Adhesion markers and the downstream targets of NF- κ B pathway were markedly increased in B16F10 cells in the HFD group, such as *intercellular adhesion molecule 1 (ICAM1)*, *cadherin 2 (N-cadherin)*, *C-X-C chemokine receptor type 7 (CXCR7)*, *CXCR4*, and *integrin subunit alpha 2 (ITGA2)* (Figure 3.12C). Moreover, bone metastasis related genes, such as *S100a8*, *TGF β 1&3*, *PTHrP*, and *BMP2*, were significantly increased in mRNA levels with a range from two to seven fold changes in B16F10 cells treated HFD than ND serum (Figure 3.12D). These data indicate that NF- κ B pathway activated in melanoma cells by HFD is possibly responsible for the tumor cell crosstalk with bone marrow adipocytes/ monocyte derived macrophages and osteoclasts in the bone tumor niche (Chen et al., 2016).

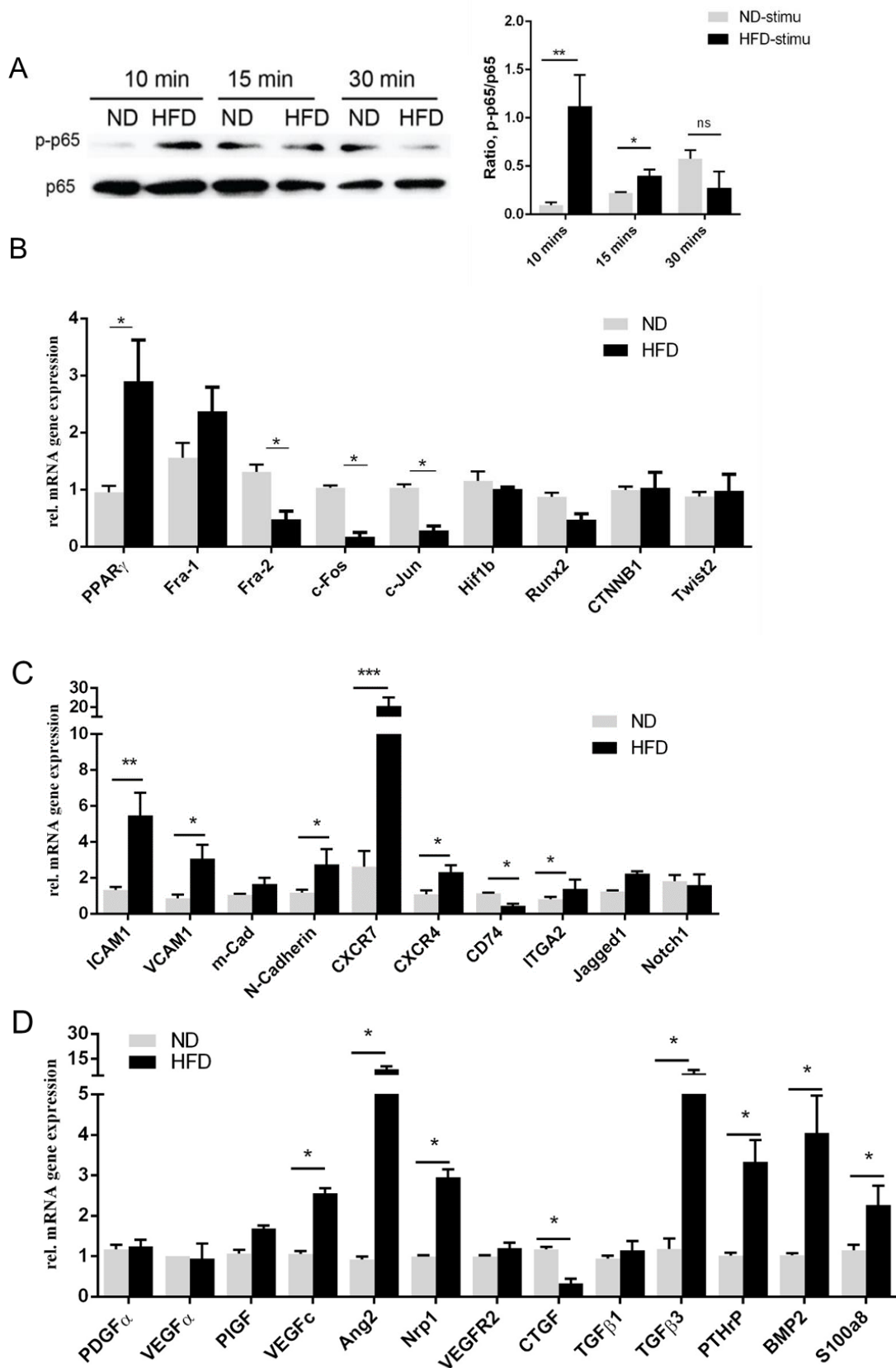


Figure 3.12 Analyses of cell signalling pathway in B16F10 cells after 2% HFD or ND serum incubation. (A) Representative western blot image of p65 and phosphorylated-p65 (p-p65) level in B16F10 cells and quantification of band intensity by the software of ImageJ. (B-C) Some selected

transcription factors mRNA levels and the downstream targets of NF- κ B signalling pathway or adhesion molecules were semi-quantified by PCR. (D) Angiogenesis and bone metastasis related genes mRNA expression. Three independent experiments were carried out in triplicate. Normal diet-fed mice, ND; high fat diet-fed mice, HFD. Data are shown as means \pm SEM. Asterisks mark statistically significant difference (ns, not significant; * P <0.05, ** P <0.01, *** P <0.001).

3.2.5 Both IL-6 and OPN are essential for CXCLs production by B16F10 melanoma cells *in vitro*

Since both serum levels of IL-6 and OPN were found increased in HFD-fed melanoma bearing mice and to determine whether these proteins could induce CXCLs expression, we treated B16F10 cells with recombinant IL-6 and OPN proteins *in vitro*. Indeed, recombinant IL-6 proteins with a concentration of 1 to 10 ng/ml upregulated CXCL1 secretion in culture supernatant by B16F10 melanoma cells (Figure 3.13A). Also, recombinant OPN proteins could induce *CXCL1* and *CXCL2* mRNA levels in B16F10 melanoma cells (Figure 3.13B) (Chen et al., 2016). These findings suggest that the increased expression of chemoattractants in melanoma cells as mediated by inflammatory cytokines may have a role in the recruitment of stromal cells into the tumor microenvironment by HFD.

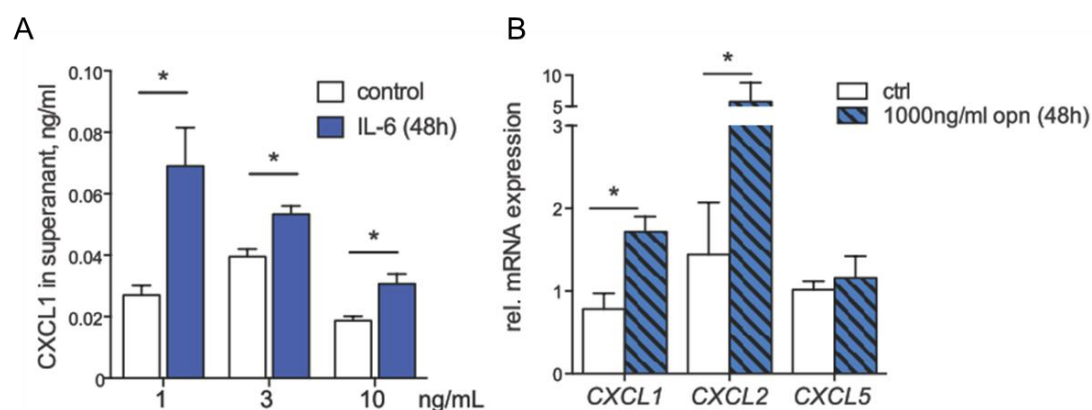


Figure 3.13 CXCLs production by B16F10 cells induced by recombinant IL-6 and OPN. (A) CXCL1 (KC) levels in culture supernatant from B16F10 cells treatment with a concentration of 1, 3, or 10 ng/ml recombinant IL-6 protein for 48h. (B) Quantification of *CXCL1,2&5* mRNA levels in B16F10 melanoma cells after 1000ng/ml OPN treatment for 48h. rel., relative. All data are means \pm SEM; Three independent experiments were carried out in triplicates. * p <0.05.

3.3 Activation of osteoclasts differentiation by melanoma cells pre-stimulated with HFD serum is dependent of cell-cell contact

3.3.1 The secretome of melanoma cells induced by HFD serum is not sufficient to promote osteoclastogenesis *in vitro*

In order to uncover the mechanism behind the enhanced osteoclastogenesis triggered by HFD in tumor bearing mice, conditioned medium (CM) was first collected from B16F10 cells, which were pre-treated with HFD or ND serum for 48h. Then, fresh bone marrow monocytes were incubated with osteoclast differentiation medium (Oc medium) plus with the above-mentioned CM (Figure 3.14 A). We did not observe significant differences in the number of TRAP+ cells in HFD compared to ND group (Figure 3.14B). Accordingly, mRNA levels of osteoclasts marker genes showed no differential expression of *NFATc1*, *OPN*, *VCAM1*, and *Cathepsin K*, while even significant lower expression of *c-Fos*, *MMP9*, and *ICAM1* were observed in HFD group compared to ND group (Figure 3.14C). These data suggest that the melanoma cells's secretome changes induced by HFD-associated circulating factors do not promote osteoclastogenesis *in vitro* (Chen et al., 2016).

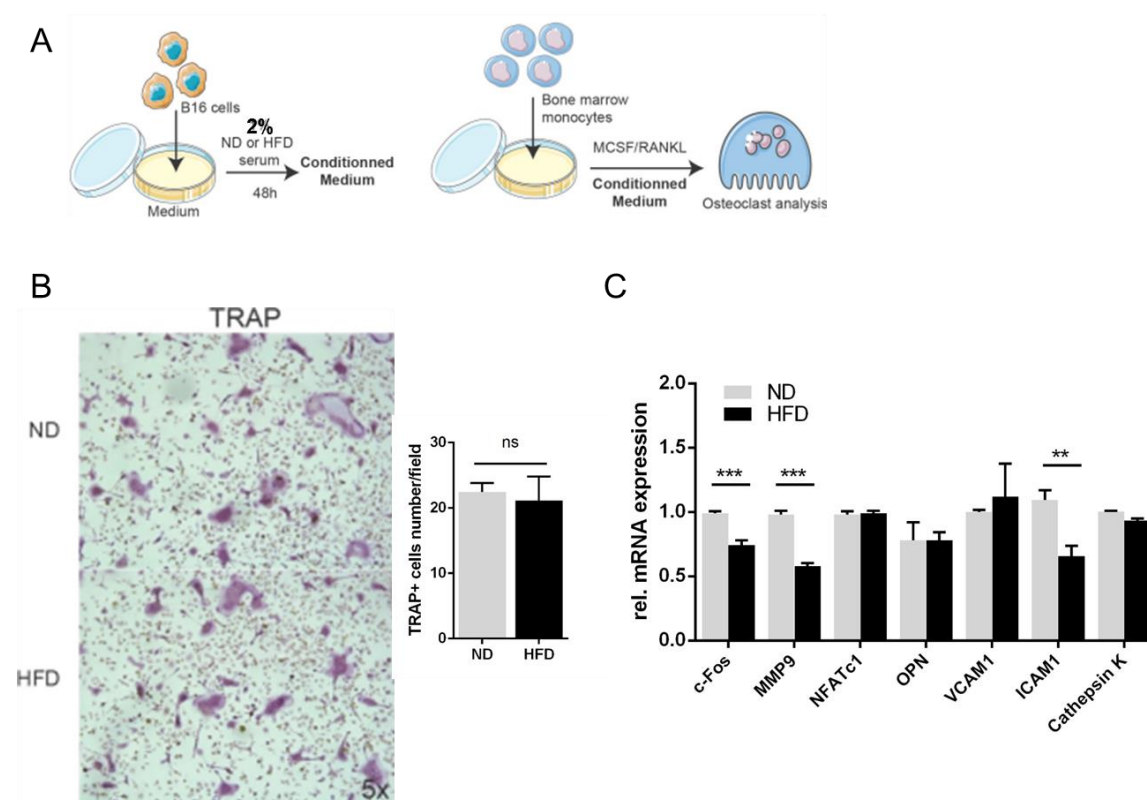


Figure 3.14 Conditioned medium from B16F10 cells pre-treated with HFD serum did not promote osteoclast differentiation compared to ND serum *in vitro*. (A) Overview of experimental setting *in vitro*. (B) Representative pictures of TRAP staining in ND and HFD group and quantification of the number of TRAP+ cells in each plate. Magnification 5×. (C) Quantitative RT-PCR analyses of osteoclast marker gene mRNA expression in ND and HFD group. Three independent experiments were carried out in triplicate. Normal diet-fed mice, ND; high fat diet-fed mice, HFD. Data were expressed as the mean ± SEM. Asterisks mark statistically significant difference (ns, not significant; * $P < 0.05$, ** $P < 0.01$, *** $P < 0.001$).

3.3.2 Melanoma cells pre-treated with HFD serum increase osteoclastogenesis in an OPN dependent manner *in vitro*

To evaluate whether the cell surface molecules expressed on melanoma cells could trigger increase in osteoclast differentiation, as previously suggested in breast cancer cells (Yagiz and Rittling, 2009), B16F10 cells were treated with HFD or ND serum for 2 days, and then fixed and co-cultured with bone marrow derived monocytes following a standard protocol for osteoclast differentiation assay *in vitro* (Figure 3.15A). As demonstrated in Figure 3.15B-C, melanoma cells pre-primed by HFD serum did raise the number of TRAP+ cells compared with ND serum. The increased osteoclastogenesis was further confirmed by a remarkable upregulation of osteoclast marker gene mRNA levels, such as *c-Fos*, *MMP9*, *OPN*, *VCAM1* and *Cathepsin K* (Figure 3.15C). Therefore, the altered expression of molecules on the melanoma cancer cell surface induced by HFD serum are responsible for the enhanced osteoclast differentiation in the HFD group. To further examine the circulating factors responsible for the above observation, we applied a neutralizing monoclonal antibody to OPN in the co-culture experiment based on the cytokine profile detailed in the section of 3.1.4 (page 57-59). Indeed, depletion of OPN in serum diminished the promoting effects on osteoclast differentiation of HFD-related circulating factors as compared with ND (Figure 3.15D). Consistently, mRNA levels of osteoclast marker genes showed a distinct decline expression of *c-Fos*, *MMP9*, *OPN* and *Cathepsin K* after clearance of OPN from the circulating factors (Figure 3.15E). Taken together, these data suggest that the increased osteoclast activation observed in the tumor area probably results from the increase of osteopontin mediated by HFD (Chen et al., 2016).

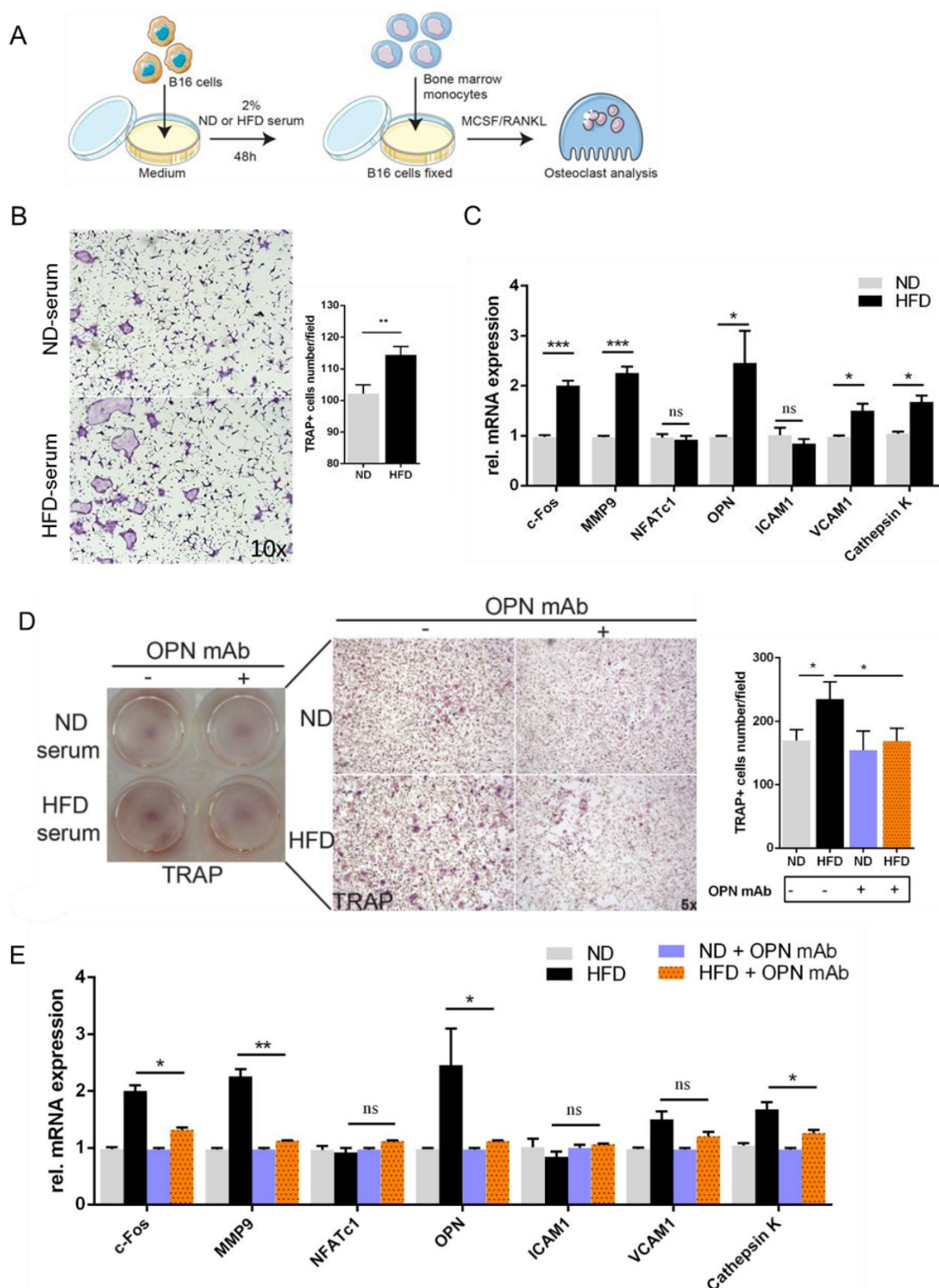


Figure 3.15 Effect of metabolic stress by HFD on osteoclast activation via cell surface molecules expressed by melanoma cells and dependent of OPN. (A) Scheme of the experiment procedures. (B) Representative TRAP staining and quantification of the number of TRAP+ cells in ND and HFD group. (C) Quantitative RT-PCR analyses of osteoclast marker gene mRNA expression in ND and HFD group. (D) Representative TRAP staining and quantification of the number of TRAP+ cells in ND and HFD group after depletion of OPN with a neutralizing monoclonal antibody (1 μ g). (E) Quantitative RT-PCR analyses of osteoclast marker gene mRNA expression in ND and HFD group after blockage of OPN. Three independent experiments were carried out in triplicate. Normal diet-fed mice, ND; high fat diet-fed

mice, HFD. Data are shown as means \pm SEM. Asterisks mark statistically significant difference (ns, not significant; * P <0.05, ** P <0.01, *** P <0.001).

3.3.3 HFD associated circulating factors also promote osteoclast differentiation *in vitro*

To explore whether HFD serum *per se* could stimulate osteoclast differentiation, we incubated bone marrow derived monocytes within osteoclast medium containing 2% heat-inactivated serum from tumor-free HFD- or ND-fed mice (Figure 3.16A). After 6 days incubation, we observed that the number of osteoclasts was higher in the HFD than the ND group (Figure 3.16B). Similarly, the levels of osteoclast marker genes were significantly increased in the HFD serum treated group than the ND serum treated group, including *MMP9*, *NFATc1*, *VCAM1*, and *Cathepsin K* (Figure 3.16C). Noticeably, no significant difference in mRNA level of OPN was observed in the HFD serum-treated group, while it was upregulated in the co-culture of melanoma cells/osteoclasts in the HFD group (Figure 3.15C). This data suggests that circulating factors from HFD-fed mice can impact osteoclastogenesis *in vitro* (Chen et al., 2016).

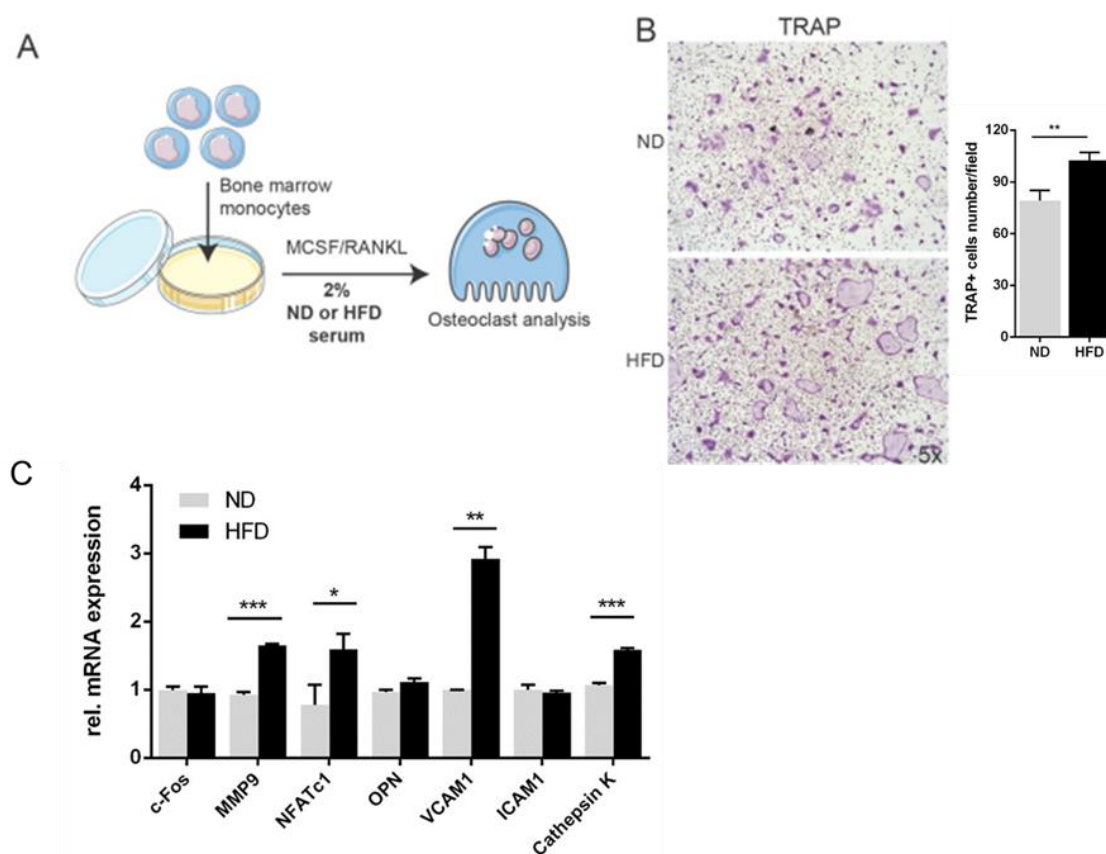


Figure 3.16 HFD associated circulating factors promote osteoclast differentiation. (A) Overview of experiment procedures. (B) Representative TRAP staining and quantification of the number of TRAP+ cells in ND and HFD group. (C) Quantitative RT-PCR analyses of osteoclast marker gene mRNA expression in ND and HFD group. Three independent experiments were carried out in triplicate. Normal diet-fed mice, ND; high fat diet-fed mice, HFD. Data are shown as the mean \pm SEM. Asterisks mark statistically significant difference (* P <0.05, ** P <0.01, *** P <0.001).

3.4 Melanoma cells potentiate a biological crosstalk with bone marrow adipocytes and osteoclasts in the bone tumor niche

3.4.1 B16F10 cells become more “aggressive” in the presence of adipocytes

To address whether bone marrow adipocytes influence the function of melanoma cells, we performed adipocyte/melanoma cell co-cultures (Figure 3.17A). As shown in Figure 3.17B, mRNA level of *c-Fos*, *Notch1*, *Jagged1* and *CD44* was increased in B16F10 cells following 48h of co-cultures. Adipocytes also triggered increases of mediator expression by the melanoma cells, including the angiogenesis molecule *VEGF α* , and pro-inflammatory cytokines *IL-6* and *IL-1 β* as well as the chemokines *CXCL1*, *CXCL2* and *CXCL5*. Together, this data indicates that melanoma cells showed increased survival

signalling and invasive properties in the presence of bone marrow adipocytes (Chen et al., 2016).

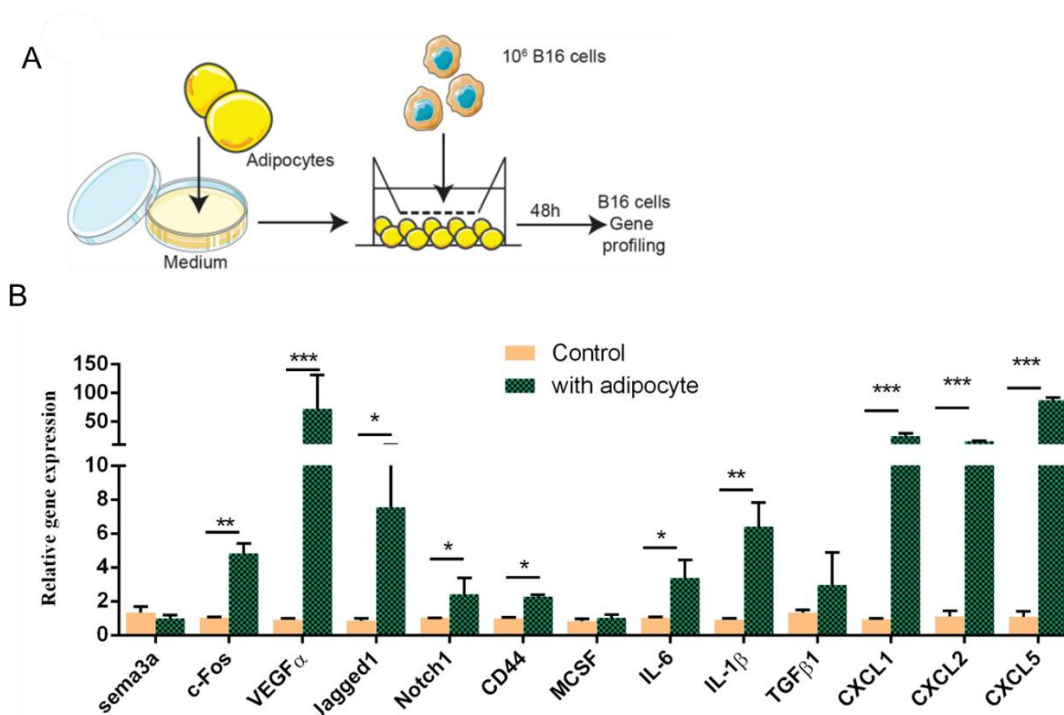


Figure 3.17 Analyses of cell signalling in B16F10 cells after incubation with bone marrow adipocytes. (A) Experimental setting for co-cultures. (B) Gene expression profiling in B16F10 cells by qPCR methods. Three independent experiments were carried out in triplicate. Data are shown as means \pm SEM. Asterisks mark statistically significant difference (* P <0.05, ** P <0.01, *** P <0.001).

3.4.2 Upregulation of chemokine (C-X-C motif) ligands and inflammatory gene expression in bone marrow adipocytes by a crosstalk of cancer cells

To further investigate how the bone marrow niche was altered by adipocytes in a crosstalk with melanoma cells, bone marrow adipocytes and B16F10 cells were co-cultured as mentioned above (section 3.4.1). After co-culture for 48h, adipocytes lost their lipid droplets (Figure 3.18A). Together with the increase mRNA levels of *Pref-1* while decline of *CEBPa β* , *PPAR γ* , *Leptin* and *aP2* were observed in adipocytes when co-cultured with melanoma cells (Figure 3.18B), suggesting that mature adipocytes undergo a dedifferentiation process. Interestingly, mRNA levels of *IL-1 β* , *IL-6*, *MCP-1*, *CXCL-1/-5*, *MCSF*, and *PDGF β* were significantly increased in the tumor-associated adipocytes after 48h of co-cultures with 10^6 B16F10 cells. These data indicate that mature adipocytes undergo a dedifferentiation process into pre-adipocyte-like cells with

a characteristic of upregulated chemokine and inflammatory cytokine secretion in the bone niche, which probably recruits macrophages and/or activates osteoclasts.

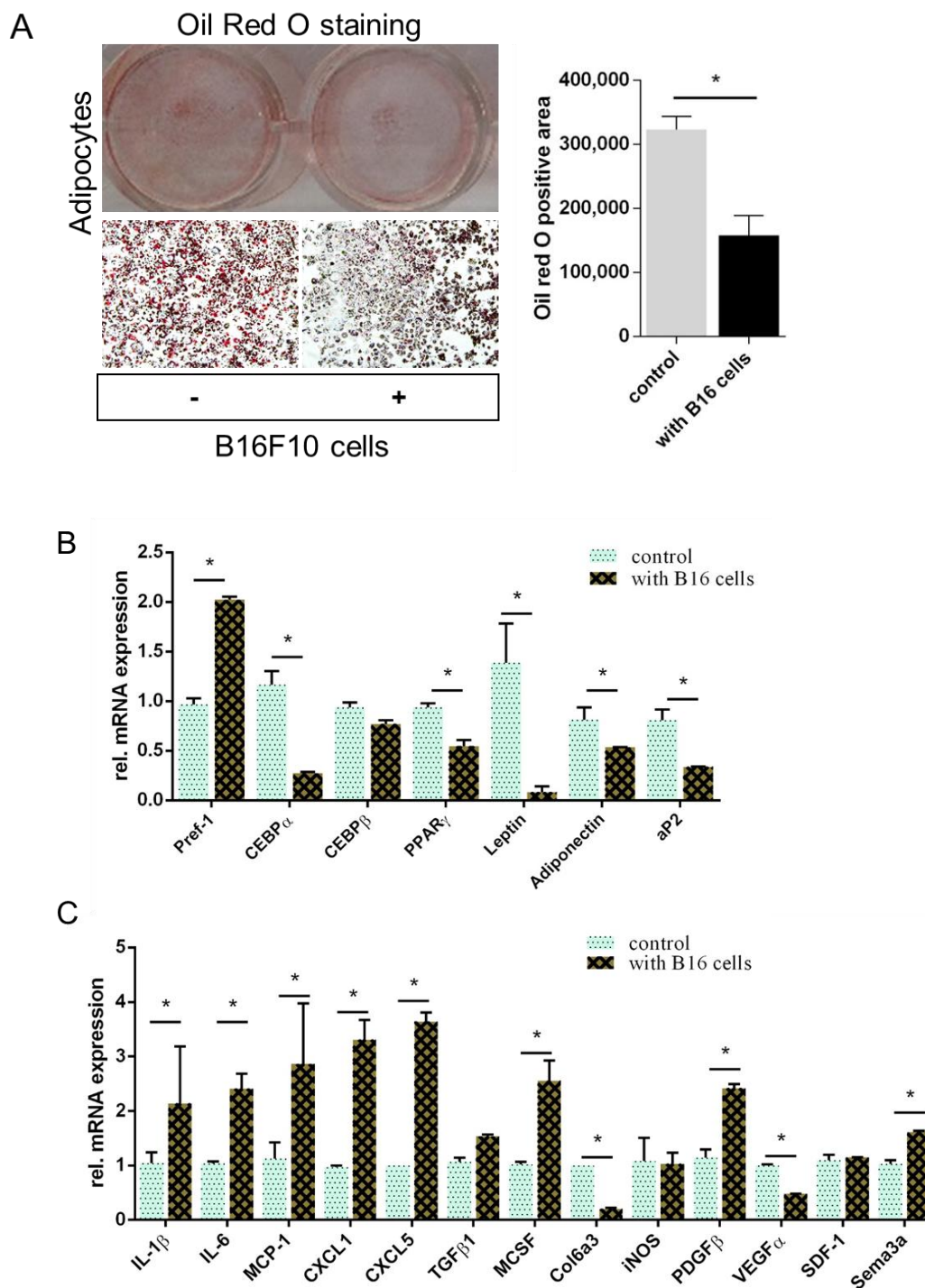


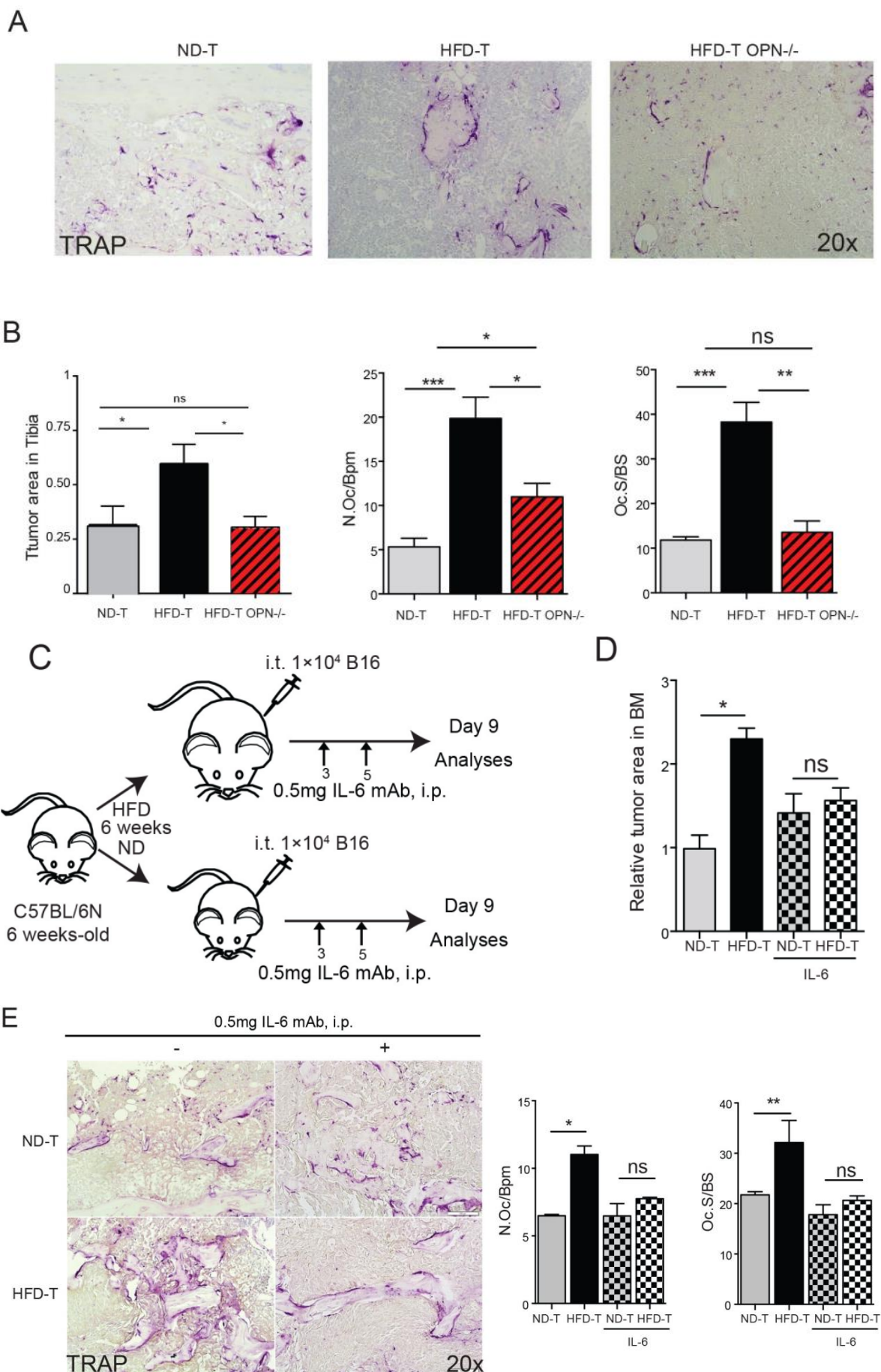
Figure 3.18 Bone marrow adipocytes become inflammatory during the co-culture with melanoma cells. (A) Oil Red O staining in adipocytes and the positive area was quantified by the software of ImageJ. Magnification 10 \times . (B) Adipocytes differentiation marker genes mRNA level in adipocytes/B16F10 co-cultures. (C) Quantitative RT-PCR analyses of inflammatory and chemokine genes mRNA level in adipocytes/B16F10 cells co-cultures. All experiments were replicated twice with triplicate. Data are

expressed as the mean \pm SEM. Asterisks mark statistically significant difference (* P <0.05, ** P <0.01, *** P <0.001).

3.5 Interruption of IL-6/JAK2-OPN axis rescue melanoma cell growth in mice exposed to HFD

3.5.1 Both IL-6 and OPN are essential for tumor growth induced by HFD *in vivo*

As reported, a close connection exists between IL-6 and OPN (Wen et al., 2015). Since both the increased serum levels of IL-6 and OPN were closely linked to the enhanced melanoma cell growth in obese mice *in vivo*, we thus hypothesized that HFD-induced melanoma cell growth might be mediated by these inflammatory cytokines. To determine the importance of osteopontin and IL-6 in the bone marrow tumor niche, we used osteopontin deficient (OPN^{-/-}) mice and an IL-6 neutralizing monoclonal antibody (mAb) treatment in the i.t. model, respectively. Interestingly, OPN deficient mice showed a significantly reduced tumor burden and significantly lower osteoclast numbers, when challenged with HFD, compared to HFD wild-type controls (Fig 3.19A-B), suggesting that OPN was a tumor-promoting and osteoclastogenic factor induced by HFD. Furthermore, neutralization of IL-6 by the mAb had a very similar effect, showing virtual restoration of the enhanced tumor growth and osteoclast activation induced by HFD (Fig 3.19C-E). In addition, administration of the IL-6 neutralizing mAb reduced OPN levels in serum of tumor bearing mice, and more strikingly in HFD tumor-bearing mice (Fig 3.19F), suggesting that IL-6 is able to initiate OPN production *in vivo*. Collectively, these data indicate that both IL-6 and OPN are essential for the tumor progression and osteoclasts activation in the bone marrow of HFD fed mice (Chen et al., 2016).



F

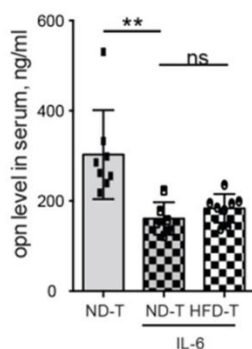


Figure 3.19 OPN deficiency or IL-6 mAb treatments rescue the increased tumor growth in tibia of high fat diet mice. (A) Representative pictures of TRAP staining in normal diet (ND), high fat diet (HFD) wild-type or HFD deficient OPN mice at day 7 post intratibial (i.t.) B16F10 cell injection (magnification 20×). Normal diet (ND)- and high fat diet (HFD)-fed mice with injection of tumor cells were defined as ND-T and HFD-T, respectively. (B) Quantification of tumor growth, osteoclast number and surface in tibia from ND, HFD wild-type or HFD deficient OPN mice at day 7 post i.t. B16F10 cells injection. (C) Schematic pictures for experimental setting of IL-6 mAb (0.5mg/mouse) intraperitoneal (i.p.) injection. (D) Relative tumor area in ND or HFD mice injected with B16F10 cells with or without mAb IL-6 treatment. (E) Representative pictures of TRAP staining (magnification 20×) and quantification of osteoclast number and surface in ND or HFD mice at day 9 post injected with B16F10 cells with or without IL-6 mAb treatment. (F) Serum levels of OPN in tumor bearing mice with or without IL-6 mAb treatment (1μg). All data are means ± SEM; (n=4 to 8 per group.) * $P < 0.05$, ** $P < 0.01$, *** $P < 0.001$.

3.5.2 Inhibition of JAK2 is essential for reducing the bone tumor cell growth and blocking IL-6 signalling *in vivo*

To further analyze the role of IL-6, we blocked downstream signalling JAK2 with the inhibitor AG490. As shown in Figure 3.20A-C, AG490 injection reduced B16F10 melanoma cell growth as well as osteoclast activation in HFD-treated mice, suggesting that the IL-6-JAK2 pathway is responsible for the enhanced tumor growth and osteoclast activation in obese mice. Consistent with the rescue of tumor growth and osteoclast activation by JAK2 inhibitor, also the HFD-induced elevation of bone marrow CD11b+Ly6C+Ly6Gint cells and the elevated levels of IL-6 were abolished *in vivo* when compared to ND melanoma bearing mice (Figure 3.20D-E). Indeed, recombinant IL-6 upregulated OPN expression, while inhibition of the IL-6 downstream JAK2 by AG490 effectively blocked OPN secretion by bone marrow-derived macrophages *in vitro* (Figure 3.20G). Also, inhibition of JAK2 by AG490 diminished the increased

CXCL1 (KC) levels in HFD tumor bearing mice *in vivo* (Figure 19G). Taken together, these data demonstrate that IL-6/JAK2 signalling and OPN are the main mediators for enhanced melanoma growth in bone marrow and the elevated CXCL1 (KC) levels following HFD (Chen et al., 2016).

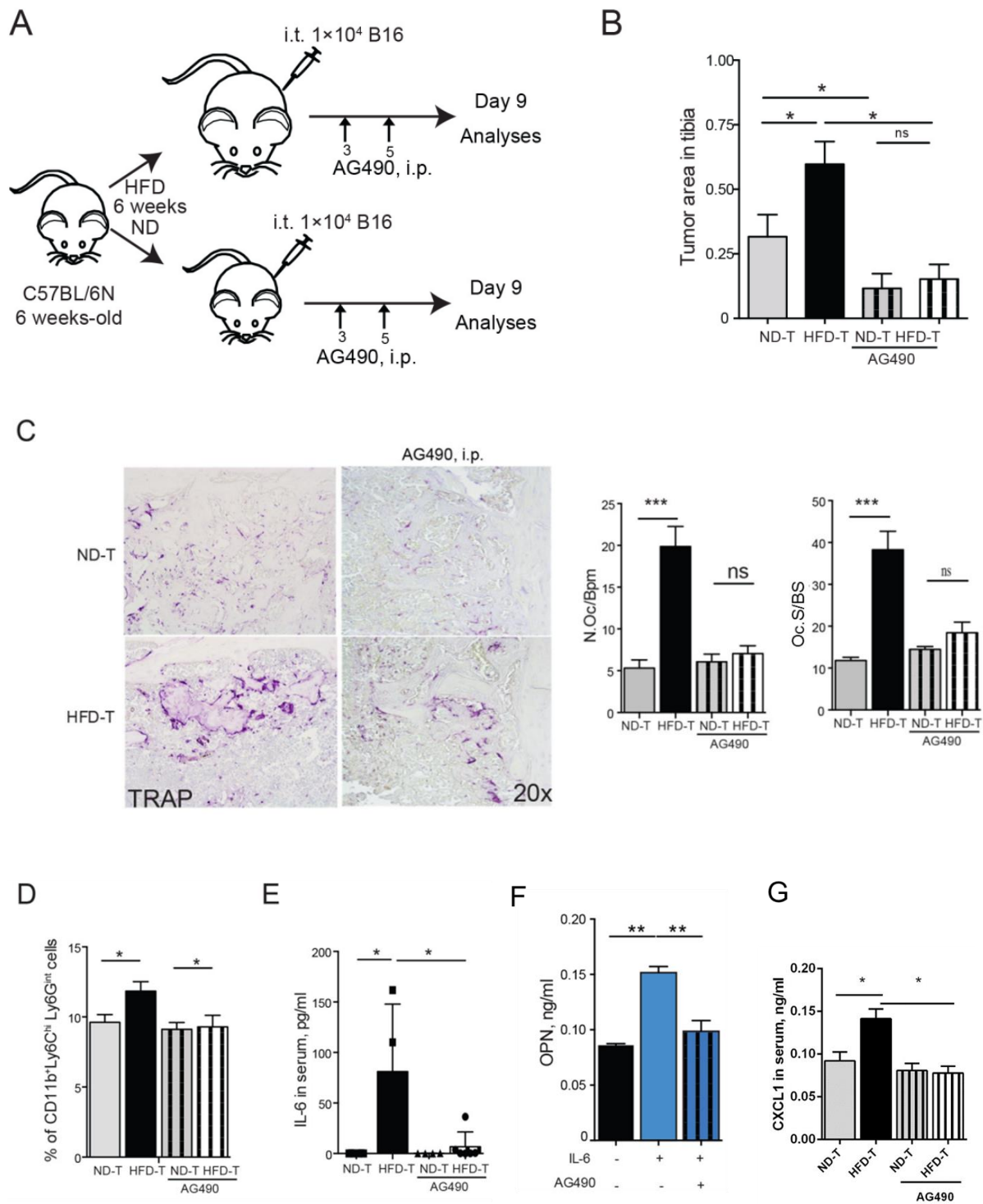


Figure 3.20 Blockade of JAK2 pathway rescues the tumor size and the number of osteoclasts infiltrated in high fat diet melanoma bearing mice. A) Schematic picture of the experimental setting: AG490 was intra-peritoneally injected every day till day 9 with the dose of 17mg/kg/mouse. Normal diet (ND)- and high fat diet (HFD)-fed mice with injection of tumor cells were defined as ND-T and HFD-T, respectively. B) Quantification of tumor size in tibia of each group. (C) Representative pictures of TRAP staining and osteoclast number and size in each group. (D) FACS analysis of CD11b+Ly6ChiLy6Gint populations in bone marrow from tumor bearing mice. (E-F) IL-6 (E) and OPN (F) levels in serum of ND-fed or HFD-fed mice injected with B16F10 cells with or without AG490 and IL-6 mAb treatment, respectively. (F) OPN levels in supernatant from bone marrow derived macrophages treated with IL-6 recombinant (10ng/ml) and AG490 (25 μ M). (G) CXCL1 levels in serum of ND-fed or HFD-fed mice injected with B16F10 cells with or without AG490 treatment. (*in vitro*) 3 independent experiments were carried out in triplicate; (*in vivo*) n=6 to 8 per group. All data are means \pm SEM; n=6 to 8 per group. *p<0.05, **p<0.01, ***p<0.001.

4. Discussion

4.1 Increased melanoma cell growth in the bone tumor niche was triggered by HFD-induced factors

Obesity increases the risk of developing certain bone marrow originated haematological malignancies, including leukaemia, lymphoma, and myeloma (Caers et al., 2007; Friedman and Herrinton, 1994; Lichtman, 2010). However, the impact of obesity on solid tumors with bone metastases has sparsely been recorded in the literature. This study shows that high fat diet (HFD) exposure induced melanoma cell growth in the bone tumor niche. In accordance, obesity also increases tumor growth in bone from metastatic prostate cancer (Hardaway et al., 2014), which preferentially metastasizes to skeletal sites. The evidence support the idea that metabolic stress induced by obesity promotes solid tumor growth in the bone marrow niche, and may worsen the prognosis of obese individuals with bone metastases.

Obesity is associated with metabolic syndrome, which is associated with increased risk of various cancers including malignant melanoma (Antoniadis et al., 2011; Berrington de Gonzalez et al., 2010; Calle et al., 2003; De Pergola and Silvestris, 2013; Kaidar-Person et al., 2011; Louer et al., 2012; Mitchell et al., 2011; Sergentanis et al., 2013; Wolin et al., 2010). Malignant melanoma is one of the most aggressive cancers, which often disseminate and metastasize to multiple sites including bone. In the bone marrow, metastatic melanoma cells grow in the bone tumor niche, which also represents as a hypoxic niche and a common site for tumor cells resistance to chemotherapy and targeted therapy and disease recurrence (Lux et al., 2014; Walker et al., 2015). During obesity developed by HFD exposure, adipocyte numbers increase in the bone marrow, as well as in adipose tissue (Luo et al., 2015). Although the effects of subcutaneous adipocytes on melanoma cell growth have been studied (Jung et al., 2015; Kushiro et al., 2012; Kwan et al., 2014), the impact of obesity on malignant melanoma growth in the bone tumor niche has yet to be investigated.

To address this, we performed two classical bone metastasis mouse models, i.e. intratibial (i.t.) and intracardiac (i.c.) injection models. In the i.t. model, melanoma

cells were directly delivered into the bone marrow niche. We observed an increased tumor burden in HFD-fed than ND-fed mice, suggesting that the increased adipocyte numbers in the HFD bone marrow niche enhanced melanoma burden in the bone tumor niche. Since the disseminating metastatic melanoma cells, *the seed*, proliferation and aggressiveness were increased by systemic factors present in HFD serum when compared to ND serum, as shown by the increases in the cell number counting and *CCND1* expression or coverage percentage in the wound healing assay. These findings suggest that *the seed* was not impaired but rather enhanced by HFD. Interestingly, a delay for the metastasized melanoma cells in initiating tumor foci in the bone marrow of HFD-fed mice was observed in the i.c. injection model compared to ND-fed mice, suggesting that the bone metastatic niche, *the soil*, is possibly impaired by HFD.

Our lab previously found that HFD changes the hematopoietic stem cell pool in the bone marrow, which results in a shift from lymphoid to myeloid cell differentiation (Luo et al., 2015). Hence, the alterations of the bone metastatic niche induced by HFD is possibly due to a decline in hematopoietic stem cell (HSC) pool (Luo et al., 2015), since the HSC niche could also be targeted by tumor cells in the bone marrow (Laharrague et al., 2000b; Luo et al., 2015; Malvi et al., 2015; Pandey et al., 2012; Reagan and Rosen, 2016; Schuettpelez and Link, 2011; Shiozawa et al., 2011). *In vitro*, we found that B16F10 cells are prone to proliferate more in HFD than ND serum. Although how HFD affect the bone marrow metastatic niche and the homing of melanoma cells from primary tumors is required for future studies, the current findings raises the question about the mechanism, behind how a fat-rich diet influences tumor growth, which is increasingly recognized in the tumor field (Brandon et al., 2009; Dirat et al., 2011; Jung et al., 2015; Kim et al., 2011a; Mori et al., 2006; Pandey et al., 2012; Parkin and Boyd, 2011; Valles et al., 2013) and becomes important facing the pandemic of obesity in the Western countries (Ribatti et al., 2010).

4.2 Inflammatory cytokines mediated the increased melanoma cell growth in the HFD bone niche

Obesity is now considered a disease associated with chronic low-grade inflammatory state (Iyengar et al., 2013; Park et al., 2014), in which a dysregulated metabolism plays an integral role (Iyengar et al., 2013; Park et al., 2014; Valles et al., 2013). Epidemiological studies have associated obesity with a range of cancer types including malignant melanoma (Ellerhorst et al., 2010; Gogas et al., 2008). Attention to the inflammatory microenvironment as a possible mechanism linking obesity with increased tumour burden has been paid (Calle and Kaaks, 2004; Dirat et al., 2011; Khandekar et al., 2011; Park et al., 2014).

In order to determine the molecular mechanisms behind the increased bone tumor burden observed in HFD-fed mice in the i.t. model, a cytokine screening was first performed. Indeed, OPN was found increased in HFD serum during steady state and following B16F10 cells injection. OPN was a good candidate for increased tumor burden, since it was previously shown to be a regulator of melanoma cell growth, angiogenesis and metastasis (Kumar et al., 2013; Yin et al., 2014). IL-6 was also found up-regulated in HFD mice after injection of B16F10 cells. Consistently with our results, Herroon MK. *et al.* (Herroon et al., 2013) proposed that upregulated levels of the inflammatory cytokines interleukin-1 β and oxidative stress protein HMOX-1 in the bone metastatic niche stimulate prostate cancer cell growth and invasiveness. Later, Hardaway A L. *et al.* (Hardaway, 2015), from the same research group, also suggested the significant contribution of CXCR2 and OPN in prostate tumor progression in bone. Thus, an enhanced inflammatory bone tumor microenvironment promoted by HFD is involved in melanoma growth in the bone melanoma niche of our HFD model.

In addition, an increase in IL-17 levels in the serum was found in HFD-fed mice compared to ND-fed mice after challenge with melanoma cells. IL-17 affects melanoma growth through a direct effect on IL-17 receptors bearing cells, including tumor cells and tumor-associated stromal cells, in the bone tumor niche. Thus, increased IL-17 levels may contribute to an increased tumor growth in obesity.

Interestingly, IL-17 could also induce IL-6 production (Chen, 2010; Gislette and Chen, 2010; Wang et al., 2009), and promote melanoma growth, in part via an IL-6 dependent mechanism (Wang et al., 2009). However, the role of IL-17 in the bone melanoma niche requires further investigation. It would be of great interest to determine whether inhibition of IL-17 may have preventive and therapeutic implications in obese patients with bone metastatic melanoma (Gislette and Chen, 2010).

4.3 Role of adipocytes in the bone melanoma niche for melanoma growth by HFD

The inflammatory bone tumor microenvironment facilitating tumor growth lead us to explore which inflammatory cells were actively involved in the bone tumor niche. In obesity, adipocytes are widely recognized as the major players in inflammatory adipose tissue (Greenberg and Obin, 2006; Stephens, 2012). Indeed, deregulated white adipocytes could release many obesity-related factors including inflammatory cytokines and chemokines (Belaid-Choucair et al., 2008; Caers et al., 2007; Cawthorn et al., 2014). However, the potential role of adipocytes in the tumor microenvironment was just recently introduced into the field of cancer research. In fact, bone marrow is also considered as an adipocyte-rich microenvironment (Herroon et al., 2013; Luo et al., 2015). However, currently their functional role is usually neglected in studies of bone metastases. Only recently, did scientists propose that bone marrow fat cells tied adipocyte-induced inflammation with skeletal metastasis in the bone-prostate cancer niche (Hardaway et al., 2014).

We have shown that adipocyte numbers increase in the bone marrow during obesity-induced by HFD (Luo et al., 2015). We thus speculated that these bone marrow changes provide an ideal microenvironment for tumor growth providing melanoma cells with a fertile niche. Our data support the concept that bone marrow adipocytes drive melanoma growth. Our results are also supported by previous observations showing adipocyte number increasing in the bone marrow with age (Lecka-Czernik et al., 2010; Takeshita et al., 2014) and the prevalence of bone metastasis in elderly melanoma patients (Macdonald et al., 2011; Markovic et al., 2007; Rogiers et al., 2015; Scutellari et al., 2003; Tellez et al., 2016).

Despite several reports on IGF1, RANKL, and the cytokine IL-8, the molecular signalling linking bone marrow adipocyte and bone tumor growth remains to be fully elucidated (Dougall et al., 2014; Lecka-Czernik et al., 2010; Takeshita et al., 2014). Indeed, adipocytes in the vicinity of the tumor cells express large amounts of IL-6, which can promote tumor growth in the bone marrow. Furthermore, earlier data have shown that adipocyte numbers in the bone marrow affect leptin levels (Laharrague et al., 1998; Laharrague et al., 2000a; Laharrague et al., 2000b), which were shown to accelerate melanoma growth (Brandon et al., 2009; Ellerhorst et al., 2010; Gogas et al., 2008; Mizutani et al., 2013). However, leptin levels decreased during tumor progression in HFD mice, suggesting that it may not be involved in the high tumor burden in the bone of HFD-exposed mice.

In fact, stress hormone promoted growth of B16-F10 melanoma metastases relies on an interleukin 6 dependent mechanism (Valles et al., 2013). The effects are activated by IL-6 and mediated by several signalling pathways, including the Janus kinase/signal transducer and transcription activator (JAK/STAT-3) (Jones et al., 2011; Na et al., 2013; Tamura et al., 1993). In our study, in support of the important role of IL-6 in promoting cancer growth in the bone marrow, we observed that blockade of IL-6 by neutralizing antibodies as well as inhibition of JAK2 by small-molecule inhibitors (AG490) significantly blocked tumor growth in the HFD model. Blocking IL-6/JAK2 pathway in the melanoma microenvironment may therefore inhibit disease progression (Na et al., 2013). Interestingly, similar observations have also been made in breast cancer models (Ara and Declerck, 2010; Dirat et al., 2011; Rahim et al., 2014; Sethi et al., 2011).

To reveal the possible role of local adipocytes in melanoma activation, we co-cultured mature bone marrow adipocytes with melanoma cells. As shown, melanoma cells were activated to express genes in the downstream of the NF- κ B pathway. Simultaneously, stressed by melanoma cells, mature bone marrow adipocytes undergo a dedifferentiation process, associated with a pro-inflammatory phenotype, less lipid content, and a gene signature similar to preadipocytes. Although apoptosis or necrosis of adipocytes may also take place (Wagner et al., 2013), these data are in line with the

observations made in other cancers, such as prostate cancer and breast cancer (Dirat et al., 2011; Hardaway, 2015; Wagner et al., 2013).

Furthermore, adipocytes could be also involved in the crosstalk of tumor cells with immune cells in tumor microenvironment. Indeed, CD4⁺ T cell subsets require distinct metabolic programs, such as glycolysis and lipid oxidation promoting effector T cell (Teff) or inducible regulatory T cell (Treg), respectively (Michalek et al., 2011). In our study, an elevated serum level of IL-17 indicate that a possible Th17 response was elicited in tumor bearing mice exposed to HFD. In addition, Sturtz, L.A. *et al.* revealed an increased expression of anti-inflammatory genes in adipose tissue from invasive breasts(Sturtz et al., 2014), suggesting a possible importance of adipocytes in aiding tumor cells to escape the surveillance of immune system. Especially the impact of adipocytes during the cancer initiation stage may be an interesting topic for the future study.

4.4 Contribution of OPN produced by macrophages and osteoclasts to the bone-melanoma niche

Macrophages in metastatic melanomas bone lesion can differentiate into osteoclasts (Lau et al., 2006). The recruitment and activation of the osteoclast by invading malignant cells is a key feature of the bone-melanoma niche, where mature osteoclasts cause bone resorption (Hiraga et al., 1995; Lau et al., 2006). In our study, osteoclasts and macrophages in the tumor area were strongly induced in bone of HFD-fed mice. Consistently, the tumor-promoting effects of osteoclasts and macrophages in the bone melanoma niche were strongly associated with enhanced bone melanoma burden.

To uncover the possible molecular mechanism linking macrophages and osteoclasts with melanoma, OPN seems a good candidate. In a cytokine profiling of sera, we found the serum level of OPN increased in HFD treated mice challenged with melanoma cells. We further showed that OPN present as a circulating factor in HFD mice is critical for B16F10 melanoma cell induced osteoclastogenesis. *In situ* of tumor area, we found that melanoma cells associated with macrophages and osteoclasts can express OPN, which seems to be important as it is released by macrophages and induce

osteoclastogenesis (Tanabe et al., 2011; Yamate et al., 1997). TRAP-negative multinucleated cells around the tumor also expressed OPN. Furthermore, OPN in the bone microenvironment have a crucial stimulatory role in melanoma progression (Kiss et al., 2015; Nemoto et al., 2001; Yin et al., 2014). Deletion of osteopontin (OPN^{-/-} mice) resulted in lower bone melanoma burden and osteoclast numbers in HFD-fed melanoma bearing mice, suggesting that this cytokine is a important driver of melanoma growth and tumor-induced bone degradation in HFD-fed mice. In line with our results, the pro-tumogenesis effect of OPN producing macrophages in prostate cancer in bone tumor niche was also suggested by Hardaway A.L. and colleagues (Hardaway, 2015). Therefore, the hypothesis that osteoclasts releasing bone matrix proteins fuels tumor cell growth, thereby creating a vicious cycle of bone destruction and tumor proliferation for the metastasized melanoma cells in the bone of HFD model.

4.5 HFD exposure drives melanoma cells to orchestrate a stromal cells-rich niche in the bone marrow

4.5.1 Impact of circulating factors on melanoma cells via the NF- κ B pathway

Obesity is associated with a marked alteration in circulating protein levels. Regarding the altered circulating factors in obesity, reports mainly focused on glucose and lipid profiles (Plourde, 2002; Szczygielska et al., 2003), elevated growth factors (Frystyk et al., 1999; Rehman et al., 2003), inflammatory cytokines (Al-Daghri et al., 2012; Dalmas et al., 2011; Rodriguez-Hernandez et al., 2013), and other mediators, that may raise the risk for health problems including cancers (Hursting and Hursting, 2012; Khan et al., 2006; Kushiro and Nunez, 2011; Lim et al., 2014; Price et al., 2012). The altered systemic factors as a link between obesity and cancers is very intriguing. Because the circulating factors may have prominent influences on the circulating tumor cells or the disseminating of cancer cells in metastatic cancer patients (AE Lohmann, 2016; RJO Dowling, 2016, 76.).

To investigate the effects of obesity-associated systemic factors on tumor cells, scientists exposed tumor cells to HFD serum. For prostate cancer, Price, R.S. *et al.*

(Price et al., 2012) reported that HFD serum increase proliferation, migration, and induce proteins critical for epithelial-mesenchymal transition (EMT) in tumor cells. Obesity-associated circulating factors also enhanced non-genomic estrogen receptor crosstalk with the PI3K/Akt and MAPK pathways in breast cancer (Bowers et al., 2013). In our study, we exposed B16F10 melanoma cells to heat-inactivated serum from HFD or ND mice. As results, the proliferation, cell cycle, migration, and osteoclast differentiation effects are enhanced in B16F10 melanoma cells by obesity-associated systemic factors. Moreover, we showed the circulating factors increased the NF- κ B pathway and its downstream targets, including CXCLs, angiogenesis, migration, adhesion, and osteoclast-promoting molecules, in melanoma cells. In accordance, serum from genetically obese mice (*ob/ob*) promotes the epithelial-mesenchymal transition (EMT) with increased Snail, Twist, and MMP9 expression in murine melanoma cells (Kushiro and Nunez, 2011). However, the expression of MMP9 is decreased in our study which may be due to the differences in the cell line and mouse model previously used.

The NF- κ B pathway is hyperactivated in human melanoma cells (Madonna et al., 2012; Yang et al., 2010). Since the transcription factor NF- κ B is a key regulator of the expression of genes involved in proliferation, cell cycle, migration, apoptosis, angiogenesis, inflammation, and tumorigenesis in cancers (Madonna et al., 2012; Yang et al., 2010). Our analysis found that the NF- κ B pathway and its downstream targets are activated in melanoma cells by obesity-associated circulating factors. As a result, the inflammation related genes are suppressed while the upregulated chemokine ligands are highly induced by systemic factors from HFD mice. The upregulated chemokine ligands, and their receptors genes, such as CXCR-4, -7, are critical for colonization and growth in the bone marrow niche. They are also enable melanoma cells to target the bone marrow niche, where they use stromal cells expressing chemokine ligand receptors, which constitute a stromal-rich niche full of adipocytes, macrophages, and endothelial cells. The increased *TGF β 3* (Hayashida, 2010; Margadant and Sonnenberg, 2010), *PTHrP* (Bryden et al., 2002; Onan et al., 2009; Soki et al., 2012), *SI00a8* (Acharyya et al., 2012), and *BMP2* (Gordon et al., 2009;

Myers et al., 2015) expression by HFD directly or indirectly provides assistance during the process (Acharyya et al., 2012). In addition, circulating factors such as OPN and induced cell-surface molecule such as ICAM1 alterations in melanoma tumor cells, could likely accelerate osteoclast differentiation *in vitro*.

Interestingly, the decreased mRNA level for AP-1 transcription factors, including Fra2, in melanoma cells might also be of relevance. Knockdown of Fra2 in murine melanoma cell lines is associated with increased migration and metastatic ability of cancer cells *in vitro*, and with prone to disseminate to distant organs, which is associated with increase of the proliferation rate, cell cycle transition, and angiogenesis *in vivo*, which are also validated in human melanoma samples (our unpublished data). Furthermore, the upregulated *PPAR γ* by systemic factors, together with reduced *Glut4* gene mRNA expression in HFD model, suggest that cancer cell metabolism is altered in HFD condition (Karnieli and Armoni, 2008). Similar observations have also been made in metastatic prostate tumors in bone (Mackenzie K. Herroon, 2015). In metastatic malignant melanoma, *PPAR γ* expression may be a predictive marker for response to therapy (Meyer et al., 2009). Due to enhanced glucose metabolism in cancer cells (Calvo et al., 2010; Karnieli and Armoni, 2008), it is proposed as a therapeutic strategy to inhibit glycolysis, which could be thought to kill the cancer cells including melanoma (Calvo et al., 2010; McBrayer et al., 2012; Parmenter et al., 2014). Indeed, obese cancer patients had a better prognosis than normal weight cancer patients after anti-cancer therapy (Daniell, 1996). A good prognosis could be possibly reach after the inhibition of NF- κ B pathway in obese patients with melanoma (Meyer et al., 2009; Nava-Villalba et al., 2015). However, more work is required to clarify the possible implications and therapeutic targets in cancer cell metabolism in obese individuals with melanoma.

4.5.2 Crosstalk of adipocytes and macrophages in the stromal cells-rich bone melanoma niche: role of IL-6-OPN-CXCLs axis

The increased adipocyte and macrophage numbers in the bone melanoma niche induced by HFD lead us to hypothesize a link with melanoma cell growth. Since the

communication between adipocytes and macrophages is very common, that could influence tumor growth in the stromal cells-rich bone melanoma niche.

As mentioned above, tumor-associated adipocytes produce IL-6, while macrophages and osteoclasts express OPN. Indeed, OPN impairs adipocyte differentiation and function, and induce a profound inflammatory cytokine secretion, such as TNF α and IL-6 (Samuvel et al., 2010; Zeyda et al., 2011). Furthermore, IL-6 was sufficient to stimulate OPN production from macrophages *in vitro*. Indeed, we showed that bone marrow adipocytes producing IL-6 seemed to induce OPN level *in vivo*, since inhibition of IL-6/JAK2 pathway reduced the OPN levels in HFD model. Additionally, we showed that adipocytes also increased secretion of CCL2 and CXCLs in response to the stress from the cancer cells, which recruit and activate macrophages. Similar results has been found in breast and prostate cancers (Arendt et al., 2013; Hardaway et al., 2015). Therefore, adipocytes and macrophages are most likely involved in a feedback loop with each other in the bone melanoma niche in HFD model. Surprisingly, OPN and IL-6 formed a positive loop, which led to CXCLs production from melanoma cancer cells. Interestingly, this activation of tumor cells appears to entail an accumulation of macrophages and in consequence also osteoclasts in the bone marrow. Indeed, while osteoclasts and macrophages were not increased in the bone marrow of HFD-treated mice, they were strongly induced after melanoma challenge in HFD-treated mice. Since adipocytes also express CXCR2/7 (Kabir et al., 2014), the tumor cells could also recruit adipocytes into the bone melanoma niche. This observation is also supported by Zhang.Y and colleagues (Zhang et al., 2009b). Importantly, blockade of OPN, IL-6/JAK2 signalling, rescue melanoma growth as well as osteoclastogenesis in the bone melanoma niche. Similar observations also were made by Kim SW *et al.* in prostate cancer (Kim et al., 2011b). Furthermore, several of these inhibitors for IL-6 are now testing in phases I and II clinical trials (Ara and Declerck, 2010), which might also be relevant for our model. Therefore, the tumor cells orchestrate the stromal cell rich niche in the bone marrow, in an OPN-IL-6-CXCLs axis dependent manner in the HFD model.

4.5.3 CD31⁺ endothelial cells in the stromal cells-rich bone melanoma niche

The stromal cell-rich bone melanoma niche contains CD31⁺ cells. CD31⁺ cells in the bone marrow represent a subpopulation of cells with high angiogenic ability. Angiogenesis plays a critical role in melanoma metastasis and progression (Jour et al., 2016; Ribatti et al., 2010). We showed that CD31⁺ cells are richer in HFD than ND model. In addition, the circulating factors, as well as adipocytes, can induce NF- κ B pathway, including *Ang-2*, *VEGF- α /c*, and *Nrp-1* angiogenic genes, in B16F10 melanoma cells. Furthermore, in the local tumor area, the increased osteoclastogenesis could also secrete PDGF isoforms (Rahman et al., 2015), which induced vascular generation. In addition, increased levels of IL-6 and OPN are also associated with the increased angiogenesis (Dai et al., 2009; Wang et al., 2009; Wang et al., 2011). Moreover, increased angiogenesis is also observed in obese mice after being inoculated subcutaneously with breast cancers, lung cancers, colon cancers, and prostate cancers (Gu et al., 2011; Park et al., 2012; Ribeiro et al., 2010; Zhang et al., 2009b). Targeting angiogenesis with neuropeptide Y suppressed melanoma growth in obese mice (Alasvand et al., 2015). In addition, several reports mentioned a strong relationship between inflammation, angiogenesis and metastasis in melanoma (Jour et al., 2016; Ribatti et al., 2010). Therefore, angiogenesis could also support the bone-resident melanoma cell growth in the bone tumor niche. However, further investigations are necessary to confirm the possible benefits for the inhibition of angiogenesis in obese melanoma patients with osteolytic metastases. Whether angiogenesis inhibitors, such as bevacizumab (humanized anti-VEGF α antibody) (Turley et al., 2012), in combination with cytotoxic agents would restrict bone tumor growth and metastasis, and potentially improve clinical outcomes in obese patients with melanoma is of great interest.

4.6 Conclusions

In conclusion, these findings provide a novel insight of how HFD influences cancer. HFD drive the tumor cells to orchestrate a stroma-rich bone marrow tumor niche, where fat cell accumulation in the bone marrow providing fuel and an inflammatory milieu for tumor cells promoting their proliferation dependent on IL-6 and JAK2. In addition, the interaction of cancer cells with the bone marrow fat facilitates the accumulation of mononuclear cells and osteoclasts in the bone marrow by expressing CXC chemokines and OPN. Moreover, increased angiogenesis could also participate in the bone melanoma niche. Hence, the IL-6-JAK2-OPN axis is a key pathway for setting up the metabolic tumor niche and an interesting therapeutic target (Figure 4.1). This is an important finding since inhibitors of IL-6, like the tocilizumab, and JAK2, like the ruxolitinib (Passamonti et al., 2011), are already in clinical use for the treatment of rheumatoid arthritis and osteomyelofibrosis, respectively.

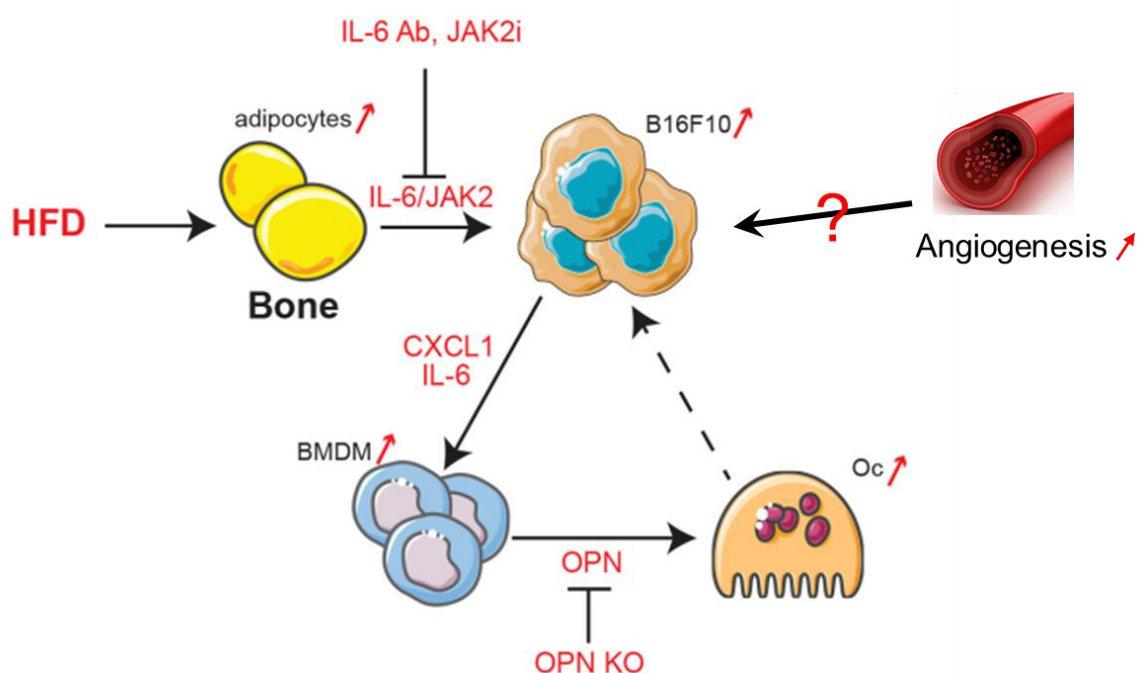


Figure 4.1 A model of crosstalk between tumor cells, adipocytes, macrophages and angiogenesis in HFD bone tumor microenvironment.

5 References

- Acharyya, S., Oskarsson, T., Vanharanta, S., *et al.* (2012). A CXCL1 paracrine network links cancer chemoresistance and metastasis. *Cell* 150, 165-178.
- AE Lohmann, M.C., RJO Dowling, M Ennis, E Amir, C Elser, C Brezden-Masley, T Vandenberg, E Lee, K Fazae, V Stambolic, PJ Goodwin (2016). Abstract P2-02-12: Association of inflammatory and tumor markers with circulating tumor cells in metastatic breast cancer. *Cancer Research* 76.
- Aebi, M. (2003). Spinal metastasis in the elderly. *Eur Spine J* 12 *Suppl* 2, S202-213.
- Akunuru, S., Palumbo, J., Zhai, Q.J., and Zheng, Y. (2011). Rac1 targeting suppresses human non-small cell lung adenocarcinoma cancer stem cell activity. *PLoS One* 6, e16951.
- Al-Daghri, N.M., Bindahman, L.S., Al-Attas, O.S., Saleem, T.H., Alokail, M.S., Alkharfy, K.M., Draz, H.M., Yakout, S., Mohamed, A.O., Harte, A.L., and McTernan, P.G. (2012). Increased circulating ANG II and TNF-alpha represents important risk factors in obese saudi adults with hypertension irrespective of diabetic status and BMI. *PLoS One* 7, e51255.
- Alasvand, M., Rashidi, B., Haghjooy Javanmard, S., and Khazaei, M. (2015). Effect of blockade of neuropeptide Y receptor on aortic intima-media thickness and adipose tissue characteristics in normal and obese mice. *Iran J Basic Med Sci* 18, 443-448.
- Amjadi, F., Javanmard, S.H., Zarkesh-Esfahani, H., Khazaei, M., and Narimani, M. (2011). Leptin promotes melanoma tumor growth in mice related to increasing circulating endothelial progenitor cells numbers and plasma NO production. *J Exp Clin Cancer Res* 30, 21.
- Andarawewa, K.L., Motrescu, E.R., Chenard, M.P., Gansmuller, A., Stoll, I., Tomasetto, C., and Rio, M.C. (2005). Stromelysin-3 is a potent negative regulator of adipogenesis participating to cancer cell-adipocyte interaction/crosstalk at the tumor invasive front. *Cancer Res* 65, 10862-10871.
- Antoniadis, A.G., Petridou, E.T., Antonopoulos, C.N., Dessypris, N., Panagopoulou, P., Chamberland, J.P., Adami, H.O., Gogas, H., and Mantzoros, C.S. (2011). Insulin resistance in relation to melanoma risk. *Melanoma Res* 21, 541-546.
- Ara, T., and Declerck, Y.A. (2010). Interleukin-6 in bone metastasis and cancer progression. *Eur J Cancer* 46, 1223-1231.
- Arendt, L.M., McCready, J., Keller, P.J., Baker, D.D., Naber, S.P., Seewaldt, V., and Kuperwasser, C. (2013). Obesity promotes breast cancer by CCL2-mediated macrophage recruitment and angiogenesis. *Cancer Res* 73, 6080-6093.
- Bakewell, S.J., Nestor, P., Prasad, S., Tomasson, M.H., Dowland, N., Mehrotra, M., Scarborough, R., Kanter, J., Abe, K., Phillips, D., and Weilbaecher, K.N. (2003).

- Platelet and osteoclast beta3 integrins are critical for bone metastasis. *Proc Natl Acad Sci U S A* 100, 14205-14210.
- Bald, T., Quast, T., Landsberg, J., *et al.* (2014). Ultraviolet-radiation-induced inflammation promotes angiotropism and metastasis in melanoma. *Nature* 507, 109-113.
- Bataille, V. (2009 -a). Epidemiology. Melanoma Molecular Map Project.
- Bataille, V. (2009 -b). Risk factors. Melanoma Molecular Map Project.
- Bedogni, B., and Powell, M.B. (2009). Hypoxia, melanocytes and melanoma - survival and tumor development in the permissive microenvironment of the skin. *Pigment Cell Melanoma Res* 22, 166-174.
- Belaid-Choucair, Z., Lepelletier, Y., Poncin, G., *et al.* (2008). Human bone marrow adipocytes block granulopoiesis through neuropilin-1-induced granulocyte colony-stimulating factor inhibition. *Stem Cells* 26, 1556-1564.
- Berrington de Gonzalez, A., Hartge, P., Cerhan, J.R., *et al.* (2010). Body-mass index and mortality among 1.46 million white adults. *N Engl J Med* 363, 2211-2219.
- Blucher, M. (2013). Adipose tissue dysfunction contributes to obesity related metabolic diseases. *Best Pract Res Clin Endocrinol Metab* 27, 163-177.
- Bochet, L., Lehuede, C., Dauvillier, S., *et al.* (2013). Adipocyte-derived fibroblasts promote tumor progression and contribute to the desmoplastic reaction in breast cancer. *Cancer Res* 73, 5657-5668.
- Bochet, L., Meulle, A., Imbert, S., Salles, B., Valet, P., and Muller, C. (2011). Cancer-associated adipocytes promotes breast tumor radioresistance. *Biochem Biophys Res Commun* 411, 102-106.
- Boespflug, A., and Thomas, L. (2016). Cobimetinib and vemurafenib for the treatment of Melanoma. *Expert Opin Pharmacother*.
- Bostel, T., Forster, R., Schlampp, I., Wolf, R., Serras, A.F., Mayer, A., Bruckner, T., Welzel, T., Schmidberger, H., Debus, J., and Rief, H. (2015). Stability, prognostic factors and survival of spinal bone metastases in malignant melanoma patients after palliative radiotherapy. *Tumori*, 0.
- Bowers, L.W., Cavazos, D.A., Maximo, I.X., Brenner, A.J., Hursting, S.D., and deGraffenried, L.A. (2013). Obesity enhances nongenomic estrogen receptor crosstalk with the PI3K/Akt and MAPK pathways to promote in vitro measures of breast cancer progression. *Breast cancer research : BCR* 15, R59.
- Braeuer, R.R., Watson, I.R., Wu, C.J., Mobley, A.K., Kamiya, T., Shoshan, E., and Bar-Eli, M. (2014). Why is melanoma so metastatic? *Pigment Cell Melanoma Res* 27, 19-36.
- Brandon, E.L., Gu, J.W., Cantwell, L., He, Z., Wallace, G., and Hall, J.E. (2009). Obesity promotes melanoma tumor growth: role of leptin. *Cancer Biol Ther* 8, 1871-1879.

- Broutzos, E., Panagiotou, I., Bafaloukos, D., and Kelekis, D. (2001). Bone metastases from malignant melanoma: a retrospective review and analysis of 28 cases. *Radiology and Oncology* 35.
- Bryden, A.A., Islam, S., Freemont, A.J., Shanks, J.H., George, N.J., and Clarke, N.W. (2002). Parathyroid hormone-related peptide: expression in prostate cancer bone metastases. *Prostate Cancer Prostatic Dis* 5, 59-62.
- Buijs, J.T., Kuijpers, C.C., and van der Pluijm, G. (2010). Targeted therapy options for treatment of bone metastases; beyond bisphosphonates. *Curr Pharm Des* 16, 3015-3027.
- Caers, J., Deleu, S., Belaid, Z., De Raeve, H., Van Valckenborgh, E., De Bruyne, E., Defresne, M.P., Van Riet, I., Van Camp, B., and Vanderkerken, K. (2007). Neighboring adipocytes participate in the bone marrow microenvironment of multiple myeloma cells. *Leukemia* 21, 1580-1584.
- Calle, E.E., and Kaaks, R. (2004). Overweight, obesity and cancer: epidemiological evidence and proposed mechanisms. *Nat Rev Cancer* 4, 579-591.
- Calle, E.E., Rodriguez, C., Walker-Thurmond, K., and Thun, M.J. (2003). Overweight, obesity, and mortality from cancer in a prospectively studied cohort of U.S. adults. *N Engl J Med* 348, 1625-1638.
- Calvo, M.B., Figueroa, A., Pulido, E.G., Campelo, R.G., and Aparicio, L.A. (2010). Potential role of sugar transporters in cancer and their relationship with anticancer therapy. *Int J Endocrinol* 2010.
- Carlinfante, G., Vassiliou, D., Svensson, O., Wendel, M., Heinegard, D., and Andersson, G. (2003). Differential expression of osteopontin and bone sialoprotein in bone metastasis of breast and prostate carcinoma. *Clin Exp Metastasis* 20, 437-444.
- Cawthorn, W.P., Scheller, E.L., Learman, B.S., *et al.* (2014). Bone marrow adipose tissue is an endocrine organ that contributes to increased circulating adiponectin during caloric restriction. *Cell Metab* 20, 368-375.
- Cetin, K., Christiansen, C.F., Jacobsen, J.B., Norgaard, M., and Sorensen, H.T. (2014). Bone metastasis, skeletal-related events, and mortality in lung cancer patients: a Danish population-based cohort study. *Lung Cancer* 86, 247-254.
- Chambers, A.F., Groom, A.C., and MacDonald, I.C. (2002). Dissemination and growth of cancer cells in metastatic sites. *Nat Rev Cancer* 2, 563-572.
- Chang, Y.S., Chen, W.Y., Yin, J.J., Sheppard-Tillman, H., Huang, J., and Liu, Y.N. (2015). EGF Receptor Promotes Prostate Cancer Bone Metastasis by Downregulating miR-1 and Activating TWIST1. *Cancer Res* 75, 3077-3086.
- Chen, G.L., Luo, Y., Eriksson, D., Meng, X., Qian, C., Bauerle, T., Chen, X.X., Schett, G., and Bozec, A. (2016). High fat diet increases melanoma cell growth in the bone marrow by inducing osteopontin and interleukin 6. *oncotarget*.

- Chen, J. (2010). The IL-23/IL-17 axis may be important in obesity-associated cancer by way of the activation of multiple signal pathways. *Int J Obes (Lond)* *34*, 1227-1228; author reply 1229.
- Chen, J., Chi, M., Chen, C., and Zhang, X.D. (2013). Obesity and melanoma: exploring molecular links. *J Cell Biochem* *114*, 1955-1961.
- Chen, Y.C., Sosnoski, D.M., and Mastro, A.M. (2010). Breast cancer metastasis to the bone: mechanisms of bone loss. *Breast Cancer Res* *12*, 215.
- Chi, M., Chen, J., Ye, Y., Tseng, H.Y., Lai, F., Tay, K.H., Jin, L., Guo, S.T., Jiang, C.C., and Zhang, X.D. (2014). Adipocytes contribute to resistance of human melanoma cells to chemotherapy and targeted therapy. *Curr Med Chem* *21*, 1255-1267.
- Coelho, P., Almeida, J., Prudencio, C., Fernandes, R., and Soares, R. (2015). Effect of Adipocyte Secretome in Melanoma Progression and Vasculogenic Mimicry. *J Cell Biochem*.
- Costache, M., Stoica, A., Contolenco, A., Costache, D., Cirstoiu, C., Simionescu, O., and George, S. (2014). Metastatic Melanoma in the Femur - Case Report with Review of Literature: a Pathologist's Point of View. *Maedica (Buchar)* *9*, 62-67.
- Cox, T.R., Rumney, R.M., Schoof, E.M., *et al.* (2015). The hypoxic cancer secretome induces pre-metastatic bone lesions through lysyl oxidase. *Nature* *522*, 106-110.
- Croset, M., Goehrig, D., Frackowiak, A., Bonnelye, E., Ansieau, S., Puisieux, A., and Clezardin, P. (2014). TWIST1 expression in breast cancer cells facilitates bone metastasis formation. *J Bone Miner Res* *29*, 1886-1899.
- Croucher, P.I., McDonald, M.M., and Martin, T.J. (2016). Bone metastasis: the importance of the neighbourhood. *Nat Rev Cancer* *16*, 373-386.
- Dai, J., Peng, L., Fan, K., *et al.* (2009). Osteopontin induces angiogenesis through activation of PI3K/AKT and ERK1/2 in endothelial cells. *Oncogene* *28*, 3412-3422.
- Dalmas, E., Rouault, C., Abdennour, M., Rovere, C., Rizkalla, S., Bar-Hen, A., Nahon, J.L., Bouillot, J.L., Guerre-Millo, M., Clement, K., and Poitou, C. (2011). Variations in circulating inflammatory factors are related to changes in calorie and carbohydrate intakes early in the course of surgery-induced weight reduction. *Am J Clin Nutr* *94*, 450-458.
- Daniell, H.W. (1996). A better prognosis for obese men with prostate cancer. *J Urol* *155*, 220-225.
- de Ferranti, S., and Mozaffarian, D. (2008). The perfect storm: obesity, adipocyte dysfunction, and metabolic consequences. *Clin Chem* *54*, 945-955.
- De Pergola, G., and Silvestris, F. (2013). Obesity as a major risk factor for cancer. *J Obes* *2013*, 291546.
- Dennis, L.K., Lowe, J.B., Lynch, C.F., and Alavanja, M.C. (2008). Cutaneous melanoma and obesity in the Agricultural Health Study. *Ann Epidemiol* *18*, 214-221.

- des Grottes, J.M., Dumon, J.C., and Body, J.J. (2001). Hypercalcaemia of melanoma: incidence, pathogenesis and therapy with bisphosphonates. *Melanoma Res* *11*, 477-482.
- Desmet, C.J., Gallenne, T., Prieur, A., *et al.* (2013). Identification of a pharmacologically tractable Fra-1/ADORA2B axis promoting breast cancer metastasis. *Proc Natl Acad Sci U S A* *110*, 5139-5144.
- Diarra, D., Stolina, M., Polzer, K., *et al.* (2007). Dickkopf-1 is a master regulator of joint remodeling. *Nat Med* *13*, 156-163.
- Diedrich, J., Gusky, H.C., and Podgorski, I. (2015). Adipose tissue dysfunction and its effects on tumor metabolism. *Horm Mol Biol Clin Investig* *21*, 17-41.
- Dirat, B., Bochet, L., Dabek, M., *et al.* (2011). Cancer-associated adipocytes exhibit an activated phenotype and contribute to breast cancer invasion. *Cancer Res* *71*, 2455-2465.
- Dougall, W.C., Holen, I., and Gonzalez Suarez, E. (2014). Targeting RANKL in metastasis. *Bonekey Rep* *3*, 519.
- Dunn, L.K., Mohammad, K.S., Fournier, P.G., McKenna, C.R., Davis, H.W., Niewolna, M., Peng, X.H., Chirgwin, J.M., and Guise, T.A. (2009). Hypoxia and TGF-beta drive breast cancer bone metastases through parallel signaling pathways in tumor cells and the bone microenvironment. *PLoS One* *4*, e6896.
- Ell, B., and Kang, Y. (2014). MicroRNAs as regulators of bone homeostasis and bone metastasis. *Bonekey Rep* *3*, 549.
- Ell, B., and Kang, Y. (2012). SnapShot: Bone Metastasis. *Cell* *151*, 690-690 e691.
- Ell, B., and Kang, Y. (2013). Transcriptional control of cancer metastasis. *Trends Cell Biol* *23*, 603-611.
- Ellerhorst, J.A., Diwan, A.H., Dang, S.M., Uffort, D.G., Johnson, M.K., Cooke, C.P., and Grimm, E.A. (2010). Promotion of melanoma growth by the metabolic hormone leptin. *Oncol Rep* *23*, 901-907.
- Erler, J.T., Bennewith, K.L., Cox, T.R., Lang, G., Bird, D., Koong, A., Le, Q.T., and Giaccia, A.J. (2009). Hypoxia-induced lysyl oxidase is a critical mediator of bone marrow cell recruitment to form the premetastatic niche. *Cancer Cell* *15*, 35-44.
- Fantozzi, A., and Christofori, G. (2006). Mouse models of breast cancer metastasis. *Breast Cancer Res* *8*, 212.
- Fidler, I.J. (2003). The pathogenesis of cancer metastasis: the 'seed and soil' hypothesis revisited. *Nat Rev Cancer* *3*, 453-458.
- Foundation., M.R. (2015). Melanoma Facts and Stats.
- Francia, G., Cruz-Munoz, W., Man, S., Xu, P., and Kerbel, R.S. (2011). Mouse models of advanced spontaneous metastasis for experimental therapeutics. *Nat Rev Cancer* *11*, 135-141.
- Franzen, A., and Heinegard, D. (1985). Isolation and characterization of two sialoproteins present only in bone calcified matrix. *Biochem J* *232*, 715-724.

- Friedman, G.D., and Herrinton, L.J. (1994). Obesity and multiple myeloma. *Cancer Causes Control* 5, 479-483.
- Frystyk, J., Skjaerbaek, C., Vestbo, E., Fisker, S., and Orskov, H. (1999). Circulating levels of free insulin-like growth factors in obese subjects: the impact of type 2 diabetes. *Diabetes Metab Res Rev* 15, 314-322.
- Furugaki, K., Moriya, Y., Iwai, T., Yorozu, K., Yanagisawa, M., Kondoh, K., Fujimoto-Ohuchi, K., and Mori, K. (2011). Erlotinib inhibits osteolytic bone invasion of human non-small-cell lung cancer cell line NCI-H292. *Clin Exp Metastasis* 28, 649-659.
- Gay, L.J., and Felding-Habermann, B. (2011). Contribution of platelets to tumour metastasis. *Nat Rev Cancer* 11, 123-134.
- Gislette, T., and Chen, J. (2010). The possible role of IL-17 in obesity-associated cancer. *ScientificWorldJournal* 10, 2265-2271.
- Gogas, H., Trakatelli, M., Dessypris, N., Terzidis, A., Katsambas, A., Chrousos, G.P., and Petridou, E.T. (2008). Melanoma risk in association with serum leptin levels and lifestyle parameters: a case-control study. *Ann Oncol* 19, 384-389.
- Gordon, K.J., Kirkbride, K.C., How, T., and Blobe, G.C. (2009). Bone morphogenetic proteins induce pancreatic cancer cell invasiveness through a Smad1-dependent mechanism that involves matrix metalloproteinase-2. *Carcinogenesis* 30, 238-248.
- Goto, H., Hozumi, A., Osaki, M., Fukushima, T., Sakamoto, K., Yonekura, A., Tomita, M., Furukawa, K., Shindo, H., and Baba, H. (2011). Primary human bone marrow adipocytes support TNF-alpha-induced osteoclast differentiation and function through RANKL expression. *Cytokine* 56, 662-668.
- Greenberg, A.S., and Obin, M.S. (2006). Obesity and the role of adipose tissue in inflammation and metabolism. *Am J Clin Nutr* 83, 461S-465S.
- Gregor, M.F., and Hotamisligil, G.S. (2011). Inflammatory mechanisms in obesity. *Annu Rev Immunol* 29, 415-445.
- Gu, J.W., Young, E., Patterson, S.G., Makey, K.L., Wells, J., Huang, M., Tucker, K.B., and Miele, L. (2011). Postmenopausal obesity promotes tumor angiogenesis and breast cancer progression in mice. *Cancer Biol Ther* 11, 910-917.
- Hall, A., Meyle, K.D., Lange, M.K., *et al.* (2013). Dysfunctional oxidative phosphorylation makes malignant melanoma cells addicted to glycolysis driven by the (V600E)BRAF oncogene. *Oncotarget* 4, 584-599.
- Hanoun, M., Zhang, D., Mizoguchi, T., Pinho, S., Pierce, H., Kunisaki, Y., Lacombe, J., Armstrong, S.A., Duhrsen, U., and Frenette, P.S. (2014). Acute myelogenous leukemia-induced sympathetic neuropathy promotes malignancy in an altered hematopoietic stem cell niche. *Cell Stem Cell* 15, 365-375.
- Hardaway, A.L. (2015). Adipocyte-Induced Inflammation In Prostate Tumor Progression In Bone: Role Of Cxcr2 And Osteopontin.

- Hardaway, A.L., Herroon, M.K., Rajagurubandara, E., and Podgorski, I. (2014). Bone marrow fat: linking adipocyte-induced inflammation with skeletal metastases. *Cancer Metastasis Rev* 33, 527-543.
- Hardaway, A.L., Herroon, M.K., Rajagurubandara, E., and Podgorski, I. (2015). Marrow adipocyte-derived CXCL1 and CXCL2 contribute to osteolysis in metastatic prostate cancer. *Clin Exp Metastasis* 32, 353-368.
- Hayashi, C., Rittling, S., Hayata, T., Amagasa, T., Denhardt, D., Ezura, Y., Nakashima, K., and Noda, M. (2007). Serum osteopontin, an enhancer of tumor metastasis to bone, promotes B16 melanoma cell migration. *J Cell Biochem* 101, 979-986.
- Hayashida, T. (2010). Integrins modulate cellular fibrogenesis at multiple levels; Regulation of TGF-beta signaling. *Endocr Metab Immune Disord Drug Targets* 10, 302-319.
- He, Q., Gao, Z., Yin, J., Zhang, J., Yun, Z., and Ye, J. (2011). Regulation of HIF-1{alpha} activity in adipose tissue by obesity-associated factors: adipogenesis, insulin, and hypoxia. *Am J Physiol Endocrinol Metab* 300, E877-885.
- Herroon, M.K., Rajagurubandara, E., Hardaway, A.L., Powell, K., Turchick, A., Feldmann, D., and Podgorski, I. (2013). Bone marrow adipocytes promote tumor growth in bone via FABP4-dependent mechanisms. *Oncotarget* 4, 2108-2123.
- Hersey, P., Watts, R.N., Zhang, X.D., and Hackett, J. (2009). Metabolic approaches to treatment of melanoma. *Clin Cancer Res* 15, 6490-6494.
- Hiraga, T., Myoui, A., Hashimoto, N., Sasaki, A., Hata, K., Morita, Y., Yoshikawa, H., Rosen, C.J., Mundy, G.R., and Yoneda, T. (2012). Bone-derived IGF mediates crosstalk between bone and breast cancer cells in bony metastases. *Cancer Res* 72, 4238-4249.
- Hiraga, T., Nakajima, T., and Ozawa, H. (1995). Bone resorption induced by a metastatic human melanoma cell line. *Bone* 16, 349-356.
- Hirano, T., Morii, H., Nakazawa, K., Murakami, D., Yamashita, A., Asahi, J., Orimo, H., Tamae, K., and Tokura, Y. (2008). Enhancement of adipogenesis induction by conditioned media obtained from cancer cells. *Cancer Lett* 268, 286-294.
- Hirbe, A.C., Roelofs, A.J., Floyd, D.H., *et al.* (2009). The bisphosphonate zoledronic acid decreases tumor growth in bone in mice with defective osteoclasts. *Bone* 44, 908-916.
- Hirbe, A.C., Uluckan, O., Morgan, E.A., Eagleton, M.C., Prior, J.L., Piwnica-Worms, D., Trinkaus, K., Apicelli, A., and Weilbaecher, K. (2007). Granulocyte colony-stimulating factor enhances bone tumor growth in mice in an osteoclast-dependent manner. *Blood* 109, 3424-3431.
- Hodi, F.S., O'Day, S.J., McDermott, D.F., *et al.* (2010). Improved survival with ipilimumab in patients with metastatic melanoma. *N Engl J Med* 363, 711-723.
- Hoejberg, L., Bastholt, L., and Schmidt, H. (2012). Interleukin-6 and melanoma. *Melanoma Res* 22, 327-333.

- Hoshino, A., Costa-Silva, B., Shen, T.L., *et al.* (2015). Tumour exosome integrins determine organotropic metastasis. *Nature* 527, 329-335.
- Hozumi, A., Osaki, M., Goto, H., Sakamoto, K., Inokuchi, S., and Shindo, H. (2009). Bone marrow adipocytes support dexamethasone-induced osteoclast differentiation. *Biochem Biophys Res Commun* 382, 780-784.
- Huang, S., and Czech, M.P. (2007). The GLUT4 glucose transporter. *Cell Metab* 5, 237-252.
- Hugo, W., Zaretsky, J.M., Sun, L., *et al.* (2016). Genomic and Transcriptomic Features of Response to Anti-PD-1 Therapy in Metastatic Melanoma. *Cell*.
- Hursting, S.D., and Hursting, M.J. (2012). Growth signals, inflammation, and vascular perturbations: mechanistic links between obesity, metabolic syndrome, and cancer. *Arterioscler Thromb Vasc Biol* 32, 1766-1770.
- Hurt, R.T., Kulisek, C., Buchanan, L.A., and McClave, S.A. (2010). The obesity epidemic: challenges, health initiatives, and implications for gastroenterologists. *Gastroenterol Hepatol (N Y)* 6, 780-792.
- Ibrahim, T., Leong, I., Sanchez-Sweatman, O., Khokha, R., Sodek, J., Tenenbaum, H.C., Ganss, B., and Cheifetz, S. (2000). Expression of bone sialoprotein and osteopontin in breast cancer bone metastases. *Clin Exp Metastasis* 18, 253-260.
- Inada, M., Takita, M., Yokoyama, S., *et al.* (2015). Direct Melanoma Cell Contact Induces Stromal Cell Autocrine Prostaglandin E2-EP4 Receptor Signaling That Drives Tumor Growth, Angiogenesis, and Metastasis. *J Biol Chem* 290, 29781-29793.
- Innocenzi, D., Alo, P.L., Balzani, A., Sebastiani, V., Silipo, V., La Torre, G., Ricciardi, G., Bosman, C., and Calvieri, S. (2003). Fatty acid synthase expression in melanoma. *J Cutan Pathol* 30, 23-28.
- Institute, N.C. (2012). Obesity and Cancer Risk.
- Ito, K., and Suda, T. (2014). Metabolic requirements for the maintenance of self-renewing stem cells. *Nat Rev Mol Cell Biol* 15, 243-256.
- Iyengar, N.M., Hudis, C.A., and Dannenberg, A.J. (2013). Obesity and inflammation: new insights into breast cancer development and progression. *Am Soc Clin Oncol Educ Book*, 46-51.
- Iyer, A., Fairlie, D.P., Prins, J.B., Hammock, B.D., and Brown, L. (2010). Inflammatory lipid mediators in adipocyte function and obesity. *Nat Rev Endocrinol* 6, 71-82.
- Jain, D., Singh, T., Kumar, N., and Daga, M.K. (2007). Metastatic malignant melanoma in bone marrow with occult primary site--a case report with review of literature. *Diagn Pathol* 2, 38.
- Jiang, C., Kim, J.H., Li, F., Qu, A., Gavrilova, O., Shah, Y.M., and Gonzalez, F.J. (2013). Hypoxia-inducible factor 1alpha regulates a SOCS3-STAT3-adiponectin signal transduction pathway in adipocytes. *J Biol Chem* 288, 3844-3857.

- Jones, D.H., Nakashima, T., Sanchez, O.H., *et al.* (2006). Regulation of cancer cell migration and bone metastasis by RANKL. *Nature* *440*, 692-696.
- Jones, S.A., Scheller, J., and Rose-John, S. (2011). Therapeutic strategies for the clinical blockade of IL-6/gp130 signaling. *J Clin Invest* *121*, 3375-3383.
- Jour, G., Ivan, D., and Aung, P.P. (2016). Angiogenesis in melanoma: an update with a focus on current targeted therapies. *J Clin Pathol*.
- Jung, J.I., Cho, H.J., Jung, Y.J., Kwon, S.H., Her, S., Choi, S.S., Shin, S.H., Lee, K.W., and Park, J.H. (2015). High-fat diet-induced obesity increases lymphangiogenesis and lymph node metastasis in the B16F10 melanoma allograft model: roles of adipocytes and M2-macrophages. *Int J Cancer* *136*, 258-270.
- Jung, U.J., and Choi, M.S. (2014). Obesity and its metabolic complications: the role of adipokines and the relationship between obesity, inflammation, insulin resistance, dyslipidemia and nonalcoholic fatty liver disease. *Int J Mol Sci* *15*, 6184-6223.
- Justesen, J., Stenderup, K., Ebbesen, E.N., Mosekilde, L., Steiniche, T., and Kassem, M. (2001). Adipocyte tissue volume in bone marrow is increased with aging and in patients with osteoporosis. *Biogerontology* *2*, 165-171.
- Kabir, S.M., Lee, E.S., and Son, D.S. (2014). Chemokine network during adipogenesis in 3T3-L1 cells: Differential response between growth and proinflammatory factor in preadipocytes vs. adipocytes. *Adipocyte* *3*, 97-106.
- Kahles, F., Findeisen, H.M., and Bruemmer, D. (2014). Osteopontin: A novel regulator at the cross roads of inflammation, obesity and diabetes. *Mol Metab* *3*, 384-393.
- Kaidar-Person, O., Bar-Sela, G., and Person, B. (2011). The two major epidemics of the twenty-first century: obesity and cancer. *Obes Surg* *21*, 1792-1797.
- Kale, S., Raja, R., Thorat, D., Soundararajan, G., Patil, T.V., and Kundu, G.C. (2014). Osteopontin signaling upregulates cyclooxygenase-2 expression in tumor-associated macrophages leading to enhanced angiogenesis and melanoma growth via alpha9beta1 integrin. *Oncogene* *33*, 2295-2306.
- Kang, Y., Siegel, P.M., Shu, W., Drobnjak, M., Kakonen, S.M., Cordon-Cardo, C., Guise, T.A., and Massague, J. (2003). A multigenic program mediating breast cancer metastasis to bone. *Cancer Cell* *3*, 537-549.
- Karnieli, E., and Armoni, M. (2008). Transcriptional regulation of the insulin-responsive glucose transporter GLUT4 gene: from physiology to pathology. *Am J Physiol Endocrinol Metab* *295*, E38-45.
- Khan, N.I., Naz, L., and Yasmeen, G. (2006). Obesity: an independent risk factor for systemic oxidative stress. *Pak J Pharm Sci* *19*, 62-65.
- Khandekar, M.J., Cohen, P., and Spiegelman, B.M. (2011). Molecular mechanisms of cancer development in obesity. *Nat Rev Cancer* *11*, 886-895.
- Kim, E.J., Choi, M.R., Park, H., Kim, M., Hong, J.E., Lee, J.Y., Chun, H.S., Lee, K.W., and Yoon Park, J.H. (2011a). Dietary fat increases solid tumor growth and metastasis

- of 4T1 murine mammary carcinoma cells and mortality in obesity-resistant BALB/c mice. *Breast Cancer Res* *13*, R78.
- Kim, H., Cho, H.J., Kim, S.W., Liu, B., Choi, Y.J., Lee, J., Sohn, Y.D., Lee, M.Y., Houge, M.A., and Yoon, Y.S. (2010a). CD31+ cells represent highly angiogenic and vasculogenic cells in bone marrow: novel role of nonendothelial CD31+ cells in neovascularization and their therapeutic effects on ischemic vascular disease. *Circ Res* *107*, 602-614.
- Kim, J.H., and Kim, N. (2014). Regulation of NFATc1 in Osteoclast Differentiation. *J Bone Metab* *21*, 233-241.
- Kim, S.W., Kim, H., Cho, H.J., Lee, J.U., Levit, R., and Yoon, Y.S. (2010b). Human peripheral blood-derived CD31+ cells have robust angiogenic and vasculogenic properties and are effective for treating ischemic vascular disease. *J Am Coll Cardiol* *56*, 593-607.
- Kim, S.W., Kim, J.S., Papadopoulos, J., Choi, H.J., He, J., Maya, M., Langley, R.R., Fan, D., Fidler, I.J., and Kim, S.J. (2011b). Consistent interactions between tumor cell IL-6 and macrophage TNF-alpha enhance the growth of human prostate cancer cells in the bone of nude mouse. *Int Immunopharmacol* *11*, 862-872.
- Kiss, T., Ecsedi, S., Vizkeleti, L., Koroknai, V., Emri, G., Kovacs, N., Adany, R., and Balazs, M. (2015). The role of osteopontin expression in melanoma progression. *Tumour Biol* *36*, 7841-7847.
- Kloting, N., and Bluher, M. (2014). Adipocyte dysfunction, inflammation and metabolic syndrome. *Rev Endocr Metab Disord* *15*, 277-287.
- Krings, A., Rahman, S., Huang, S., Lu, Y., Czernik, P.J., and Lecka-Czernik, B. (2012). Bone marrow fat has brown adipose tissue characteristics, which are attenuated with aging and diabetes. *Bone* *50*, 546-552.
- Kruger, T.E., Miller, A.H., Godwin, A.K., and Wang, J. (2014). Bone sialoprotein and osteopontin in bone metastasis of osteotropic cancers. *Crit Rev Oncol Hematol* *89*, 330-341.
- Kruglikov, I.L., Scherer, P.E., and Wollina, U. (2016). Are dermal adipocytes involved in psoriasis? *Exp Dermatol*.
- Kucerova, L., and Skolekova, S. (2013). Tumor microenvironment and the role of mesenchymal stromal cells. *Neoplasma* *60*, 1-10.
- Kudo-Saito, C., Fuwa, T., Murakami, K., and Kawakami, Y. (2013). Targeting FSTL1 prevents tumor bone metastasis and consequent immune dysfunction. *Cancer Res* *73*, 6185-6193.
- Kudo-Saito, C., Shirako, H., Takeuchi, T., and Kawakami, Y. (2009). Cancer metastasis is accelerated through immunosuppression during Snail-induced EMT of cancer cells. *Cancer Cell* *15*, 195-206.

- Kumar, S., Sharma, P., Kumar, D., Chakraborty, G., Gorain, M., and Kundu, G.C. (2013). Functional characterization of stromal osteopontin in melanoma progression and metastasis. *PLoS One* 8, e69116.
- Kushiro, K., Chu, R.A., Verma, A., and Nunez, N.P. (2012). Adipocytes Promote B16BL6 Melanoma Cell Invasion and the Epithelial-to-Mesenchymal Transition. *Cancer Microenviron* 5, 73-82.
- Kushiro, K., and Nunez, N.P. (2011). Ob/ob serum promotes a mesenchymal cell phenotype in B16BL6 melanoma cells. *Clin Exp Metastasis* 28, 877-886.
- Kwan, H.Y., Fu, X., Liu, B., Chao, X., Chan, C.L., Cao, H., Su, T., Tse, A.K., Fong, W.F., and Yu, Z.L. (2014). Subcutaneous adipocytes promote melanoma cell growth by activating the Akt signaling pathway: role of palmitic acid. *J Biol Chem* 289, 30525-30537.
- Kwan Tat, S., Padrines, M., Theoleyre, S., Heymann, D., and Fortun, Y. (2004). IL-6, RANKL, TNF-alpha/IL-1: interrelations in bone resorption pathophysiology. *Cytokine Growth Factor Rev* 15, 49-60.
- Laharrague, P., Larrouy, D., Fontanilles, A.M., Truel, N., Campfield, A., Tenenbaum, R., Galitzky, J., Corberand, J.X., Penicaud, L., and Casteilla, L. (1998). High expression of leptin by human bone marrow adipocytes in primary culture. *FASEB J* 12, 747-752.
- Laharrague, P., Oppert, J.M., Brousset, P., Charlet, J.P., Campfield, A., Fontanilles, A.M., Guy-Grand, B., Corberand, J.X., Penicaud, L., and Casteilla, L. (2000a). High concentration of leptin stimulates myeloid differentiation from human bone marrow CD34+ progenitors: potential involvement in leukocytosis of obese subjects. *Int J Obes Relat Metab Disord* 24, 1212-1216.
- Laharrague, P., Truel, N., Fontanilles, A.M., Corberand, J.X., Penicaud, L., and Casteilla, L. (2000b). Regulation by cytokines of leptin expression in human bone marrow adipocytes. *Horm Metab Res* 32, 381-385.
- Lau, Y.S., Sabokbar, A., Giele, H., Cerundolo, V., Hofstetter, W., and Athanasou, N.A. (2006). Malignant melanoma and bone resorption. *Br J Cancer* 94, 1496-1503.
- Lecka-Czernik, B., Rosen, C.J., and Kawai, M. (2010). Skeletal aging and the adipocyte program: New insights from an "old" molecule. *Cell Cycle* 9, 3648-3654.
- Lee, J.H., Kim, H.N., Kim, K.O., Jin, W.J., Lee, S., Kim, H.H., Ha, H., and Lee, Z.H. (2012). CXCL10 promotes osteolytic bone metastasis by enhancing cancer outgrowth and osteoclastogenesis. *Cancer Res* 72, 3175-3186.
- Lee, Y.H., Petkova, A.P., and Granneman, J.G. (2013). Identification of an adipogenic niche for adipose tissue remodeling and restoration. *Cell Metab* 18, 355-367.
- Li, J., Karaplis, A.C., Huang, D.C., Siegel, P.M., Camirand, A., Yang, X.F., Muller, W.J., and Kremer, R. (2011). PTHrP drives breast tumor initiation, progression, and metastasis in mice and is a potential therapy target. *J Clin Invest* 121, 4655-4669.

- Li, Y., Malaeb, B.S., Li, Z.Z., Thompson, M.G., Chen, Z., Corey, D.R., Hsieh, J.T., Shay, J.W., and Koeneman, K.S. (2010). Telomerase enzyme inhibition (TEI) and cytolytic therapy in the management of androgen independent osseous metastatic prostate cancer. *Prostate* 70, 616-629.
- Lichtman, M.A. (2010). Obesity and the risk for a hematological malignancy: leukemia, lymphoma, or myeloma. *Oncologist* 15, 1083-1101.
- Lim, Y.Z., Wang, Y., Wluka, A.E., Davies-Tuck, M.L., Hanna, F., Urquhart, D.M., and Cicuttini, F.M. (2014). Association of obesity and systemic factors with bone marrow lesions at the knee: a systematic review. *Semin Arthritis Rheum* 43, 600-612.
- Lin, C.N., Wang, C.J., Chao, Y.J., Lai, M.D., and Shan, Y.S. (2015). The significance of the co-existence of osteopontin and tumor-associated macrophages in gastric cancer progression. *BMC Cancer* 15, 128.
- Liu, Y., and Cao, X. (2016). Organotropic metastasis: role of tumor exosomes. *Cell Res* 26, 149-150.
- Liu, Y., Zhang, N., Wang, Y., Xu, M., Liu, N., Pang, X., Cao, J., Ma, N., Pang, H., Liu, L., and Zhang, H. (2012). Zinc finger E-box binding homeobox 1 promotes invasion and bone metastasis of small cell lung cancer in vitro and in vivo. *Cancer Sci* 103, 1420-1428.
- Liu, Y.N., Yin, J., Barrett, B., Sheppard-Tillman, H., Li, D., Casey, O.M., Fang, L., Hynes, P.G., Ameri, A.H., and Kelly, K. (2015). Loss of Androgen-Regulated MicroRNA 1 Activates SRC and Promotes Prostate Cancer Bone Metastasis. *Mol Cell Biol* 35, 1940-1951.
- Livak, K.J., and Schmittgen, T.D. (2001). Analysis of relative gene expression data using real-time quantitative PCR and the 2(-Delta Delta C(T)) Method. *Methods* 25, 402-408.
- Louer, C.R., Furman, B.D., Huebner, J.L., Kraus, V.B., Olson, S.A., and Guilak, F. (2012). Diet-induced obesity significantly increases the severity of posttraumatic arthritis in mice. *Arthritis Rheum* 64, 3220-3230.
- Lu, X., Mu, E., Wei, Y., *et al.* (2011). VCAM-1 promotes osteolytic expansion of indolent bone micrometastasis of breast cancer by engaging alpha4beta1-positive osteoclast progenitors. *Cancer Cell* 20, 701-714.
- Lu, X., Wang, Q., Hu, G., Van Poznak, C., Fleisher, M., Reiss, M., Massague, J., and Kang, Y. (2009). ADAMTS1 and MMP1 proteolytically engage EGF-like ligands in an osteolytic signaling cascade for bone metastasis. *Genes Dev* 23, 1882-1894.
- Lumeng, C.N., and Saltiel, A.R. (2011). Inflammatory links between obesity and metabolic disease. *J Clin Invest* 121, 2111-2117.
- Lund, S.A., Giachelli, C.M., and Scatena, M. (2009). The role of osteopontin in inflammatory processes. *J Cell Commun Signal* 3, 311-322.

- Luo, Y., Chen, G.L., Hannemann, N., Ipseiz, N., Kronke, G., Bauerle, T., Munos, L., Wirtz, S., Schett, G., and Bozec, A. (2015). Microbiota from Obese Mice Regulate Hematopoietic Stem Cell Differentiation by Altering the Bone Niche. *Cell Metab* 22, 886-894.
- Lux, A., Seeling, M., Baerenwaldt, A., *et al.* (2014). A humanized mouse identifies the bone marrow as a niche with low therapeutic IgG activity. *Cell Rep* 7, 236-248.
- Macdonald, J.B., Dueck, A.C., Gray, R.J., Wasif, N., Swanson, D.L., Sekulic, A., and Pockaj, B.A. (2011). Malignant melanoma in the elderly: different regional disease and poorer prognosis. *J Cancer* 2, 538-543.
- Mackenzie K. Herroon, E.R., Aimalie L. Hardaway, and Izabela Podgorski (2015). Abstract B04: Exploring the roles of bone marrow adipocytes in metabolic adaptation of metastatic prostate tumors in bone. *Cancer Research B04*.
- Madonna, G., Ullman, C.D., Gentilcore, G., Palmieri, G., and Ascierto, P.A. (2012). NF-kappaB as potential target in the treatment of melanoma. *J Transl Med* 10, 53.
- Malvi, P., Chaube, B., Pandey, V., Vijayakumar, M.V., Boreddy, P.R., Mohammad, N., Singh, S.V., and Bhat, M.K. (2015). Obesity induced rapid melanoma progression is reversed by orlistat treatment and dietary intervention: role of adipokines. *Mol Oncol* 9, 689-703.
- Mao, Y., Keller, E.T., Garfield, D.H., Shen, K., and Wang, J. (2013). Stromal cells in tumor microenvironment and breast cancer. *Cancer Metastasis Rev* 32, 303-315.
- Margadant, C., and Sonnenberg, A. (2010). Integrin-TGF-beta crosstalk in fibrosis, cancer and wound healing. *EMBO Rep* 11, 97-105.
- Markovic, S.N., Erickson, L.A., Rao, R.D., *et al.* (2007). Malignant melanoma in the 21st century, part 1: epidemiology, risk factors, screening, prevention, and diagnosis. *Mayo Clin Proc* 82, 364-380.
- Maru, G.B., Gandhi, K., Ramchandani, A., and Kumar, G. (2014). The role of inflammation in skin cancer. *Adv Exp Med Biol* 816, 437-469.
- Maryland, U.o. (2003). *Medicine Facts about Skin Cancer*.
- Mauer, J., Chaurasia, B., Goldau, J., *et al.* (2014). Signaling by IL-6 promotes alternative activation of macrophages to limit endotoxemia and obesity-associated resistance to insulin. *Nat Immunol* 15, 423-430.
- McBrayer, S.K., Cheng, J.C., Singhal, S., Krett, N.L., Rosen, S.T., and Shanmugam, M. (2012). Multiple myeloma exhibits novel dependence on GLUT4, GLUT8, and GLUT11: implications for glucose transporter-directed therapy. *Blood* 119, 4686-4697.
- Melnikova, V.O., and Bar-Eli, M. (2009). Inflammation and melanoma metastasis. *Pigment Cell Melanoma Res* 22, 257-267.
- Meyer, S., Vogt, T., Landthaler, M., Berand, A., Reichle, A., Bataille, F., Marx, A.H., Menz, A., Hartmann, A., Kunz-Schughart, L.A., and Wild, P.J. (2009). Cyclooxygenase 2 (COX2) and Peroxisome Proliferator-Activated Receptor Gamma (PPARG) Are

- Stage-Dependent Prognostic Markers of Malignant Melanoma. *PPAR Res* 2009, 848645.
- Michalek, R.D., Gerriets, V.A., Jacobs, S.R., Macintyre, A.N., MacIver, N.J., Mason, E.F., Sullivan, S.A., Nichols, A.G., and Rathmell, J.C. (2011). Cutting edge: distinct glycolytic and lipid oxidative metabolic programs are essential for effector and regulatory CD4⁺ T cell subsets. *J Immunol* 186, 3299-3303.
- Mitchell, N.S., Catenacci, V.A., Wyatt, H.R., and Hill, J.O. (2011). Obesity: overview of an epidemic. *Psychiatr Clin North Am* 34, 717-732.
- Mizutani, H., Fukushima, S., Masuguchi, S., Yamashita, J., Miyashita, A., Nakahara, S., Aoi, J., Inoue, Y., Jinnin, M., and Ihn, H. (2013). Serum levels of leptin receptor in patients with malignant melanoma as a new tumor marker. *Exp Dermatol* 22, 748-749.
- Mizutani, K., Sud, S., McGregor, N.A., Martinovski, G., Rice, B.T., Craig, M.J., Varsos, Z.S., Roca, H., and Pienta, K.J. (2009). The chemokine CCL2 increases prostate tumor growth and bone metastasis through macrophage and osteoclast recruitment. *Neoplasia* 11, 1235-1242.
- Mock, K., Preca, B.T., Brummer, T., Brabletz, S., Stemmler, M.P., and Brabletz, T. (2015). The EMT-activator ZEB1 induces bone metastasis associated genes including BMP-inhibitors. *Oncotarget* 6, 14399-14412.
- Monteiro, A.C., Leal, A.C., Goncalves-Silva, T., Mercadante, A.C., Kestelman, F., Chaves, S.B., Azevedo, R.B., Monteiro, J.P., and Bonomo, A. (2013). T cells induce pre-metastatic osteolytic disease and help bone metastases establishment in a mouse model of metastatic breast cancer. *PLoS One* 8, e68171.
- Morgan, G., and Lipton, A. (2010). Antitumor effects and anticancer applications of bisphosphonates. *Semin Oncol* 37 Suppl 2, S30-40.
- Mori, A., Sakurai, H., Choo, M.K., Obi, R., Koizumi, K., Yoshida, C., Shimada, Y., and Saiki, I. (2006). Severe pulmonary metastasis in obese and diabetic mice. *Int J Cancer* 119, 2760-2767.
- Mouawad, R., Benhammouda, A., Rixe, O., Antoine, E.C., Borel, C., Weil, M., Khayat, D., and Soubrane, C. (1996). Endogenous interleukin 6 levels in patients with metastatic malignant melanoma: correlation with tumor burden. *Clin Cancer Res* 2, 1405-1409.
- Muruganandan, S., and Sinal, C.J. (2014). The impact of bone marrow adipocytes on osteoblast and osteoclast differentiation. *IUBMB Life*.
- Myers, T.J., Longobardi, L., Willcockson, H., Temple, J.D., Tagliaferro, L., Ye, P., Li, T., Esposito, A., Moats-Staats, B.M., and Spagnoli, A. (2015). BMP2 Regulation of CXCL12 Cellular, Temporal, and Spatial Expression is Essential During Fracture Repair. *J Bone Miner Res* 30, 2014-2027.
- Na, Y.R., Lee, J.S., Lee, S.J., and Seok, S.H. (2013). Interleukin-6-induced Twist and N-cadherin enhance melanoma cell metastasis. *Melanoma Res* 23, 434-443.

- Nava-Villalba, M., Nunez-Anita, R.E., Bontempo, A., and Aceves, C. (2015). Activation of peroxisome proliferator-activated receptor gamma is crucial for antitumoral effects of 6-iodolactone. *Mol Cancer* *14*, 168.
- Naveiras, O., Nardi, V., Wenzel, P.L., Hauschka, P.V., Fahey, F., and Daley, G.Q. (2009). Bone-marrow adipocytes as negative regulators of the haematopoietic microenvironment. *Nature* *460*, 259-263.
- Nemoto, H., Rittling, S.R., Yoshitake, H., Furuya, K., Amagasa, T., Tsuji, K., Nifuji, A., Denhardt, D.T., and Noda, M. (2001). Osteopontin deficiency reduces experimental tumor cell metastasis to bone and soft tissues. *J Bone Miner Res* *16*, 652-659.
- Nieman, K.M., Kenny, H.A., Penicka, C.V., *et al.* (2011). Adipocytes promote ovarian cancer metastasis and provide energy for rapid tumor growth. *Nat Med* *17*, 1498-1503.
- Nieman, K.M., Romero, I.L., Van Houten, B., and Lengyel, E. (2013). Adipose tissue and adipocytes support tumorigenesis and metastasis. *Biochim Biophys Acta* *1831*, 1533-1541.
- Nikki A. Ford, J.D., Stephen D. Hursting (2013). Metabolic Perturbations Associated with Adipose Tissue Dysfunction and the Obesity-Cancer Link. *Adipose Tissue and Cancer*, pp 1-14.
- Nomiyama, T., Perez-Tilve, D., Ogawa, D., Gizard, F., Zhao, Y., Heywood, E.B., Jones, K.L., Kawamori, R., Cassis, L.A., Tschop, M.H., and Bruemmer, D. (2007). Osteopontin mediates obesity-induced adipose tissue macrophage infiltration and insulin resistance in mice. *J Clin Invest* *117*, 2877-2888.
- O'Connell, M.E., Powell, B.W., O'Connell, J.M., and Harmer, C.L. (1989). Spontaneous regression of multiple bone metastases in malignant melanoma. *Br J Radiol* *62*, 1095-1100.
- Odenbro, A., Gillgren, P., Bellocco, R., Boffetta, P., Hakansson, N., and Adami, J. (2007). The risk for cutaneous malignant melanoma, melanoma in situ and intraocular malignant melanoma in relation to tobacco use and body mass index. *Br J Dermatol* *156*, 99-105.
- Ohyama, Y., Nemoto, H., Rittling, S., Tsuji, K., Amagasa, T., Denhardt, D.T., Nifuji, A., and Noda, M. (2004). Osteopontin-deficiency suppresses growth of B16 melanoma cells implanted in bone and osteoclastogenesis in co-cultures. *J Bone Miner Res* *19*, 1706-1711.
- Onan, D., Allan, E.H., Quinn, J.M., Gooi, J.H., Pompolo, S., Sims, N.A., Gillespie, M.T., and Martin, T.J. (2009). The chemokine Cxcl1 is a novel target gene of parathyroid hormone (PTH)/PTH-related protein in committed osteoblasts. *Endocrinology* *150*, 2244-2253.
- Organization, W.H. (2015). Fact sheet: obesity and overweight.
- Ortiz, A., and Lin, S.H. (2012). Osteolytic and osteoblastic bone metastases: two extremes of the same spectrum? *Recent Results Cancer Res* *192*, 225-233.

- Paget, S. (1989). The distribution of secondary growths in cancer of the breast. 1889. *Cancer Metastasis Rev* 8, 98-101.
- Pandey, V., Vijayakumar, M.V., Ajay, A.K., Malvi, P., and Bhat, M.K. (2012). Diet-induced obesity increases melanoma progression: involvement of Cav-1 and FASN. *Int J Cancer* 130, 497-508.
- Parfitt, A.M., Drezner, M.K., Glorieux, F.H., Kanis, J.A., Malluche, H., Meunier, P.J., Ott, S.M., and Recker, R.R. (1987). Bone histomorphometry: standardization of nomenclature, symbols, and units. Report of the ASBMR Histomorphometry Nomenclature Committee. *J Bone Miner Res* 2, 595-610.
- Park, H., Kim, M., Kwon, G.T., Lim do, Y., Yu, R., Sung, M.K., Lee, K.W., Daily, J.W., 3rd, and Park, J.H. (2012). A high-fat diet increases angiogenesis, solid tumor growth, and lung metastasis of CT26 colon cancer cells in obesity-resistant BALB/c mice. *Mol Carcinog* 51, 869-880.
- Park, J., Morley, T.S., Kim, M., Clegg, D.J., and Scherer, P.E. (2014). Obesity and cancer--mechanisms underlying tumour progression and recurrence. *Nat Rev Endocrinol* 10, 455-465.
- Park, J., and Scherer, P.E. (2012). Adipocyte-derived endotrophin promotes malignant tumor progression. *J Clin Invest* 122, 4243-4256.
- Parkin, D.M., and Boyd, L. (2011). 8. Cancers attributable to overweight and obesity in the UK in 2010. *Br J Cancer* 105 Suppl 2, S34-37.
- Parmenter, T.J., Kleinschmidt, M., Kinross, K.M., *et al.* (2014). Response of BRAF-mutant melanoma to BRAF inhibition is mediated by a network of transcriptional regulators of glycolysis. *Cancer Discov* 4, 423-433.
- Passamonti, F., Maffioli, M., Caramazza, D., and Cazzola, M. (2011). Myeloproliferative neoplasms: from JAK2 mutations discovery to JAK2 inhibitor therapies. *Oncotarget* 2, 485-490.
- Patel, L.R., Camacho, D.F., Shiozawa, Y., Pienta, K.J., and Taichman, R.S. (2011). Mechanisms of cancer cell metastasis to the bone: a multistep process. *Future Oncol* 7, 1285-1297.
- Pavlovic, M., Arnal-Estape, A., Rojo, F., *et al.* (2015). Enhanced MAF Oncogene Expression and Breast Cancer Bone Metastasis. *J Natl Cancer Inst* 107, djv256.
- Peinado, H., Aleckovic, M., Lavotshkin, S., *et al.* (2012). Melanoma exosomes educate bone marrow progenitor cells toward a pro-metastatic phenotype through MET. *Nat Med* 18, 883-891.
- Perez, M., Migliaccio, S., Taranta, A., Festuccia, C., Orru, L., Brama, M., Bologna, M., Faraggiana, T., Baron, R., and Teti, A. (2001). Melanoma cells stimulate osteoclastogenesis, c-Src expression and osteoblast cytokines. *Eur J Cancer* 37, 629-640.
- Plourde, G. (2002). Impact of obesity on glucose and lipid profiles in adolescents at different age groups in relation to adulthood. *BMC Fam Pract* 3, 18.

- Pluijm, G., Lowik, C., and Papapoulos, S. (2000). Tumour progression and angiogenesis in bone metastasis from breast cancer: new approaches to an old problem. *Cancer Treat Rev* 26, 11-27.
- Pollard, J.W. (2004). Tumour-educated macrophages promote tumour progression and metastasis. *Nat Rev Cancer* 4, 71-78.
- Poon, M., Zeng, L., Zhang, L., Lam, H., Emmenegger, U., Wong, E., Bedard, G., Lao, N., Chow, R., and Chow, E. (2013). Incidence of skeletal-related events over time from solid tumour bone metastases reported in randomised trials using bone-modifying agents. *Clin Oncol (R Coll Radiol)* 25, 435-444.
- Price, R.S., Cavazos, D.A., De Angel, R.E., Hursting, S.D., and deGraffenried, L.A. (2012). Obesity-related systemic factors promote an invasive phenotype in prostate cancer cells. *Prostate Cancer Prostatic Dis* 15, 135-143.
- Price, T., and Sipkins, D.A. (2014). Rewiring the niche: sympathetic neuropathy drives malignant niche transformation. *Cell Stem Cell* 15, 261-262.
- Psaila, B., and Lyden, D. (2009). The metastatic niche: adapting the foreign soil. *Nat Rev Cancer* 9, 285-293.
- Raes, G., De Baetselier, P., Noel, W., Beschin, A., Brombacher, F., and Hassanzadeh Gh, G. (2002). Differential expression of FIZZ1 and Ym1 in alternatively versus classically activated macrophages. *J Leukoc Biol* 71, 597-602.
- Rahim, F., Hajizamani, S., Mortaz, E., Ahmadzadeh, A., Shahjahani, M., Shahrabi, S., and Saki, N. (2014). Molecular regulation of bone marrow metastasis in prostate and breast cancer. *Bone Marrow Res* 2014, 405920.
- Rahman, M.M., Matsuoka, K., Takeshita, S., and Ikeda, K. (2015). Secretion of PDGF isoforms during osteoclastogenesis and its modulation by anti-osteoclast drugs. *Biochem Biophys Res Commun* 462, 159-164.
- Ramakrishna, R., and Rostomily, R. (2013). Seed, soil, and beyond: The basic biology of brain metastasis. *Surg Neurol Int* 4, S256-264.
- Rao, G., Wang, H., Li, B., *et al.* (2013). Reciprocal interactions between tumor-associated macrophages and CD44-positive cancer cells via osteopontin/CD44 promote tumorigenicity in colorectal cancer. *Clin Cancer Res* 19, 785-797.
- Reagan, M.R., and Rosen, C.J. (2016). Navigating the bone marrow niche: translational insights and cancer-driven dysfunction. *Nat Rev Rheumatol* 12, 154-168.
- Rehman, J., Considine, R.V., Bovenkerk, J.E., Li, J., Slavens, C.A., Jones, R.M., and March, K.L. (2003). Obesity is associated with increased levels of circulating hepatocyte growth factor. *J Am Coll Cardiol* 41, 1408-1413.
- Ren, G., Esposito, M., and Kang, Y. (2015). Bone metastasis and the metastatic niche. *J Mol Med (Berl)* 93, 1203-1212.
- Ribatti, D., Annese, T., and Longo, V. (2010). Angiogenesis and melanoma. *Cancers (Basel)* 2, 114-132.

- Ribeiro, A.M., Andrade, S., Pinho, F., Monteiro, J.D., Costa, M., Lopes, C., Aguas, A.P., and Monteiro, M.P. (2010). Prostate cancer cell proliferation and angiogenesis in different obese mice models. *Int J Exp Pathol* 91, 374-386.
- Rivera-Gonzalez, G., Shook, B., and Horsley, V. (2014). Adipocytes in skin health and disease. *Cold Spring Harb Perspect Med* 4.
- RJO Dowling, M.C., AE Lohmann, M Ennis, E Amir, C Elser, C Brezden-Masley, T Vandenberg, E Lee, K Fazae, V Stambolic, PJ Goodwin (2016, 76.). Abstract P2-02-09: Obesity associated factors are inversely associated with circulating tumor cells in metastatic breast cancer. *Cancer Research*.
- Roato, I. (2014). Bone metastases: When and how lung cancer interacts with bone. *World J Clin Oncol* 5, 149-155.
- Roberts, E., Cossigny, D.A., and Quan, G.M. (2013). The role of vascular endothelial growth factor in metastatic prostate cancer to the skeleton. *Prostate Cancer* 2013, 418340.
- Robey, I.F., Lien, A.D., Welsh, S.J., Baggett, B.K., and Gillies, R.J. (2005). Hypoxia-inducible factor-1alpha and the glycolytic phenotype in tumors. *Neoplasia* 7, 324-330.
- Rodriguez-Hernandez, H., Simental-Mendia, L.E., Rodriguez-Ramirez, G., and Reyes-Romero, M.A. (2013). Obesity and inflammation: epidemiology, risk factors, and markers of inflammation. *Int J Endocrinol* 2013, 678159.
- Rogiers, A., van den Oord, J.J., Garmyn, M., Stas, M., Kenis, C., Wildiers, H., Marine, J.C., and Wolter, P. (2015). Novel Therapies for Metastatic Melanoma: An Update on Their Use in Older Patients. *Drugs Aging* 32, 821-834.
- Roodman, G.D. (2004). Mechanisms of bone metastasis. *N Engl J Med* 350, 1655-1664.
- Roszer, T. (2015). Understanding the Mysterious M2 Macrophage through Activation Markers and Effector Mechanisms. *Mediators Inflamm* 2015, 816460.
- Sakamoto, S., Inoue, H., Ohba, S., Kohda, Y., Usami, I., Masuda, T., Kawada, M., and Nomoto, A. (2015). New metastatic model of human small-cell lung cancer by orthotopic transplantation in mice. *Cancer Sci* 106, 367-374.
- Samuvel, D.J., Sundararaj, K.P., Li, Y., Lopes-Virella, M.F., and Huang, Y. (2010). Adipocyte-mononuclear cell interaction, Toll-like receptor 4 activation, and high glucose synergistically up-regulate osteopontin expression via an interleukin 6-mediated mechanism. *The Journal of biological chemistry* 285, 3916-3927.
- Sawant, A., Deshane, J., Jules, J., Lee, C.M., Harris, B.A., Feng, X., and Ponnazhagan, S. (2013). Myeloid-derived suppressor cells function as novel osteoclast progenitors enhancing bone loss in breast cancer. *Cancer Res* 73, 672-682.
- Scheller, J., Chalaris, A., Schmidt-Arras, D., and Rose-John, S. (2011). The pro- and anti-inflammatory properties of the cytokine interleukin-6. *Biochim Biophys Acta* 1813, 878-888.

- Schuettpelz, L.G., and Link, D.C. (2011). Niche competition and cancer metastasis to bone. *J Clin Invest* *121*, 1253-1255.
- Scutellari, P.N., Antinolfi, G., Galeotti, R., and Giganti, M. (2003). Metastatic bone disease. Strategies for imaging. *Minerva Med* *94*, 77-90.
- Sergentanis, T.N., Antoniadis, A.G., Gogas, H.J., Antonopoulos, C.N., Adami, H.O., Ekblom, A., and Petridou, E.T. (2013). Obesity and risk of malignant melanoma: a meta-analysis of cohort and case-control studies. *Eur J Cancer* *49*, 642-657.
- Sethi, N., Dai, X., Winter, C.G., and Kang, Y. (2011). Tumor-derived JAGGED1 promotes osteolytic bone metastasis of breast cancer by engaging notch signaling in bone cells. *Cancer Cell* *19*, 192-205.
- Shalapour, S., and Karin, M. (2015). Immunity, inflammation, and cancer: an eternal fight between good and evil. *J Clin Invest* *125*, 3347-3355.
- Shiozawa, Y., Eber, M.R., Berry, J.E., and Taichman, R.S. (2015). Bone marrow as a metastatic niche for disseminated tumor cells from solid tumors. *Bonekey Rep* *4*, 689.
- Shiozawa, Y., Pedersen, E.A., Havens, A.M., *et al.* (2011). Human prostate cancer metastases target the hematopoietic stem cell niche to establish footholds in mouse bone marrow. *J Clin Invest* *121*, 1298-1312.
- Shors, A.R., Solomon, C., McTiernan, A., and White, E. (2001). Melanoma risk in relation to height, weight, and exercise (United States). *Cancer Causes Control* *12*, 599-606.
- Slipicevic, A., Jorgensen, K., Skrede, M., Rosnes, A.K., Troen, G., Davidson, B., and Florenes, V.A. (2008). The fatty acid binding protein 7 (FABP7) is involved in proliferation and invasion of melanoma cells. *BMC Cancer* *8*, 276.
- Soki, F.N., Park, S.I., and McCauley, L.K. (2012). The multifaceted actions of PTHrP in skeletal metastasis. *Future Oncol* *8*, 803-817.
- Soleimani, M., and Nadri, S. (2009). A protocol for isolation and culture of mesenchymal stem cells from mouse bone marrow. *Nat Protoc* *4*, 102-106.
- Stacer, A.C., Fenner, J., Cavnar, S.P., Xiao, A., Zhao, S., Chang, S.L., Salomonson, A., Luker, K.E., and Luker, G.D. (2015). Endothelial CXCR7 regulates breast cancer metastasis. *Oncogene*.
- Steiner, G., and MacDonald, J. (1972). Metastases to bone from malignant melanoma. *Clinical radiology* *23*, 52-57.
- Stephens, J.M. (2012). The fat controller: adipocyte development. *PLoS Biol* *10*, e1001436.
- Stiff, A., Trikha, P., Wesolowski, R., *et al.* (2016). Myeloid-derived suppressor cells express Bruton's tyrosine kinase and can be depleted in tumor bearing hosts by ibrutinib treatment. *Cancer Res*.

- Sturtz, L.A., Deyarmin, B., van Laar, R., Yarina, W., Shriver, C.D., and Ellsworth, R.E. (2014). Gene expression differences in adipose tissue associated with breast tumorigenesis. *Adipocyte* 3, 107-114.
- Sumantran, V.N., Mishra, P., and Sudhakar, N. (2015). Microarray analysis of differentially expressed genes regulating lipid metabolism during melanoma progression. *Indian J Biochem Biophys* 52, 125-131.
- Szczygielska, A., Widomska, S., Jaraszkievicz, M., Knera, P., and Muc, K. (2003). Blood lipids profile in obese or overweight patients. *Ann Univ Mariae Curie Sklodowska Med* 58, 343-349.
- Takayanagi, H. (2007). The role of NFAT in osteoclast formation. *Ann N Y Acad Sci* 1116, 227-237.
- Takayanagi, H., Kim, S., Koga, T., *et al.* (2002). Induction and activation of the transcription factor NFATc1 (NFAT2) integrate RANKL signaling in terminal differentiation of osteoclasts. *Dev Cell* 3, 889-901.
- Takeshita, S., Fumoto, T., Naoe, Y., and Ikeda, K. (2014). Age-related marrow adipogenesis is linked to increased expression of RANKL. *J Biol Chem* 289, 16699-16710.
- Takita, M., Inada, M., Maruyama, T., and Miyaura, C. (2007). Prostaglandin E receptor EP4 antagonist suppresses osteolysis due to bone metastasis of mouse malignant melanoma cells. *FEBS Lett* 581, 565-571.
- Tamura, T., Udagawa, N., Takahashi, N., Miyaura, C., Tanaka, S., Yamada, Y., Koishihara, Y., Ohsugi, Y., Kumaki, K., Taga, T., and *et al.* (1993). Soluble interleukin-6 receptor triggers osteoclast formation by interleukin 6. *Proc Natl Acad Sci U S A* 90, 11924-11928.
- Tan, J., Buache, E., Chenard, M.P., Dali-Youcef, N., and Rio, M.C. (2011). Adipocyte is a non-trivial, dynamic partner of breast cancer cells. *Int J Dev Biol* 55, 851-859.
- Tanabe, N., Wheal, B.D., Kwon, J., Chen, H.H., Shugg, R.P., Sims, S.M., Goldberg, H.A., and Dixon, S.J. (2011). Osteopontin signals through calcium and nuclear factor of activated T cells (NFAT) in osteoclasts: a novel RGD-dependent pathway promoting cell survival. *J Biol Chem* 286, 39871-39881.
- Tang, K.D., Liu, J., Jovanovic, L., *et al.* (2016). Adipocytes promote prostate cancer stem cell self-renewal through amplification of the cholecystokinin autocrine loop. *Oncotarget* 7, 4939-4948.
- Tas, F. (2012). Metastatic behavior in melanoma: timing, pattern, survival, and influencing factors. *J Oncol* 2012, 647684.
- Tellez, A., Rueda, S., Conic, R.Z., Powers, K., Galdyn, I., Mesinkovska, N.A., and Gastman, B. (2016). Risk factors and outcomes of cutaneous melanoma in women less than 50 years of age. *J Am Acad Dermatol*.

- Templeton, Z.S., Lie, W.R., Wang, W., Rosenberg-Hasson, Y., Alluri, R.V., Tamaresis, J.S., Bachmann, M.H., Lee, K., Maloney, W.J., Contag, C.H., and King, B.L. (2015). Breast Cancer Cell Colonization of the Human Bone Marrow Adipose Tissue Niche. *Neoplasia* 17, 849-861.
- Tomei, S., Wang, E., Delogu, L.G., Marincola, F.M., and Bedognetti, D. (2014). Non-BRAF-targeted therapy, immunotherapy, and combination therapy for melanoma. *Expert Opin Biol Ther* 14, 663-686.
- Turley, R.S., Fontanella, A.N., Padussis, J.C., Toshimitsu, H., Tokuhisa, Y., Cho, E.H., Hanna, G., Beasley, G.M., Augustine, C.K., Dewhirst, M.W., and Tyler, D.S. (2012). Bevacizumab-induced alterations in vascular permeability and drug delivery: a novel approach to augment regional chemotherapy for in-transit melanoma. *Clin Cancer Res* 18, 3328-3339.
- Udagawa, N., Takahashi, N., Akatsu, T., Tanaka, H., Sasaki, T., Nishihara, T., Koga, T., Martin, T.J., and Suda, T. (1990). Origin of osteoclasts: mature monocytes and macrophages are capable of differentiating into osteoclasts under a suitable microenvironment prepared by bone marrow-derived stromal cells. *Proc Natl Acad Sci U S A* 87, 7260-7264.
- Valles, S.L., Benloch, M., Rodriguez, M.L., Mena, S., Pellicer, J.A., Asensi, M., Obrador, E., and Estrela, J.M. (2013). Stress hormones promote growth of B16-F10 melanoma metastases: an interleukin 6- and glutathione-dependent mechanism. *J Transl Med* 11, 72.
- van Kruijsdijk, R.C., van der Wall, E., and Visseren, F.L. (2009). Obesity and cancer: the role of dysfunctional adipose tissue. *Cancer Epidemiol Biomarkers Prev* 18, 2569-2578.
- Vasiliadou, I., and Holen, I. (2013). The role of macrophages in bone metastasis. *J Bone Oncol* 2, 158-166.
- Veierod, M.B., Thelle, D.S., and Laake, P. (1997). Diet and risk of cutaneous malignant melanoma: a prospective study of 50,757 Norwegian men and women. *Int J Cancer* 71, 600-604.
- Wagner, M., Bjerkvig, R., Wiig, H., and Dudley, A.C. (2013). Loss of adipocyte specification and necrosis augment tumor-associated inflammation. *Adipocyte* 2, 176-183.
- Walker, N.D., Patel, J., Munoz, J.L., Hu, M., Guiro, K., Sinha, G., and Rameshwar, P. (2015). The bone marrow niche in support of breast cancer dormancy. *Cancer Lett.*
- Wang, H., Yu, C., Gao, X., *et al.* (2015). The osteogenic niche promotes early-stage bone colonization of disseminated breast cancer cells. *Cancer Cell* 27, 193-210.
- Wang, J., Loberg, R., and Taichman, R.S. (2006). The pivotal role of CXCL12 (SDF-1)/CXCR4 axis in bone metastasis. *Cancer Metastasis Rev* 25, 573-587.

- Wang, L., Yi, T., Kortylewski, M., Pardoll, D.M., Zeng, D., and Yu, H. (2009). IL-17 can promote tumor growth through an IL-6-Stat3 signaling pathway. *J Exp Med* 206, 1457-1464.
- Wang, Y., Ma, J., Yan, X., Chen, X., Si, L., Liu, Y., Han, J., Hao, W., and Zheng, Q. (2016). Isoliquiritigenin inhibits proliferation and induces apoptosis via alleviating hypoxia and reducing glycolysis in melanoma B16F10 cells. *Recent Pat Anticancer Drug Discov*.
- Wang, Y., Yan, W., Lu, X., *et al.* (2011). Overexpression of osteopontin induces angiogenesis of endothelial progenitor cells via the avbeta3/PI3K/AKT/eNOS/NO signaling pathway in glioma cells. *Eur J Cell Biol* 90, 642-648.
- Weilbaecher, K.N., Guise, T.A., and McCauley, L.K. (2011). Cancer to bone: a fatal attraction. *Nat Rev Cancer* 11, 411-425.
- Weischenfeldt, J., and Porse, B. (2008). Bone Marrow-Derived Macrophages (BMM): Isolation and Applications. *CSH Protoc* 2008, pdb prot5080.
- Wen, Y., Feng, D., Wu, H., Liu, W., Li, H., Wang, F., Xia, Q., Gao, W.Q., and Kong, X. (2015). Defective Initiation of Liver Regeneration in Osteopontin-Deficient Mice after Partial Hepatectomy due to Insufficient Activation of IL-6/Stat3 Pathway. *Int J Biol Sci* 11, 1236-1247.
- WHO, J., and Consultation, F.E. (2003). Diet, nutrition and the prevention of chronic diseases. *World Health Organ Tech Rep Ser* 916.
- Wolchok, J.D., Kluger, H., Callahan, M.K., *et al.* (2013). Nivolumab plus ipilimumab in advanced melanoma. *N Engl J Med* 369, 122-133.
- Wolfson, B., Eades, G., and Zhou, Q. (2015). Adipocyte activation of cancer stem cell signaling in breast cancer. *World J Biol Chem* 6, 39-47.
- Wolin, K.Y., Carson, K., and Colditz, G.A. (2010). Obesity and cancer. *Oncologist* 15, 556-565.
- Wong, E.W.P., Shen, L., Shieh, J.-H., and Moore, M.A. (2014). Enhanced adipogenesis of bone marrow-derived stromal cells by ovarian cancer cells via BMP4 and IL8 is associated with increase in cancer stem/progenitor cells and cancer cell proliferation. [abstract]. In: *Proceedings of the 105th Annual Meeting of the American Association for Cancer Research; 2014 Apr 5-9; San Diego, CA. Philadelphia (PA): AACR; Cancer Res* 74, AM2014-4866.
- Wu, Y. (2006). Overweight and obesity in China. *BMJ* 333, 362-363.
- Wu, Z., McRoberts, K.S., and Theodorescu, D. (2007). The role of PTEN in prostate cancer cell tropism to the bone micro-environment. *Carcinogenesis* 28, 1393-1400.
- Yagiz, K., and Rittling, S.R. (2009). Both cell-surface and secreted CSF-1 expressed by tumor cells metastatic to bone can contribute to osteoclast activation. *Exp Cell Res* 315, 2442-2452.

- Yamate, T., Mocharla, H., Taguchi, Y., Igietseme, J.U., Manolagas, S.C., and Abe, E. (1997). Osteopontin expression by osteoclast and osteoblast progenitors in the murine bone marrow: demonstration of its requirement for osteoclastogenesis and its increase after ovariectomy. *Endocrinology* *138*, 3047-3055.
- Yang, J., Splittgerber, R., Yull, F.E., Kantrow, S., Ayers, G.D., Karin, M., and Richmond, A. (2010). Conditional ablation of *Ikkb* inhibits melanoma tumor development in mice. *J Clin Invest* *120*, 2563-2574.
- Yang, M., Jiang, P., Sun, F.X., Hasegawa, S., Baranov, E., Chishima, T., Shimada, H., Moossa, A.R., and Hoffman, R.M. (1999). A fluorescent orthotopic bone metastasis model of human prostate cancer. *Cancer Res* *59*, 781-786.
- Yin, M., Soikkeli, J., Jahkola, T., Virolainen, S., Saksela, O., and Holtta, E. (2014). Osteopontin promotes the invasive growth of melanoma cells by activating integrin $\alpha v \beta 3$ and down-regulating tetraspanin CD9. *Am J Pathol* *184*, 842-858.
- Yoneda, T., and Hiraga, T. (2005). Crosstalk between cancer cells and bone microenvironment in bone metastasis. *Biochem Biophys Res Commun* *328*, 679-687.
- Zeyda, M., Gollinger, K., Todoric, J., Kiefer, F.W., Keck, M., Aszmann, O., Prager, G., Zlabinger, G.J., Petzelbauer, P., and Stulnig, T.M. (2011). Osteopontin is an activator of human adipose tissue macrophages and directly affects adipocyte function. *Endocrinology* *152*, 2219-2227.
- Zhang, X.H., Wang, Q., Gerald, W., Hudis, C.A., Norton, L., Smid, M., Foekens, J.A., and Massague, J. (2009a). Latent bone metastasis in breast cancer tied to Src-dependent survival signals. *Cancer Cell* *16*, 67-78.
- Zhang, Y., Daquinag, A., Traktuev, D.O., Amaya-Manzanares, F., Simmons, P.J., March, K.L., Pasqualini, R., Arap, W., and Kolonin, M.G. (2009b). White adipose tissue cells are recruited by experimental tumors and promote cancer progression in mouse models. *Cancer Res* *69*, 5259-5266.
- Zheng, H., and Kang, Y. (2015). Cradle of evil: osteogenic niche for early bone metastasis. *Cancer Cell* *27*, 153-155.
- Zhuang, J., Zhang, J., Lwin, S.T., Edwards, J.R., Edwards, C.M., Mundy, G.R., and Yang, X. (2012). Osteoclasts in multiple myeloma are derived from Gr-1+CD11b+myeloid-derived suppressor cells. *PLoS One* *7*, e48871.

6. Appendix

6.1 Abbreviations

Akt	Via thymoma viral proto-oncogene 1
BM	Bone marrow
BMI	Body mass index
BMPs	Bone morphogenetic proteins
BRAF	B-Raf proto-oncogene, serine/threonine kinase
BSA	Bovine Serum Albumin
BV/TV	Bone volume per total volume
CAAs	Cancer-associated adipocytes
CEBP β	CCAAT/enhancer-binding protein beta
c-Fos	FBJ Murine Osteosarcoma Viral Oncogene Homolog
CM	Conditioned medium
COX-2	Cyclooxygenase-2
CSF-1	Colony stimulating factor 1
CTGF	Connective tissue growth factor
CTGF	Connective tissue growth factor
CTLA4	Cytotoxic T-lymphocyte-associated protein 4
CXCL	CXC-chemokine ligand
CXCR2	Chemokine (C-X-C motif) receptor 2
DCs	Dendritic cells
DMEM	Dulbecco's Modified Eagle Medium
DMSO	Dimethyl Sulfoxide
EDTA	Ethylenediaminetetraacetic Acid
ELISA	Enzyme Linked Immunosorbent Assay
EMT	Epithelial-mesenchymal transition
ERK	Extracellular signal-regulated kinase
Eta-1	Early T-lymphocyte activation-1
FABP4	Fatty acid-binding protein 4

FACS	Fluorescence Activated Cell Sorting
FASN	Fatty acid synthase
FBS	Fetal Bovine Serum
FGFs	Fibroblast growth factors
FIZZ1	Cysteine-rich secreted A12-alpha-like protein 1
FN	Fibronectin
Fra1	Fos-related antigen 1
FSL1	Follistatin-like protein 1
Glut	Glucose transport proteins
hAJs	Heterotypic adherens junctions
HFD	High fat diet
HIF-1 α	Hypoxia-inducible factor-1 alpha
HRP	Horseradish Peroxidase
HSCs	Haematopoietic stem cells
HSPG	Heparan sulfate proteoglycan
i.c.	Intracardiac
i.t.	Intratibial
ICAM1	Intercellular adhesion molecule 1
IGFs	insulin like growth factors
IHC	Immunohistochemistry
IHC	Immunohistochemistry
IL	Interlukin
JAK2	Janus kinase 2
JNK	c-Jun NH2-terminal kinase
KO	Knock-out
LOX	Lysyl oxidase
M2	Alternative activation of macrophages
MAF	v-maf avian musculoaponeurotic fibrosarcoma oncogene homolog

MCSF	Macrophage colony stimulating factor 1
M-CSF	Macrophage Colony Stimulating Factor
MDSCs	Myeloid derived monocyte cells
MEK	Mitogen-activated protein kinase kinase
MEM	Minimal Essential Medium
MIP	Macrophage inflammatory protein
MM	Malignant melanoma
MMP9	Matrix metalloproteinase 9
MMPs	Matrix metalloproteinases
MSCs	Mesenchemal stem cells
N.Oc/B.Pm	Number of osteoclasts per bone perimeter
N.Oc/B.Pm	Number of osteoclasts per bone perimeter
N.Oc/BS	Osteoclast number/bone surface
N.Oc/BS	Osteoclast number/bone surface
ND	Normal diet
NFATc1	Nuclear factor-activated T cells c1
NF- κ B	Nuclear factor kappa beta
Notch1	Notch homolog 1, translocation-associated
Notch1	Notch homolog 1, translocation-associated
OPN	Osteopontin
PAI-1	Plasminogen activator inhibitor-1
PBS	Phosphate Buffered Saline
PD1	Programmed cell death protein 1
PI3K	Phosphoinositide 3-kinase
PTHrP	Parathyroid hormone-like related protein
RANKL	Receptor Activator of NF- κ B Ligand
RNA	Ribonucleic Acid
RT-PCR	Reverse Transcription Polymerase Chain Reaction
SDS-PAGE	Sodium Dodecyl sulfate-Polyacrylamide gel electrophoresis

SEM	Standard error of the mean
SIBLINGs	Small integrin-binding ligand N-linked glycoproteins
sIL-6R	Soluble IL-6 receptor
Snail	Snail Family Zinc Finger 1
SPP1	Secreted phosphoprotein 1
Src	SRC proto-oncogene, non-receptor tyrosine kinase
SREs	Skeletal-related events
STAT3	Signal transducer and activator of transcription 3
T2DM	Type 2 diabetes mellitus
TAMs	Tumor associated macrophages
Tb.Th	Trabecular bone thickness
TBS	Tris Buffered Saline
TFs	Transcription factors
TGF β 1	Transforming growth factor β 1
TIMPs	Tissue inhibitors of metalloproteinases
TNF- α	Tumor necrosis factor- alpha
TRAP	Tartrate Resistant Acid Phosphatase
Twist1	Twist Basic Helix-Loop-Helix Transcription Factor 1
uPAs	Urokinase-type plasminogen activators
VCAM1	Vascular cell adhesion molecule 1
VEGF	Vascular endothelial growth factor
WB	Western blot
Ym-1	Chitinase-like 3
Zeb1	Zinc finger E-box binding homeobox 1

6.2 Acknowledgements

I appreciate my supervisor Prof. Gerog Schett for the opportunity to perform my MD thesis at his institute, the Internal Medicine 3 with excellent working conditions.

I appreciate my co-supervisor Prof. Aline Bozec, for the opportunity to perform my MD thesis at her laboratory in the department of Internal Medicine 3 of Universitätsklinikum Erlangen, for her excellent scientific guidance, constant scientific interest and support with ideas, and her passion and enthusiasm, letting me feel freedom in doing experimental research. All of those provided me endless motivation in scientific work.

I appreciate my colleagues of the group of Aline Bozec for the great atmosphere, the support, and the fun we had. Special thanks to Yubin, Xianyi, Zhu, Bettina, Nicole, Kay, Kenia and Mireia for giving suggestions and help during my work.

I thank Prof. Aline Bozec, Dr. Bettina Grötsch geb. Herbort, Daniel, and Christian for their careful revision of the thesis.

I thank Christine and Barbara for their outstanding technique support. I would also thank Prof. Martin Herrmann, Dr. Wolfgang Baum, Dr. Ulrike Harre, Olga, Katja and Katharina for their kind help during my work.

I thank Prof. Dov Zipori (Department of Molecular Cell Biology, The Weizmann Institute of Science, Rehovot, Israel), who kindly provided me the murine bone marrow adipocyte cell line 14F1.1.

I also appreciate Prof. Xiao-Xiang Chen, Prof. Cheng Qian, and my tutor of master degree, Prof. Shuang Ye, for their great support in pursuing my doctoral study in Germany.

Finally, I would like to thank my parents for the selfless love and support. Special thanks to my girlfriend, Juan Wang, for her romantic love.